Rotorua heat flow survey 2018

AM Seward
EK Mroczek
CJ Bromley
N Macdonald
S Lor
F Sanders
RR Reeves
T Brakenrig
DJ Graham

GNS Science Consultancy Report 2018/94
August 2018

GNS SCIENCE
TE PŪ AO

DISCLAIMER

This report has been prepared by the Institute of Geological and Nuclear Sciences Limited (GNS Science) exclusively for and under contract to Bay of Plenty Regional Council. Unless otherwise agreed in writing by GNS Science, GNS Science accepts no responsibility for any use of or reliance on any contents of this report by any person other than Bay of Plenty Regional Council and shall not be liable to any person other than Bay of Plenty Regional Council, on any ground, for any loss, damage or expense arising from such use or reliance.

Use of Data:

Client consent required to use data.

BIBLIOGRAPHIC REFERENCE

Seward AM, Sanders F, Mroczek EK, Reeves RR, Bromley CJ, Brakenrig T, Macdonald N, Graham DJ, Lor S. 2018. Rotorua heat flow survey 2018. Wairakei (NZ): GNS Science. 63 p. (GNS Science consultancy report; 2018/94).

CONTENTS

EXECUTIVE SUMMARY ..... **IV**

1.0 INTRODUCTION **1**

1.1 Background 1
1.2 Project Objectives 1
1.3 Historic Surveys 1

2.0 DATA COLLECTION **4**

2.1 2018 Survey Design 4
2.2 Survey Detail 4
2.3 Collection Methods 7
2.3.1 Spring Surveying and Sampling 7
2.3.2 Geothermal Pool Surveying 7
2.3.3 Measurement of Streams and Waterways 7
2.3.4 Near Surface Ground Temperature Measurements 9

3.0 ANALYSIS METHODS **10**

3.1 Heat Flow from Springs 10
3.2 Heat Flow from Pools 10
3.2.1 Heat Loss from Pools 10
3.2.1.1 Other Methods 11
3.3 Heat Flow from Streams 11
3.4 Heat Flow from Heated Ground 12
3.4.1 Heat Flow Determined from Temperatures Measured at 15 cm (Dawson 1964) 12
3.4.2 Heat Flow Determined Using a Portable Calorimeter 13
3.4.3 Conductive Heat Flow Through Soils 14
3.4.4 Convective Heat Flow Through Soils 14

4.0 RESULTS **15**

4.1 Heat Flow from Springs 15
4.2 Heat Flow from Pools 18
4.2.1 Uncertainties 20
4.3 Heat Flow from Streams 21
4.3.1 Puarenga Stream – Whakarewarewa 21
4.3.2 Tawera Stream – Kuirau Park Outflow 23
4.4 Heat Flow from Heated Ground 24
4.4.1 Calorimetry 24
4.4.2 Soil Temperature Profiles 26
4.4.3 Uncertainties 27

5.0 SUMMARY AND DISCUSSION **29**

5.1 Results Summary 29
5.2 Comparisons to Historical Heat Loss Surveys 30

6.0 CONCLUSIONS **32**

6.1 Recommendations 32

7.0 REFERENCES **33**

TABLES

Table E1 Summary of results. iv

Table E2 Comparison of heat loss from Whakarewarewa over time standardised to a constant wind speed and air temperature. v

Table 4.1 Determined heat loss and average Cl/SO_4 due to surface discharge. 15

Table 4.2 Summary of total heat loss (MW) from pool surfaces in each of the survey areas. 18

Table 4.3 Gauging and chemistry results from Puarenga Stream surveyed on 20 March 2018. 22

Table 4.4 Gauging and chemistry results from Puarenga Stream surveyed on 19 April 2018. 22

Table 4.5 Chloride-, Sulphate-fluxes, molar ratio, Thermal output (calculated from chloride flux) and calculated heat flow (from water temperature) of the Puarenga Stream surveyed in March and April 2018. 22

Table 4.6 Average measurements for the Tawera stream outflow of Kuirau Park. 23

Table 4.7 Measured heat fluxes (Wm^{-2}) and inferred boiling point depth (m). 24

Table 4.8 Total heat loss through the ground. 27

Table 5.1 Summary of results. Heat flows are given MW. 29

Table 5.2 Comparison between heat loss calculated using Dawson (1964) for 38 features common between the surveys at Whakarewarewa. 31

Table 5.3 Comparison of heat loss results from Whakarewarewa over time. 31

FIGURES

Figure 1.1 Thermal infra-red image over Rotorua city (Reeves et al. 2014). 3

Figure 2.1 Locations of water features surveyed during the 2018 heat flow survey. 5

Figure 2.2 Sites of soil temperature gradient measurements made during the 2018 heat flow survey of Rotorua 6

Figure 2.3 The gauging site locations along the Puarenga Stream. Aerial photography sourced from BOPLASS (2011). 8

Figure 2.4 The site of the data logger placed in the outlet from Kuirau Park. Aerial photography sourced from BOPLASS (2011). 8

Figure 4.1 Chloride concentration of Rotorua spring water. Red colours represent greatest chloride content. Aerial photography sourced from BOPLASS (2011) 16

Figure 4.2 Sulphate concentration of Rotorua spring water 17

Figure 4.3 Calculated heat flux for each surveyed pool. Aerial photography sourced from BOPLASS (2011) 19

Figure 4.4 The effect of windspeed on the calculated evaporative heat flux at different pool temperatures (40°C, 60°C and 80°C) using the equations of Dawson (1964) and Adam et al. (1990) 20

Figure 4.5 Water temperature, air temperature measured with the temperature logger compared with the flow data recorded by EK406461. 23

Figure 4.6 Locations of the Calorimeter sites of the 2018 heat flow survey 25

Figure 4.7 Total heat flux verses boiling point depth for the Wairakei – Tauhara sites (black circles) and from the six sites from this survey (red circles) 26

Figure 4.8 Comparisons between temperatures measured at 5 cm, and the inferred temperature of the related pixel on the 2014 TIR. 27

Figure 4.9 Comparison between ground heat flux calculated using the measured 15 cm ground temperature (Qdawson), and the heat flux determined using conductive and convective heat flux calculated by the methods of Seward et al. (2018a), showing a linear best fit correlation. 28

Figure 4.10 Inferred relationship between Q_{tot} and the 5 cm deep ground temperature for collected Rotorua soil data. 28

APPENDICES

APPENDIX 1: DATA COLLECTION AND FIELD NOTES 36

A1.1 Field Notes 36
A1.2 Weather Details for Survey Dates 37

APPENDIX 2: SPRING DATA CHEMICAL ANALYSIS 39

APPENDIX 3: POOL DATA 40

APPENDIX 4: CHEMICAL ANALYSIS OF PUARENGA STREAM 42

A4.1 Puarenga Stream Gauging Reports 42
A4.2 Puarenga Stream Chemistry 42

APPENDIX 5: GROUND TEMPERATURE DATA 43

A5.1 Soil Temperature Data 43
A5.2 Soil Temperature Profiles 47
A5.3 Calorimeter Data Plots 56
A5.4 Determining Heat Loss from TIR Heat Signature for Area Estimation 63

APPENDIX TABLES

Table A 1.1 Survey details. 37
Table A 2.1 Heat flow and chloride concentrations of surveyed springs. 39
Table A 3.1 Surface heat loss from pools. 40
Table A 5.1 Temperatures and heat flux determined at ground temperature sites. 43
Table A 5.2 Summary of heat loss determined in each area using the TIR image. 63

APPENDIX FIGURES

Figure A 5.1 Soil temperature profiles recorded at the ambient reference site. 47
Figure A 5.2 Soil temperature profiles measured at Kuirau Park. 48
Figure A 5.3 Soil temperature profiles collected at Sulphur Bay / Government gardens 49
Figure A 5.4 Soil temperature profiles collected at Whakarewarewa / Te Puia 50
Figure A 5.5 Soil temperature profiles collected at Arikikapakapa. 55
Figure A 5.6 Plot of raw data collected at Calorimeter site R1. 56
Figure A 5.7 Plot of raw data collected at Calorimeter site R2. 57
Figure A 5.8 Plot of raw data collected at Calorimeter site R4. 58
Figure A 5.9 Plot of raw data collected at Calorimeter site W1. 59
Figure A 5.10 Plot of raw data collected at Calorimeter site W7. 60
Figure A 5.11 Plot of raw data collected at Calorimeter site W8. 61
Figure A 5.12 Plot of raw data collected at Calorimeter site 99-calorimeter 62

ENCLOSURES

USB drive
Appendix A1.1 – Field Notes
Appendix 2 – Spring Data Chemical Analysis
Appendix A4.1 – Puarenga Stream Gauging Reports
Appendix A4.2 – Puarenga Stream Chemistry ..... back cover

EXECUTIVE SUMMARY

This report describes the data collection, analysis, methods and results from an assessment of surface heat loss from the Rotorua Geothermal Field conducted by GNS Science between February 26 and April 19, 2018. The surface heat loss from the Whakarewarewa, Arikikapakapa, Sulphur Bay and Government Gardens, and Kuirau Park areas have been calculated from advective, evaporative and radiative heat losses from pools, springs and ground surfaces, using:

1. Flow rates, water temperatures and water chemistry (chloride and sulphate concentrations) of significant flowing hot **springs.**
2. Surface temperatures and area of geothermal **pools.**
3. Water temperature, flow rate and water chemistry (chloride and sulphate concentrations) of **streams and rivers** with geothermal inflows.
4. Ground temperature-depth profiles and terrestrial calorimetry (**surface heat flux**).

The surface heat flux was not measured at Ngapuna and Ohinemutu because these areas were outside the scope of the report.

Two methods of calculating evaporative heat loss are presented. The method of Adam et al. (1990) is believed to be the most accurate assessment method, however the method of Dawson (1964) is also used so that the results in this report can be compared to previous estimates of heat loss that use the latter methodology.

The total surface heat loss calculations for the areas surveyed indicate a heat loss of 184 MW and 299 MW using the evaporative heat flux methods of Adam et al. (1990) and Dawson (1964) respectively. The main difference in these estimates is caused by the way the different methods account for the cooling effect of wind on surface evaporation in the heat loss calculations.

Table E1 summarises the calculated heat loss for each area.

Table E1 Summary of results. Heat loss are given MW.

Area	Evaporation and radiation (pools)		Discharge (springs and streams)	Ground heat flow	Total	
	Dawson	Adam			Dawson	Adam
Whakarewarewa	97.7	55.3	36.0	9.81	141	98.6
Sulphur Bay	6.2	4.0	Not accounted for	6.62	12.8	10.6
Arikikapakapa	71.5	32.3	-	0.48	72	32.8
Kuirau Park	72.6	41.6	0.024	0.77	73.4	42.4
Total	**248**	**133.2**	**36.0**	**17.7**	**299.2**	**184.4**

Table E2 summarises the results from this survey compared to historical heat loss surveys, and focusses on the Whakarewarewa area. Note the calculated heat loss from the 2018 study (Table E2) differs from values in Table E1, because Table E2 assumes a constant ambient air temperature of 12°C and windspeed of 1 ms^{-1} in the evaporative calculations, in order to be consistent with the two previous assessments.

An increase of approximately 22 MW is evident between 1985 and 2018. This equates to about 80% of the total heat loss measured in 1969. The increase in heat loss can be interpreted as a sign of increased heat flow caused by more geothermal fluids reaching the surface.

Table E2 Comparison of heat loss from Whakarewarewa over time standardised to a constant wind speed and air temperature. Discharged heat loss is calculated from water temperatures relative to 12°C.

Survey	1969	1985	2018
Evaporation and radiation	95.5	58.7	62.9
Discharge	27	17	33.5
Ground surface heat flux	10.3	7.9	9.8
Total	132.8	83.6	106.2

1.0 INTRODUCTION

1.1 Background

Estimating heat loss from a geothermal field provides an indication of thermal activity present in the geothermal system at depth. Geothermal surface features (such as hot springs, pools and hot ground) occur where geothermal fluids discharge at the surface. Changes in the activity of the geothermal surface features over time can indicate changes that may be occurring within the geothermal reservoir due to either natural or anthropogenic causes. Measurements of heat loss can be used as a proxy to monitor the combined heat discharge from large areas. Heat loss monitoring can reveal when and where large-scale changes in the thermal regime (aquifer pressure and temperature) are occurring within a geothermal system and can provide useful inputs into calibrating numerical models of geothermal systems and therefore improved forecasting of the effects of energy use through scenario modelling (e.g., Ratouis et al. 2016).

Bay of Plenty Regional Council (BOPRC) are interested in estimating the surface heat loss from the Rotorua Geothermal Field (RGF), to provide an overall heat loss estimate that can be used to help calibrate numerical models of the system and inform policy. Numerical models aid in testing and understanding conceptual models of the complex hydrothermal system and underlying reservoir. They are used to inform policy on use and protection of the geothermal resource. Results from this study will be used to update the current models of Rotorua.

1.2 Project Objectives

The objectives of the project were to:

1. Determine appropriate methodologies for estimating heat loss.
2. Estimate geothermal-field scale terrestrial heat loss from the RGF. This will include the Whakarewarewa, Kuirau Park, Arikikapakapa and Sulphur Bay and Government Gardens areas (Figure 1.1) in the RGF. The Ngapuna and Ohinemutu geothermal areas (Figure 1.1) are omitted from this study.
3. Compare historic heat loss measurements from Whakarewarewa to the 2018 survey to estimate changes in heat loss over time.

1.3 Historic Surveys

Previous heat loss surveys in the RGF are largely confined to the Whakarewarewa geothermal area. Lloyd (1969a, 1969b) mapped and surveyed 538 accessible natural geothermal features to provide a dataset against which future surveys could be compared. Features are described in detail with the prominent characteristics of each feature including, where possible, estimates of flow rate, ebullitions, pond size, pulsing characteristics, surrounding foliage and other distinguishing characteristics. Additionally, a survey of ground temperature at 15 cm depth was undertaken in 1968.

Cody et al. (1984a, 1984b) repeated the heat loss survey in 1984–1985. Their survey involved repeat observations of the initial 538 features surveyed in 1969, and an additional 279 features that had been formed or had become accessible since the first survey. Ground temperatures at 15 cm were again measured at over 1000 locations in 1985.

Heat loss from 28 springs in Whakarewarewa are reported by Gordon et al. (2001). He reported an increase in heat loss of 30% over heat loss reported for the sample features in 1984/85. The 2001 survey, however, was only based on the discharge flows of a subset of spring located along the Puarenga Stream (Figure 1.1), and no estimates were made of evaporative heat loss or ground heat.

In 2010–2011, a survey of ~100 water features and 140 ground-temperature sites was undertaken at Whakarewarewa (Scott et al. 2016). That survey did not show the same increase in heat loss as Gordon et al. (2001). The heat loss from the surveyed features indicated a decrease in surface heat loss relative to 1985. This may have been in part due to the subset of features that was surveyed in the 2010–2011 survey, and in part due to the large decrease in surface temperature of Lake Roto-A-Tamaheke (Figure 1.1). Lake Roto-A-Tamaheke accounts for a large proportion of the total evaporative heat loss at Whakarewarewa due to its large surface area (>8000 m^2). Historic temperature measurements of the lake are 64°C (1969), 49°C (1985) and 39.4°C (2010), and the decreasing surface temperature of the lake over time will have a large effect on the total heat loss.

Much of the geothermal discharge at Whakarewarewa flows into the Puarenga Stream. Determining heat content, chloride and sulphate concentrations of the Puarenga Stream provides a better determination of geothermal heat loss than from individual features. The heat and chemical mass flow into the Puarenga Stream was regularly measured (~monthly) between 1982 and 1993 at Hemo Gorge and at the FRI sites. Hemo Gorge is upstream of any known geothermal activity; the FRI is downstream of Whakarewarewa Village. The stream flow was automatically gauged at these two sites between 1982 and 1985, and manually thereafter (Glover 1988, 1992).

Glover (1988, 1992) explored the heat and mass output from the Whakarewarewa geothermal area by measuring temperature changes and assessing changes in chemical composition in the Puarenga Stream, upstream and downstream of surface manifestations in the geothermal area. It is assumed all springs and subterranean flow from the geothermal area follow the natural contours of the landscape and flow into the Puarenga Stream. Glover collected two years of data and showed an average inflow from the Whakarewarewa geothermal valley of between 137 and 160 Ls^{-1} between Hemo Gorge and FRI (Figure 1.1). A mean average water temperature increase of 5.8°C was measured. This suggested that a heat inflow from the geothermal activity in the valley was approximately 39–43 MW.

Reeves and Rae (2016) reported changes in the surface thermal area of Rotorua between 1990 and 2014 using aerial thermal infrared (TIR) data. They indicated little change in the size of surface areas of geothermal activity in Ngapuna, Ohinemutu, Kuirau Park and Arikikapakapa, but a decrease in geothermal surface area in Sulphur Bay and Whakarewarewa.

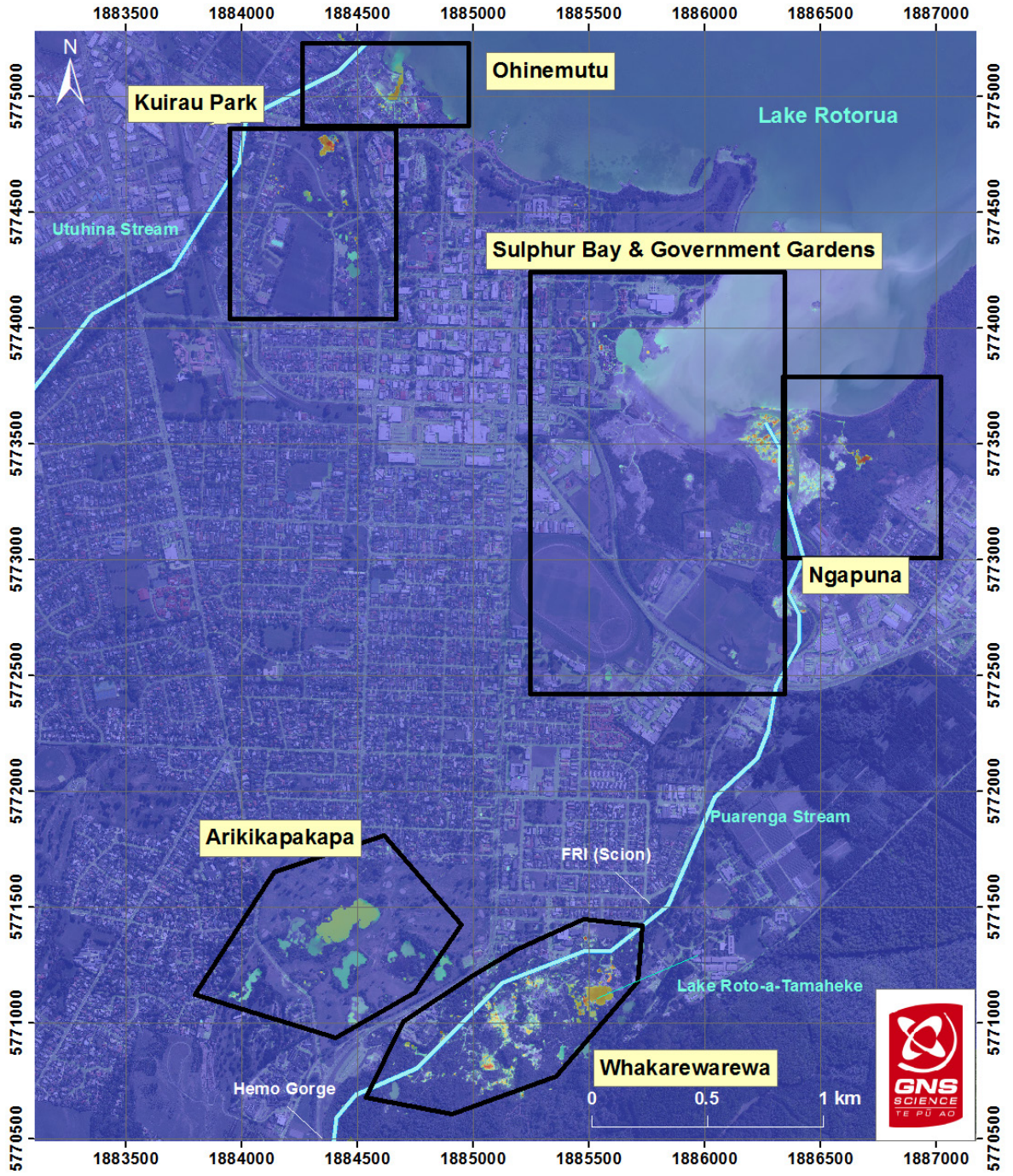

Figure 1.1 Thermal infra-red image over Rotorua city (Reeves et al. 2014). Higher thermal signatures (red) suggest higher surface heat flux.

2.0 DATA COLLECTION

2.1 2018 Survey Design

Time, budgetary and access constraints usually mean that not every geothermal feature can be surveyed in a heat loss survey. Therefore, prioritisation of features to be surveyed is required to ensure that a heat loss estimation for an area is valid. Generally, large, hot and/or flowing geothermal features will be selected because these features will have the largest heat losses relative to ambient conditions.

The targeted geothermal surface features for the Rotorua heat loss survey were determined using high resolution TIR images collected in 2014 (Figure 1.1; Reeves et al. 2014). Surface temperatures were estimated from the thermal images. A proxy for heat output based on inferred surface temperature and surface area was calculated to determine the features to be targeted. Additionally, features that had previously been surveyed as part of the Rotorua monitoring program (e.g., Pearson-Grant et al. 2015) were also targeted.

Access permission was granted for the areas of Whakarewarewa Village and Te Puia (from here referred to as Whakarewarewa), Arikikapakapa, Kuirau Park, Sulphur Bay and Government Gardens.

A total of 116 water features were surveyed. Thirty-four of these sites were also sampled for chloride and sulphate concentrations which enabled chloride balances to be estimated. One hundred and thirty-one ground temperature profiles were measured and six calorimeter sites were surveyed. Additionally, the Puarenga Stream was gauged at five locations as it flows through Whakarewarewa to identify areas of stream gain/loss. Water samples were collected at the gauging sites. This was repeated a month later as inconsistent flow data had been collected on the first attempt.

2.2 Survey Detail

Field data was collected between 27 February and 19 April 2018 (Appendix 1). Data collection was limited to days where there was little or no rain, as large amounts of meteoric water can cool water surfaces of pools, dilute spring water chemistries and dampen near surface soil temperatures.

Four key data sets were collected during the field campaign. They consisted of:

1. Flow rates, temperatures and water quality (chloride and sulphate concentrations) of geothermal flowing **springs.**
2. Surface temperatures, area and outflow rates of geothermal **pools.**
3. Water temperature, flow rate and water quality (chloride and sulphate concentrations) of **streams and waterways.**
4. Ground temperature-depth profiles to a maximum depth of 1 m, and terrestrial calorimetry (**surface heat flow**).

Care was taken to survey water features as close together in time as possible to minimise effects of changes in atmospheric pressure and weather patterns on the heat output of the geothermal surface features. Most of the observations of water features were completed within the first two weeks of surveying.

Figures 2.1 and 2.2 show the geothermal water feature sites and ground temperature sites surveyed during this campaign.

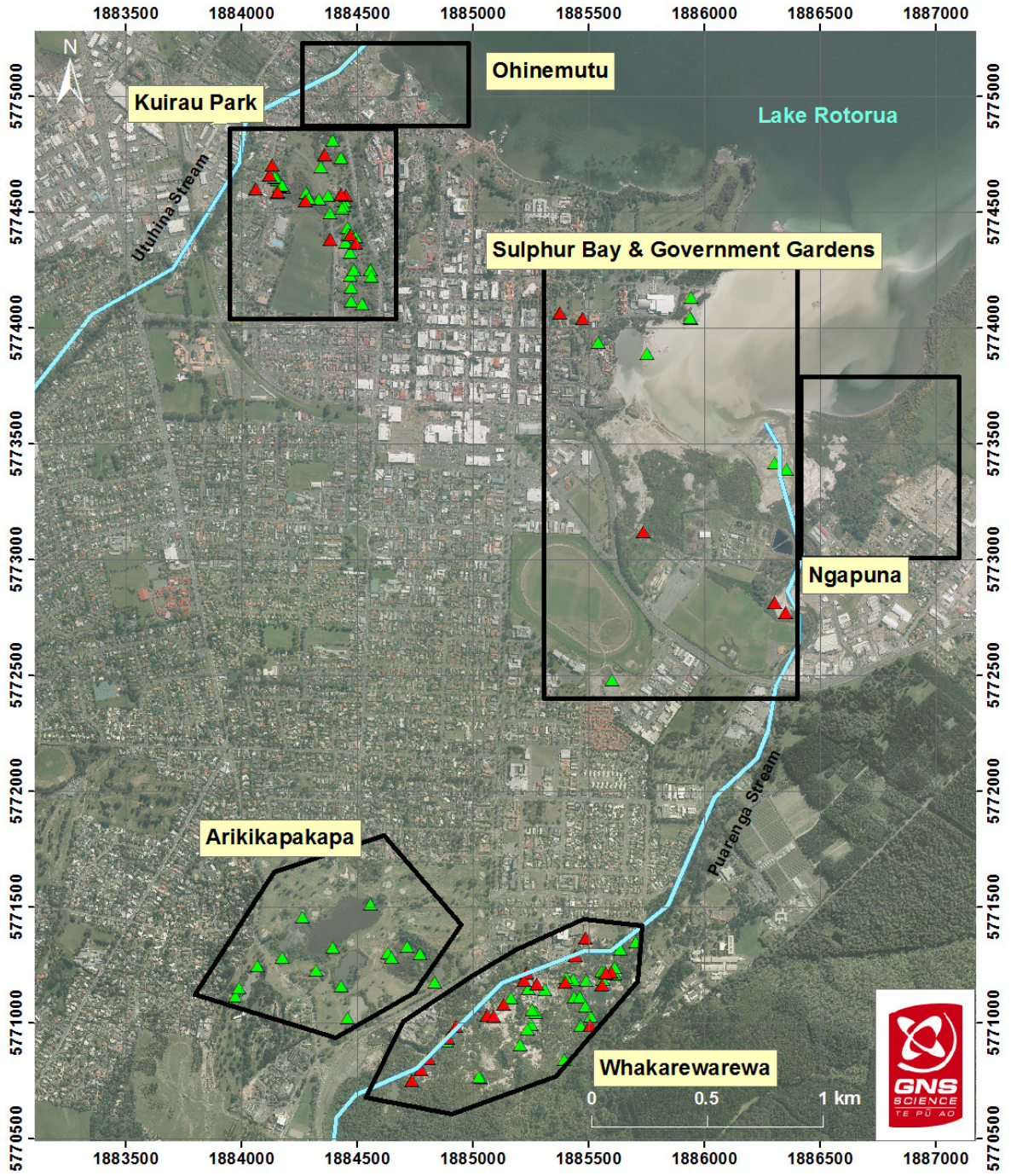

Figure 2.1 Locations of water features surveyed during the 2018 heat flow survey. Red triangle indicates the sites where water samples were taken. Aerial photography sourced from BOPLASS (2011).

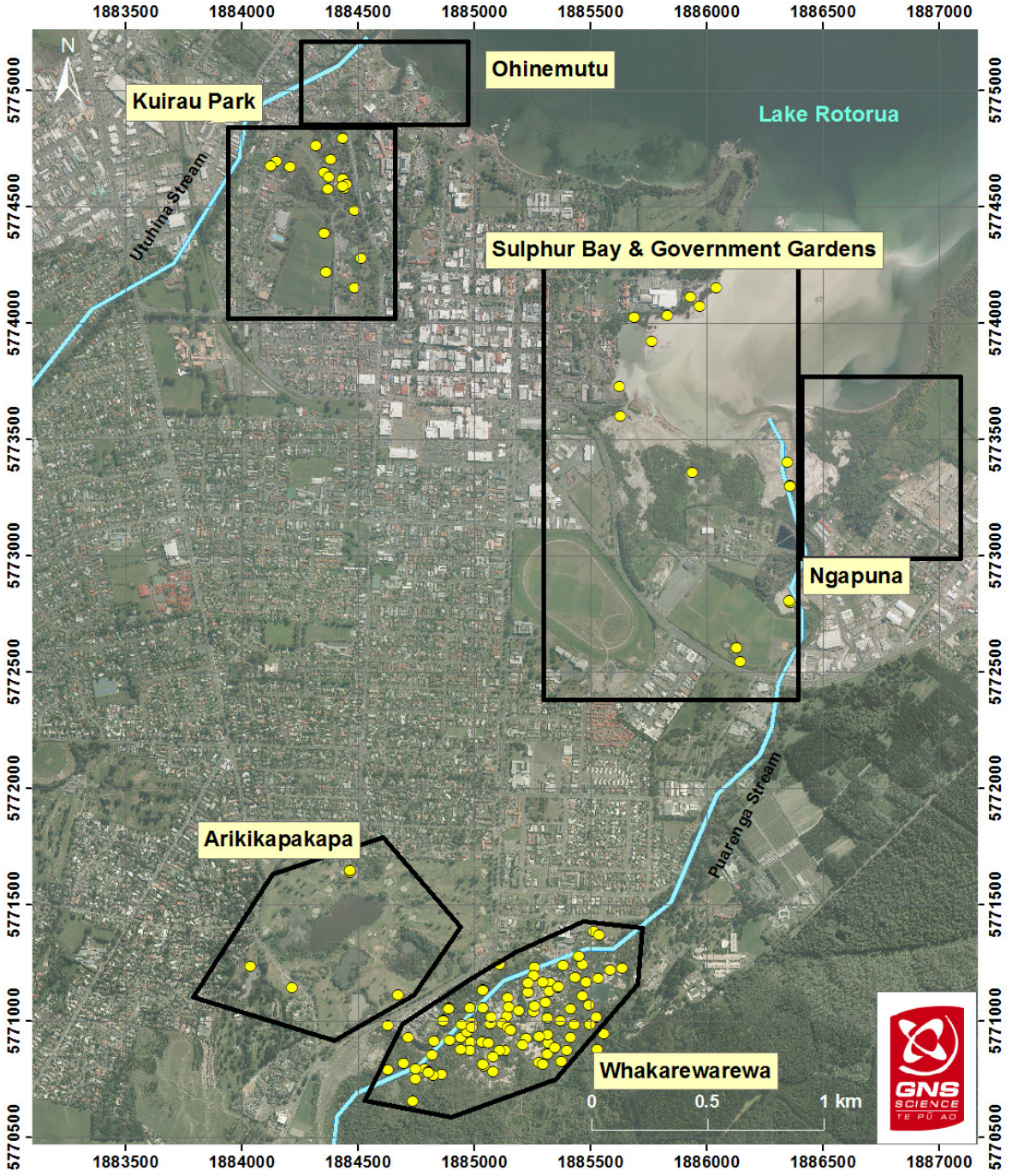

Figure 2.2 Sites of soil temperature gradient measurements made during the 2018 heat flow survey of Rotorua. Sites of known warm ground were targeted, with a higher concentration of measurements made in the Whakarewarewa area to re-create the coverage of previous surveys. Aerial photography sourced from BOPLASS (2011).

2.3 Collection Methods

Measurements made in the field were recorded using a tablet installed with a GNS Science (GNS) built application. Observations for each dataset are described below, but include, measurements, feature descriptions, photographs, and atmospheric conditions.

Site locations were recorded in NZTM 2000 coordinate system using a Garmin GPSmap 62sc at the site of survey measurement. Water and ground temperature measurements were made using a Yokogawa TX10 digital meter and K-type thermocouple. Wind speed measurements were measured using a Digitech anemometer.

Air temperature and windspeed were recorded on site, while hourly atmospheric pressure and humidity were recorded at the Rotorua Racecourse (National Institute of Water and Atmospheric Research (NIWA) climate station – agent number 41077).

2.3.1 Spring Surveying and Sampling

Springs were surveyed for water temperature, flow rate and water chemistry. Water samples were collected, and water temperatures were measured mid-flow and close to source. Survey procedures outlined in GNS (2017a) were adopted for observation information, feature location, feature description, colour and turbidity, odour, ebullience, eruption and for measurement of temperature and wind speed. Water sampling procedures described in GNS (2017b) were used for sampling features where water samples were required. Raw 500 ml and 100 ml filtered water samples were collected and submitted to the New Zealand Geothermal Analytical Laboratory (NZGAL) to be analysed for chloride and sulphate concentrations.

2.3.2 Geothermal Pool Surveying

Geothermal pools were surveyed using the procedures described in GNS (2017a). Geothermal pools with the largest thermal signatures, as detected by the 2014 TIR survey (Reeves et al. 2014) were targeted. Surface water temperatures were measured at <2 cm below the pool surface.

2.3.3 Measurement of Streams and Waterways

Water temperature, flow rate and water chemistry were collected from selected streams. The Puarenga Stream, which runs through the Whakarewarewa geothermal valley, has historically been surveyed at five locations (Figure 2.3). NIWA was subcontracted to gauge the flow at these five sites using a Teledyne RD Instrument Streampro Acoustic doppler Current Profiler (ADCP). The ADCP provides a quick, easy and accurate method of measuring the stream flow.

Water samples were collected at each gauging site along the Puarenga Stream, as per the methodology in the GNS (2017b). Raw 500 ml and 100 ml filtered water samples were collected and submitted to NZGAL to be analysed for chloride and sulphate.

A Trutrack datalogger (model pt-HR) was installed to record water temperatures 2 m upstream of the Tarawera gauging station EK406461 (Figure 2.4), which monitors the outflow from Kuirau Park. Water temperature data was collected every 5 minutes between 9:00, 26 February 2018 and 17:00, 4 April, 2018. Water samples were collected on 27 February 2018 as per the methodology in the GNS (2017b). Raw 500 ml and 100 ml filtered water samples were collected and submitted to NZGAL to be analysed for chloride and sulphate.

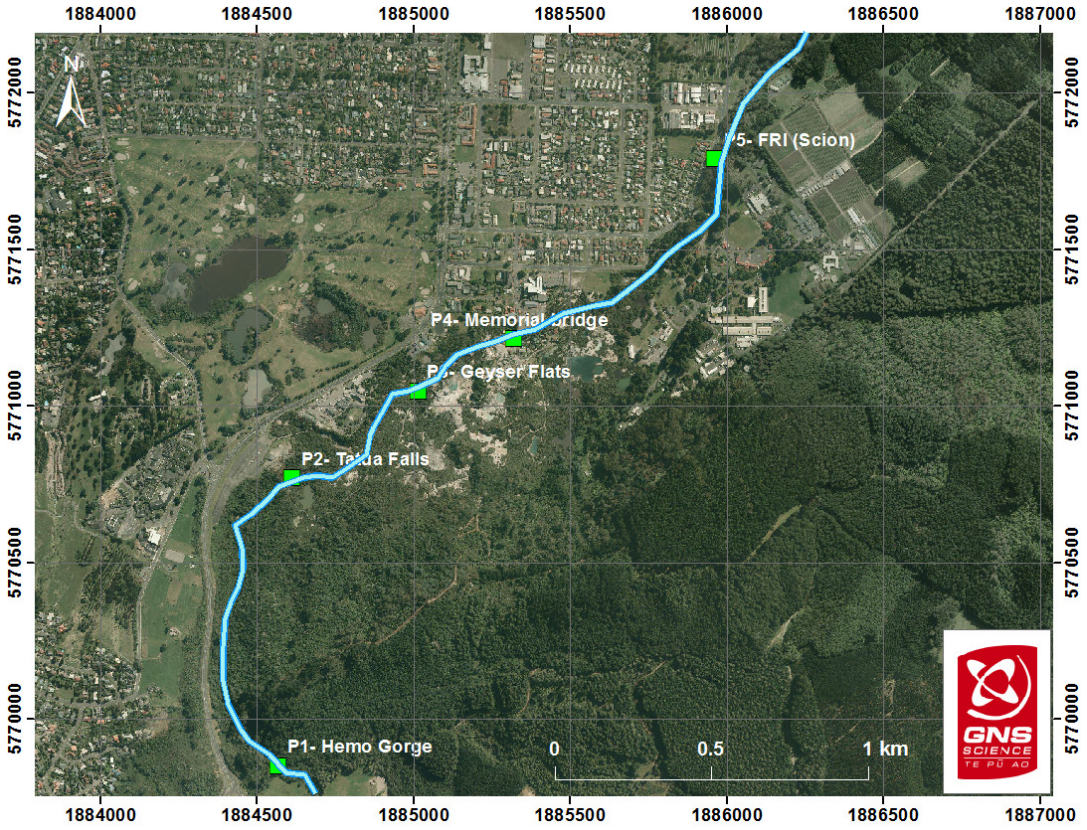

Figure 2.3 The gauging site locations along the Puarenga Stream. Aerial photography sourced from BOPLASS (2011).

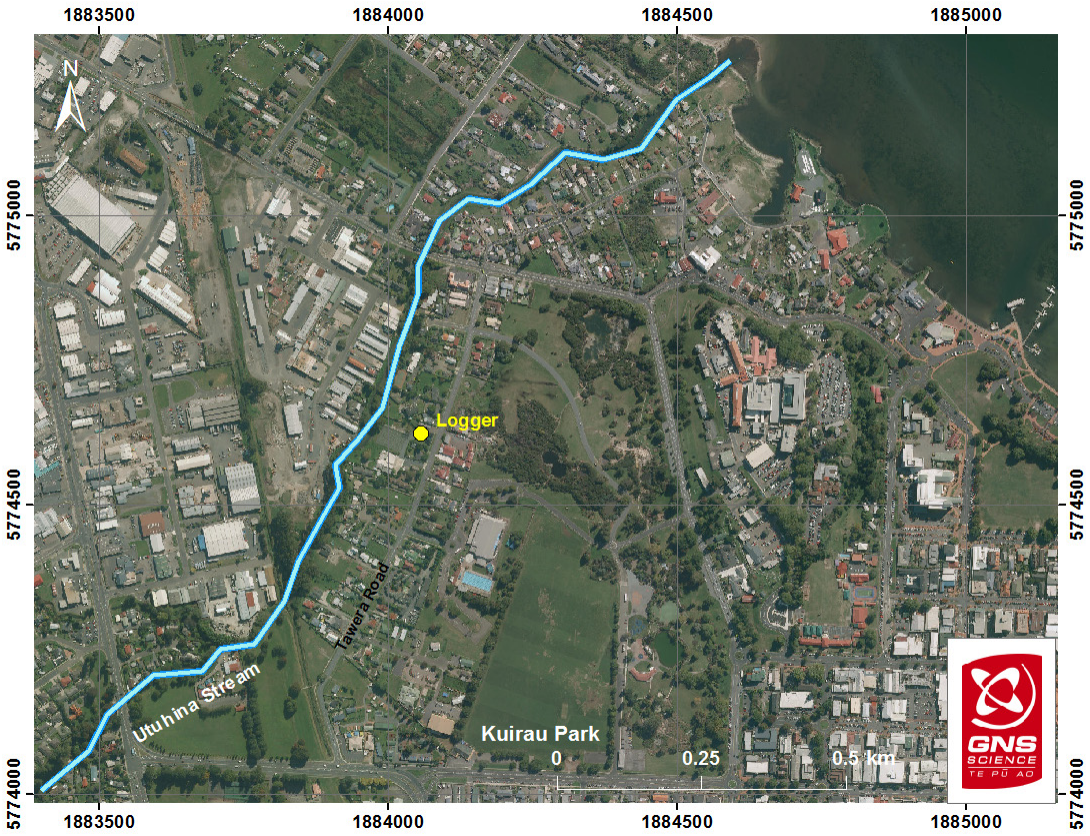

Figure 2.4 The site of the data logger placed in the outlet from Kuirau Park. Aerial photography sourced from BOPLASS (2011).

2.3.4 Near Surface Ground Temperature Measurements

Near-surface ground temperature measurements were made using a TX10 and k-thermocouple, at 5, 10, 15, 20, 25, 50 and 100 cm depth. These temperatures are used to determine thermal gradients at sites from which conductive heat flow can be determined.

Calorimetry measurements are undertaken at selected high-temperature or steaming ground sites, to determine convective heat flux. Calorimetry data was collected following the procedure described by Seward et al. (2018b).

3.0 ANALYSIS METHODS

This section outlines the methods used to determine surface heat loss from the RGF. Methods are based on historic methodologies for ease of comparisons with previous heat flow surveys of the area. Advances and alternative methods are also outlined for result comparison.

Note that the terms heat loss refers to the heat output of a feature or area (generally in Watts (W) or MW), while heat flux refers to heat output at a location standardised for area (Wm^{-2}).

3.1 Heat Flow from Springs

The measurement of the heat content of a stream into which springs discharge is preferred to individual measurements, as springs often discharge a percentage of their heat by subsurface flow (Miotti et al. 2010).

Heat flow from springs is determined by:

- calculating the evaporative heat loss from the water surface using the calculations described below for a pool, and
- an estimation of the heat discharge using a measurement of water temperature (°C), and volumetric flow rate (Ls^{-1}).

$$Q_{spring} = 0.001 M_w (h_w - h_{atm}) \qquad \text{kW}$$

where M_w is the mass flow of heated water in kgs^{-1}, h_w is the enthalpy of the discharging water in $KJkg^{-1}$ and h_{atm} is the enthalpy of water at the atmospheric temperature in $KJkg^{-1}$ (Sorey and Colvard 1994).

3.2 Heat Flow from Pools

3.2.1 Heat Loss from Pools

Heat flux from heated pools consists of heat lost predominantly through evaporative processes (Q_E) and radiative processes (Q_R). The conductive heat loss (Q_C) is often over an order a magnitude smaller than the other mechanisms. Total heat loss from pool can be calculated by summing the three components:

$$Q_{pool} = Q_E + Q_C + Q_R$$

Equations described by Dawson (1964) and used by Simpson (1985) to determine heat loss from the surface of geothermal pools are described and converted into SI units by Fridriksson et al. (2006). These converted equations are described below and used to determine the surface heat loss from the surface of pools in this survey.

The heat flux from a pool by evaporation is calculated by

$$Q_E = A\left(h_{s,tp} - h_{w,tp}\right)(0.0065 + 0.0029w)\frac{\left(P_{H2O,tp} - P_{H2O,atm}\right)}{P_{ATM}} \qquad \text{(W)}$$

Where A is the area of the pool (m^2), $h_{s,tp}$ is the enthalpy of the steam at pool temperature (t_p) ($J\ kg^{-1}$), $h_{w,tp}$ is the enthalpy of water at pool temperature, w is the wind speed (ms^{-1}), $P_{H2O,tp}$ is the vapour pressure of water at t_p (bar), $P_{H2O,atm}$ is the atmospheric vapour pressure (bar) and P_{ATM} is the atmospheric pressure in bar.

For vigorously boiling surfaces an additional evaporative heat loss is determined by

$$Q_e = 1.7\ h$$

where *h* is the height of observed ebullitions (cm).

The heat loss by conduction and molecular diffusion, Q_C, is related to Q_E by the Bowen ratio, RB (Sutton 1953).

$$RB = \frac{Q_C}{Q_E} = 6.1 \times 10^{-4} P_{tot} \frac{(t_p - t_{atm})}{(P_{H2O,tp} - P_{H2O,atm})}$$

where t_{atm} is the atmospheric temperature in °C.

Radiative heat loss, Q_R, is calculated by

$$Q_R = A\varepsilon\sigma(T_P^4 - T_{atm}^4) \qquad \text{(W)}$$

where ε is emissivity, equal to 0.955 for water, σ is the Stefan-Boltzman constant equal to 5.68 x 10^{-8} $Wm^{-2}K^{-4}$, and T_P and T_{amt} refer to the temperature of the pool (*P*) and ambient air (*amt*) temperature in Kelvin.

3.2.1.1 Other Methods

Historically, the methods of Dawson (1964) to calculate surface heat loss from pool surface have been used to assess the heat loss in Rotorua (Cody and Simpson 1985; Simpson 1985). However, experimental investigations into the evaporative heat flux (Ryan et al. 1974; Adam et al. 1990; Sartori 2000) suggest that Dawson's equation overestimate the surface heat loss, when environmental factors, such as wind, are introduced. In this study we have calculated the surface heat loss using both the methods described by Dawson (1964) (converted into SI units, Fridriksson et al. (2006)) and Adam et al. (1990), to allow a more consistent estimation of evaporative heat output, as well as a comparison to historic data.

Adam et al. (1990) uses an equation which combines forced and free convective components to determine a total evaporative heat flux.

$$Q_E = \sqrt{(2.7\Delta T^{1/3})^2 + (5.1A^{-0.05}w)^2}\left(p_{H2O,tp} - p_{H2O,atm}\right) \qquad \text{(MW)}$$

where ΔT is the difference between the surface temperature of the pool and the ambient air temperature (°C), A is the surface area of the pool (m^2), w is the onsite windspeed at the time of the temperature measurement (ms^{-1}), and $p_{H2O,tp}$, $p_{H2O,atm}$at the vapour pressure of water at t_p and atmospheric conditions (bar).

3.3 Heat Flow from Streams

The heat flow into the Puarenga Stream is estimated from the water composition, temperature and flow data collected both upstream and downstream of Whakarewarewa geothermal area. Identified changes in temperature, chloride and sulphate concentrations are assumed to be due to addition of geothermal waters. A chloride and sulphate flux is calculated by multiplying the concentrations (mgL^{-1}) by the measured flow rate (Ls^{-1}) at the survey site. The heat flow is calculated by multiplying the measured flow rate by the enthalpy of the stream water at a measured temperature. The enthalpy and density of water is determined by using *water97_v13.xla* add-in for excel, which calculated the thermodynamic and transport properties of water and steam using the industrial standard IAPWS-IF97 (Spang 2002).

An alternative method for determining thermal output into a stream is calculated from the chloride flux and enthalpy of the water (Glover 1992). The enthalpy of the Puarenga stream is assumed to be 0.58 MJ/g.

The flows of the Puarenga Stream can be effected by large, variable takes upstream by the Rotorua Lakes Council (RLC) as a water supply and takes for the Waipa Mill for commercial purposes.

A temperature logger was placed in the Tawera Stream outflow of Kuirau Park, at 12:43 on February 27, 2018. It was left in place until April 6, 2018. The data logger was located approximately 2 m upstream of the BOPRC gauging site (EK406461) and was recording a measurement of air and water temperature every 5 seconds.

3.4 Heat Flow from Heated Ground

Areas of heated ground are common in geothermally active areas. Most surface expressions come along with diffuse discharges of ground vapour consisting of conductive heat flux as well as convective flows (Hochstein and Bromley 2005). Convective heat flux accounts for a large percentage of the total heat flux from warm ground, in some cases up to 50% (Bromley et al. 2011).

There are several methods used to determine heat flow through heated ground in geothermally active areas. These include methods described by Dawson (1964), and Hochstein and Bromley (2005). The method described by Dawson (1964) was used in the heat determination of Simpson (1985) and again here. More recent surveys have used the method described by Hochstein and Bromley (2005) in which the thermal gradient of the top 1 m of the soils (if linear) is used directly to determine heat flux if a thermal conductivity of the soil is known. If non-linear, extrapolation is used to determine a depth to boiling point, which is then used to infer surface heat loss using an empirical equation derived between heat loss from calorimetry and boiling point depth. Calorimetry is also used in several locations, to directly measure the surface heat flux at the surface of heated ground. Details of each method are given below:

3.4.1 Heat Flow Determined from Temperatures Measured at 15 cm (Dawson 1964)

Dawson (1964) uses an empirical relationship between heat flow (q_s) and the temperature at a depth of 15 cm (t_{15}) to determine heat loss. He derived this relationship by relating measured heat flux (measured using a calorimeter) to ground temperatures at 15 cm depth. The relationship is given below.

$$q_s = 1.24\ x\ 10^{-6}\ \ t_{15}^4 \qquad \text{cal m}^{-2}\,\text{s}^{-1}$$

A more recent study by Fridriksson et al. (2006) separates soils temperature at 15 cm into two categories: (1) soils with measured temperatures less than 97°C, and (2) soils with temperatures equal to or greater than 97°C at 15 cm depth. This is a result of a change in characteristics in heat transfer as temperatures reach boiling temperatures (~98.8°C at Rotorua). For temperatures, less than 97°C he used the equation given by Dawson (1964), converted below into S.I. units.

$$q_s = 5.2\ x\ 10^{-6}\ \ t_{15}^4 \qquad \text{W m}^{-2}$$

and for $t_{15} \geq 97°C$, he used equation:

$$q_s = 10^{\left(\frac{logd_{97}-3.548}{-0.84}\right)} \qquad \text{W m}^{-2}$$

where d_{97} is the depth at which a temperature of 97°C is reached.

Hochstein and Bromley (2005) suggested ground temperatures recorded at 15 cm depth are greatly influenced by atmospheric conditions, and that the heat flux determined from temperature gradients at greater than 50 cm depth are more reliable (see Section 3.4.3 for more details on this method).

To determine a surface heat loss for Rotorua, the measured point heat fluxes were extrapolated using the thermal signatures detected in the 2014 TIR images (Reeves et al. 2014), to calculate a total area of similar ground temperature. This assumes that the surface temperature is indicative of heat flux properties. Inferred ground temperatures (Reeves et al. 2014) are categorised into 2° bands. The total area of ground with temperatures within a band are used to estimate a total heat loss through the ground. This method differs to the methods used in the previous survey, where the area was estimated by contouring the measurements sites.

3.4.2 Heat Flow Determined Using a Portable Calorimeter

Total surface heat flux can be measured using the water-based calorimeter by recording increases in the temperature of the water, starting from near-ambient conditions. A linear rate of temperature increase is caused by steady ground heat transfer over a short time-period (typically 5 minutes). These measurements allow a total heat flux from the surface, within the foot print of the calorimeter, to be determined using equation (Hochstein and Bromley 2005).

$$q_{tot} = \frac{mc\left(\frac{\Delta T_{rd}}{\Delta t} - \frac{\Delta T_{dr}}{\Delta t}\right)}{A} \qquad \text{W m}^{-2}$$

where $\frac{\Delta T_{rd}}{\Delta t}$ denotes the temperature-rise recorded during the measurement interval, and $\frac{\Delta T_{dr}}{\Delta t}$ is the background temperature drift, *m* is the water mass, *c* is the specific heat and *A* is the area covered by the calorimeter.

At each calorimeter site, a total heat flux (Q_{tot}) was determined by placing the calorimeter on the ground for 5 minutes and measuring the temperature increase of the water placed in the calorimeter. To measure heat loss due only to advective steam flux and radiation processes, the same procedure was followed, but by placing the calorimeter on a 2 cm thick plastic ring to lift it off the ground, and then measuring the temperature change. Effects from warm ambient air were measured in between ground measurements, by recording any temperature increase or decrease caused by the surrounding air, while the calorimeter is on an insulated block. Ambient air affects are also minimised as the calorimeter is fully insulated with polystyrene, except for the base. Full details of the calorimeter design and processing procedure are described by Hochstein and Bromley (2005). At each site 1 m temperature profiles were also measured at 5, 10, 15, 20, 25, 50 and 100 cm depths. These ground temperatures are used to determine conductive temperature gradients and depths at which boiling temperatures are reached (98.8°C for Rotorua).

3.4.3 Conductive Heat Flow Through Soils

An alternative method for determining surface heat loss through the near-surface is to determine the geothermal gradient of the top meter. With a measured (or known) thermal conductivity of the soil, the conductive surface heat flux can be calculated using equation:

$$q_c = \frac{\Delta T}{\Delta z}\lambda \qquad \text{W m}^{-2}$$

where q_c is the conductive heat flux, ΔT is the change in temperature over depth range Δz, and λ is the near-surface thermal conductivity of the soil.

3.4.4 Convective Heat Flow Through Soils

The largest mechanism for heat flow through the ground in heated areas is through convection (or advection of steam). The convective component of heat transfer can be calculated through an exponential relationship determined by comparing calorimeter data to boiling point temperatures determined from temperature gradients.

The depth to boiling point can be either measured directly for Z_{BP} <1 m, or inferred from extrapolating a fitted exponential function to the measured temperature-depth data.

$$Z_{BP} = \exp[c_1(T_{BP} - T_z)]$$

where T_z is the temperature at depth z, T_{BP} is the boiling point temperatures (at atmospheric pressure; 98.8°C for Rotorua) and c_1 is a constant (assessed empirically to be -0.025 (Hochstein and Bromley 2005)).

Once the boiling point depth is established, a surface heat flux (q_{ZB}) can be calculated using an empirical power-law relationship:

$$q_{ZB} = a\left[\frac{Z_{BP}}{Z_0}\right]^{-b}$$

Seward et al. (2018a) determined the values of *a* and *b* to be 147.87 and 0.84, respectively. These values were determined using 85 q_{tot} (from calorimeter measurements) and Z_{BP} (from temperature-depth profiles) values collected at both the Wairakei and Tauhara Geothermal Fields and are assumed to be similar and applicable to the Rotorua near surface geology.

4.0 RESULTS

4.1 Heat Flow from Springs

Heat flow from springs were calculated using the methods outlined for analysis of springs in Section 3.1. Water sample results are presented in Appendix 2. In general, higher chloride (Cl) concentrations point to a higher fraction of deep geothermal water source, while higher sulphate (SO_4) concentrations, suggest higher dilution by shallow steam heated waters. Figures 4.1 and 4.2 show the chloride and sulphate concentrations of the water samples collected at selected springs. Several historically sampled springs could not be accessed due to safety reasons, and therefore were not sampled during this survey. The water level of many features was low at the time of survey, resulting in no surface outflow at many spring sites. Table A 2.1 lists the results for the springs surveyed.

Table 4.1 summarises the heat loss and chloride / sulphate characteristics of the respective surveyed areas.

Table 4.1 Determined heat loss and average Cl/SO_4 due to surface discharge.

Area	Discharging heat flow (kW)	Average chloride concentration (mgL^{-1})	Average sulphate concentration (mgL^{-1})	Average Cl/SO_4 mass ratio
Total	**33.1**			
Kuirau Park	20.3	337	98	4.3
Sulphur Bay/ Government Gardens	0.1	969	175	8.7
Whakarewarewa	12.7	530	181	4.8
Arikikapakapa	*No flow*			

The features surveyed at Kuirau Park have similar sulphate and chloride concentrations, with chloride ranging from 281 to 396 mgL^{-1}, and sulphate ranging from 44 to 227 mgL^{-1}. While the features surveyed in Sulphur Bay and Whakarewarewa show variation within the area (Figures 4.1 and 4.2). There is a distinct difference in chemistry between those features surveyed in Government Gardens (RRF3175, RRF3178 and RRF3177) and those surveyed along the banks of the Puarenga Stream near Ngapuna (RRF3167 and RRF3168). The Government Garden features have chloride concentrations ranging from 542 to 658 mgL^{-1}, while those near Ngapuna show more than double the chloride content (1242 mgL^{-1} and 1851 mgL^{-1}). This is consistent with the view of Mroczek et al. (2011) that the Ngapuna springs are feed primarily from the deep geothermal water. High chloride content is also seen at RRF0952 (THC Blowout), in Whakarewarewa, which has a chloride content of 1036 mgL^{-1} and very little sulphate content (62 mgL^{-1}). The remainder of the springs surveyed in the Whakarewarewa area show a relatively similar chloride content, ranging between 450 and 627 mgL^{-1}. Figure 4.2 shows a clear distinction between sulphate content of springs along the Puarenga Stream (<230 mgL^{-1}) and features further away (>230 mgL^{-1}). This suggests that there is less shallow mixing of the spring water near the stream.

Comparison with previous compositional data shows that Cl and SO_4 concentrations are very similar to other surveys undertaken over the last decade. The exception to this is at Malfroy's Geyser (RRF3177), where chloride has increased since 2008 from 497 mgL^{-1} to 658 mgL^{-1} (Mroczek et al. 2011) with little change in sulphate composition.

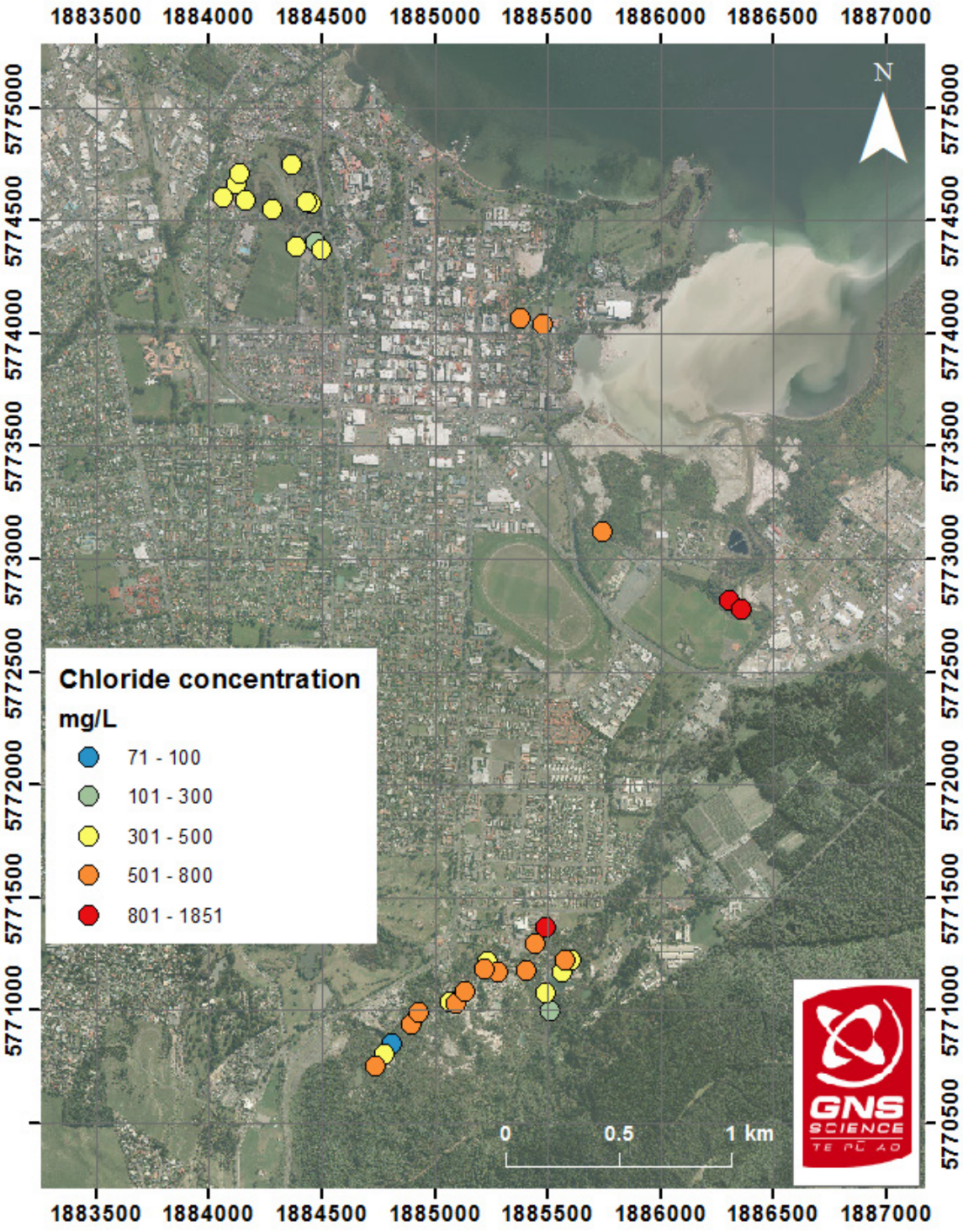

Figure 4.1 Chloride concentration of Rotorua spring water. Red colours represent greatest chloride content. Aerial photography sourced from BOPLASS (2011)

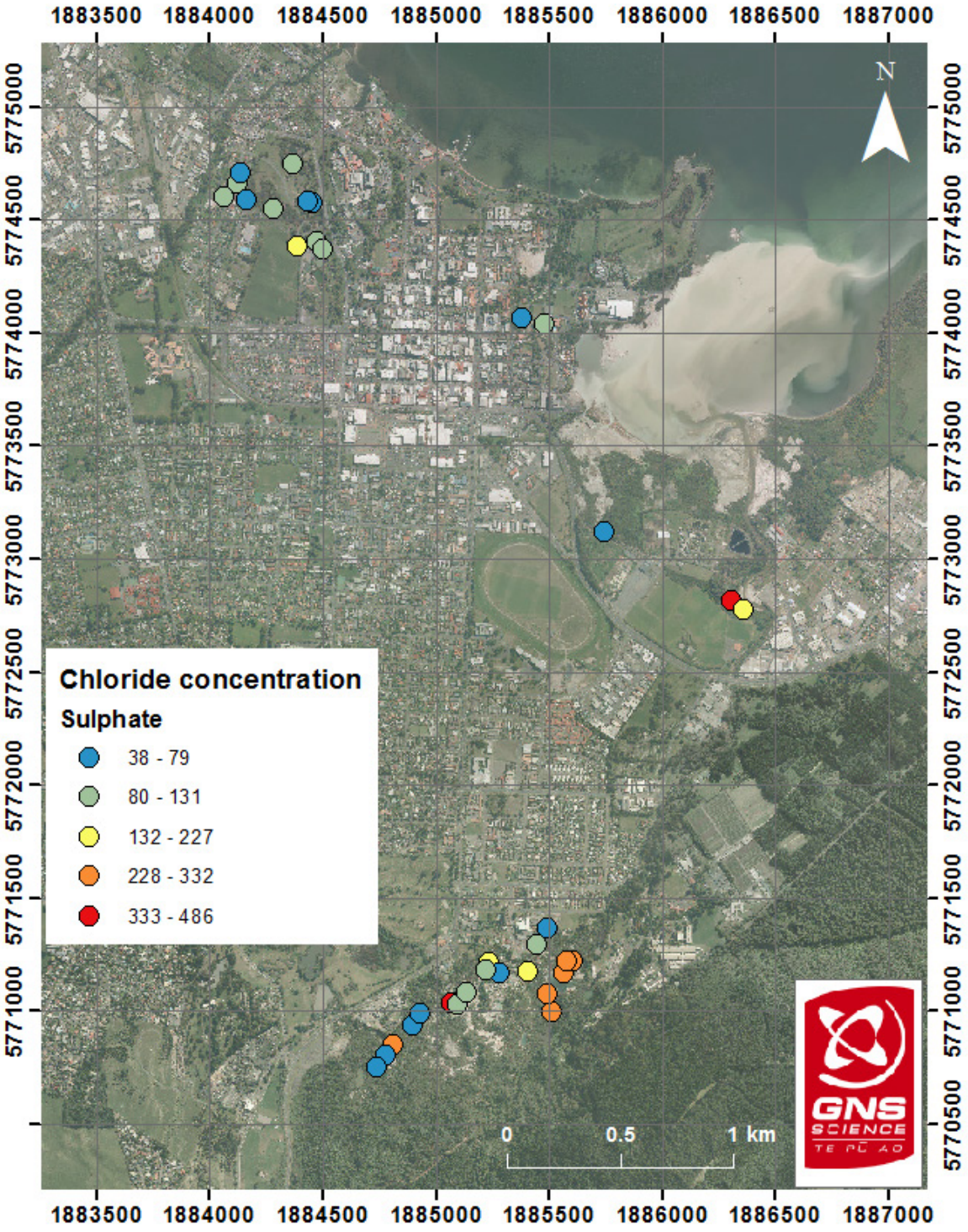

Figure 4.2 Sulphate concentration of Rotorua spring water. Red colours represent greatest sulphate content. Aerial photography sourced from BOPLASS (2011)

4.2 Heat Flow from Pools

Appendix 3 summarises the collected data and calculated heat loss using the Dawson (1964) and the Adam et al. (1990) methods. Figure 4.3 shows the heat flux calculated for each water feature using Adams equations. Table 4.2 lists the heat loss from pool surfaces at Whakarewarewa, Arikikapakapa, Sulphur Bay (and Government Gardens) and Kuirau Park. It is important to note that the method of Adam et al. (1990) only accounts for the evaporative component of the heat loss. The evaporative component is generally an order of magnitude greater that the other components. For completeness, the conductive and radiated heat loss is added to the evaporative heat loss determined using Adam et al. (1990) to give a total heat loss from pools (Table 4.2).

Table 4.2 Summary of total heat loss (MW) from pool surfaces in each of the survey areas.

Area	Total heat loss determined using Dawson (1964)	Total heat loss determined using Adam et al. (1990)
Whakarewarewa	97.7	55.3
Arikikapakapa	71.5	32.3
Sulphur Bay	6.2	4.0
Kuirau Park	72.6	41.6
Total	248.0 MW	133.2 MW

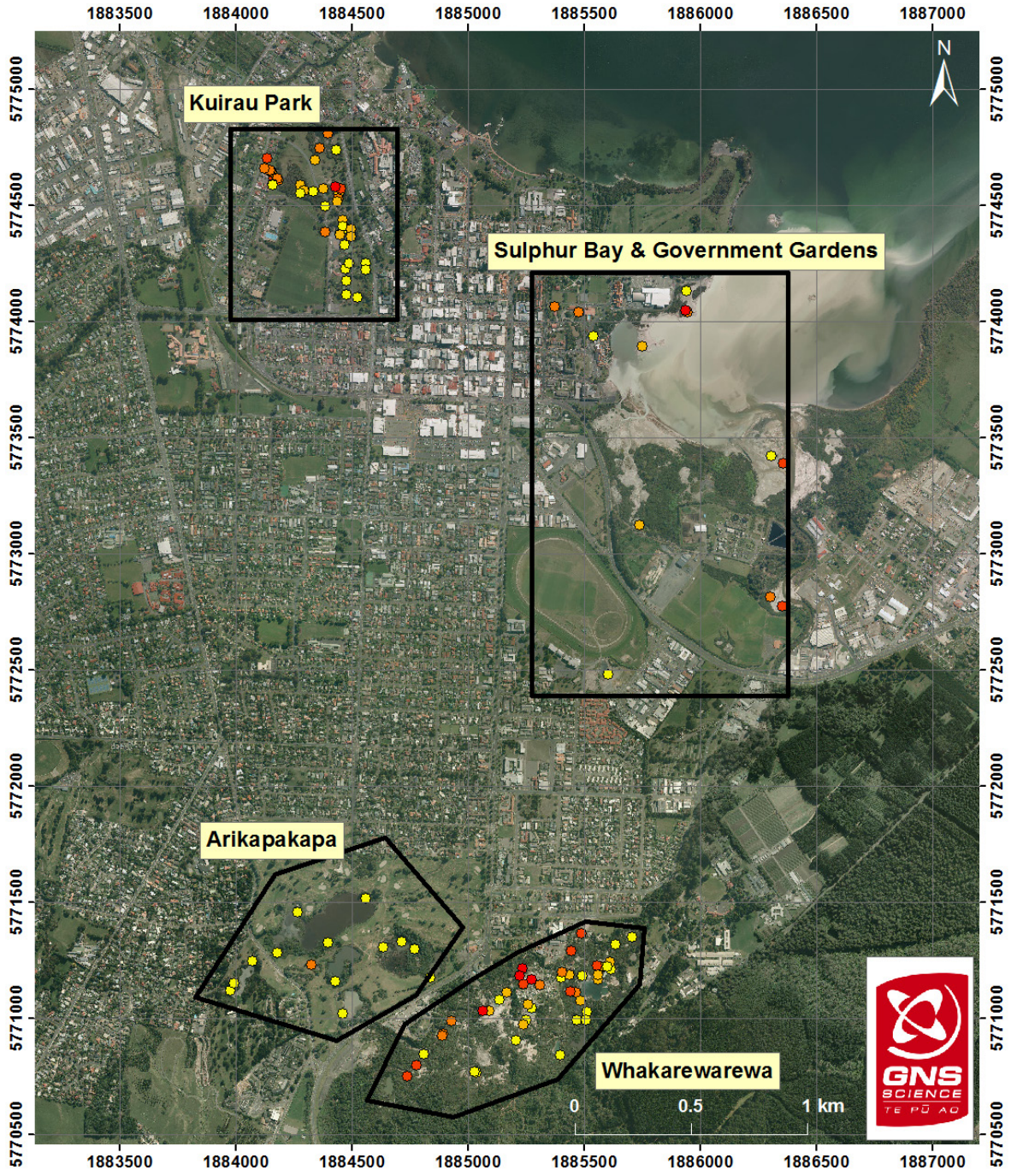

Figure 4.3 Calculated heat flux for each surveyed pool. Aerial photography sourced from BOPLASS (2011)

4.2.1 Uncertainties

Figure 4.4 shows the effect of the variation in windspeed on the evaporative heat flux from a pool surface, using the methods of Dawson (1964) and Adam et al. (1990) to calculate heat loss. It is our opinion that the behaviour of evaporative heat flux with respect to windspeed is best accounted for using the equations derived by Adam et al. (1990). Figure 4.4 suggests that the method of Dawson underestimates surface heat flux at low wind speed, especially for hotter pools, and over estimates the heat loss at higher wind speed.

Errors in estimating the area of a pool from ground-based observations can be large. For the analysis presented in this report, aerial images were used to assess the surface area of pools. High resolution aerial images of Whakarewarewa were obtained on April 4, 2018 (Macdonald et al. 2018). For areas outside of Whakarewarewa, aerial images collected in 2015 and 2016 available from Land Information New Zealand (LINZ) (2018) were used. Care was taken to assess the surface area using these images, however there is some ambiguity for some pools due to shadows in the images. In these situations, personal knowledge and images collected from the ground survey were used to interpret the pool area. Since there is natural variability in the water-level of pools over time especially between seasons, we assume that the surface areas presented in this survey are accurate to within 10%.

Additional uncertainty in the heat loss estimates occur by assuming a constant surface temperature over the whole area in pools or lakes of large surface areas. The temperature measured at one location is unlikely to be representative of the whole lake surface, especially in lakes such as Roto-A-Tamaheke, and Kuirau Lake. TIR images show zones of hotter and cooler temperatures with apparent surface temperature variations of up to 5°C.

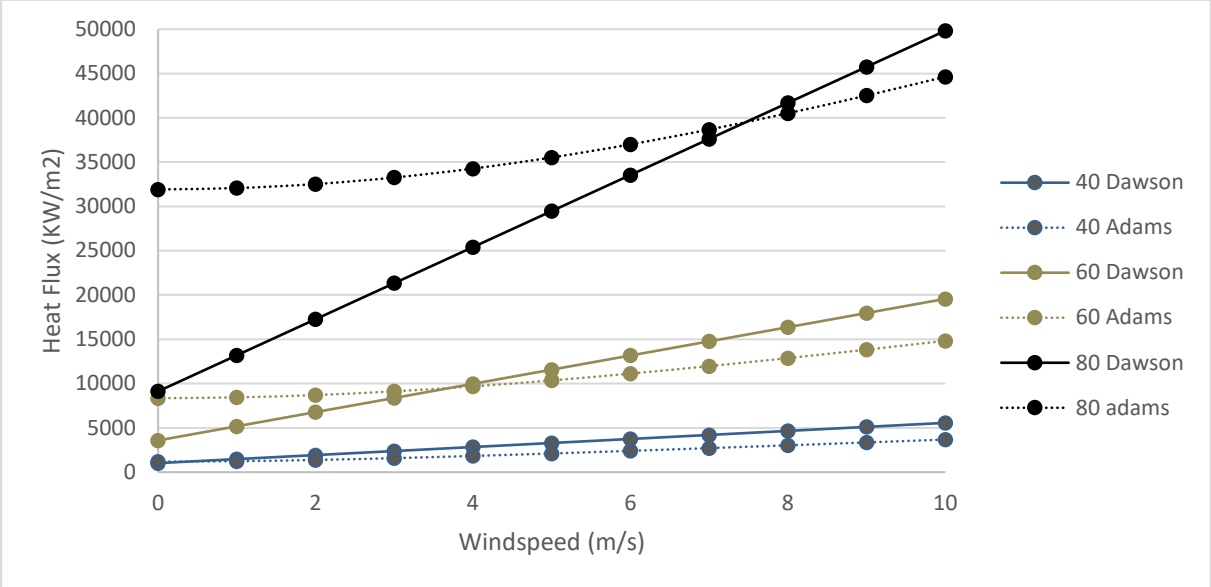

Figure 4.4 The effect of windspeed on the calculated evaporative heat flux at different pool temperatures (40°C, 60°C and 80°C) using the equations of Dawson (1964) and Adam et al. (1990). These are based on a reference ambient air temperature of 20°C, and a surface area of 5000 m^2.

4.3 Heat Flow from Streams

4.3.1 Puarenga Stream – Whakarewarewa

The Puarenga Stream was gauged at five locations (Figure 2.3) on March 20, 2018 with the first location (Hemo Gorge) being surveyed at 10:50 am. The RLC pumps were turned off from 6:33 am to 10:15 (NZST) allowing 3hr 45 min of full-volume water travel downstream (Note: the Waipa Saw Mill was extracting 1225 m^3/day on this date; Ede (2018)). Water samples were collected at each gauging site. Table 4.3 shows the gauging and water composition (Appendix 4).

The negative flow differences indicated in Table 4.3 suggests water is lost from the stream between Tatua Falls and Geyser Flat, and between Memorial bridge and FRI (Scion). After discussion with Janine Barber (BOPRC), it was decided to re-gauge the Puarenga Stream to check these results, as a previous survey in 2013 had not seen a decrease in water volume. At this time the amount of water being extracted by the Waipa Mill was unknown. The repeat gauging was undertaken on April 19, 2018, at four of the original sites (excluding Tatua Falls). Again, the RLC pumps were turned off for the gauging, however the Waipa Mill pumps were still running. Table 4.4 shows the gauging and water chemistry results for the April survey. Volume of water extracted by the Saw Mill on April 19, 2018 totalled 967 m^3/day (Ede 2018), however, the time and volume of the water extraction are unknown, and therefore the effect of the water extraction on the gauging measurements is unknown.

A small increase in flow was detected between Hemo Gorge and FRI (Scion) in the April survey, however it is within the uncertainty of the measurements, and likely negligible. An increase in chloride and sulphate concentrations were observed downstream in both surveys. It is our view that the small negative flows measured are more likely a combination of variations in the upstream abstraction and stream gauging errors rather than a loss of water to groundwater. However, this mechanism is a common source of recharge to groundwater in many streams and cannot be discounted.

Table 4.5 lists the calculated chloride-, sulphate- and heat- flux at each gauging site.

The increase in chloride flux as the stream flows down the valley (comparisons between Hemo Gorge and FRI (Scion)) was calculated to be 60.75 g/s and 63.24 g/s for the March 20 and April 19 surveys respectively. Sulphate fluxes increase by 48.5 g/s and 51.4 g/s between Hemo Gorge and FRI (Scion) for the March and April surveys. An increase in surface heat flow of 37.1 MW and 30.0 MW were calculated from measured water temperature increases for each survey. The thermal output determined using the chloride flux results in a comparative increase between Hemo gorge and FRI (Scion) of 35.2 MW and 36.7 MW.

Table 4.3 Gauging and chemistry results from Puarenga Stream surveyed on 20 March 2018.

Site	Time (NZST)	Flow (L/s)	STD (L/s)	Flow difference (L/s)	Water temperature (°C)	Chloride (mg/L)	Sulphate (mg/L)
Hemo Gorge	10:50	1884	49		13.1	9.7	8.9
Tatua Falls	12:06	1888	62	6	13.5	10.0	9.4
Geyser Flat	13:19	1790	67	-98	15.6	13.7	11.7
Memorial bridge	14:40	1954	67	164	17.5	28.0	18.9
FRI (Scion)	15:24	1796	27	-158	18.7	44.0	27.0

Table 4.4 Gauging and chemistry results from Puarenga Stream surveyed on 19 April 2018.

Site	Time (NZST)	Flow (L/s)	STD (L/s)	Flow difference (L/s)	Water temperature (°C)	Chloride (mg/L)	Sulphate (mg/L)
Hemo Gorge	11:19	1890			12.0	7.8	6.4
Geyser Flat	13:09	1917		27	12.6	13.8	11.6
Memorial bridge	14:20	2030		113	14.4	28.0	19.3
FRI (Scion)	15:24	1902		-128	15.7	41.0	27.0

Table 4.5 Chloride-, Sulphate-fluxes, molar ratio, Thermal output (calculated from chloride flux) and calculated heat flow (from water temperature) of the Puarenga Stream surveyed in March and April 2018.

	20 March 2018					19 April 2018				
Site	Cl flux (g/s)	SO_4 flux (g/s)	Cl/SO_4 (Molar ratio)	Cl thermal output (MW)	Heat flow (MW)	Cl flux (g/s)	SO_4 flux (g/s)	Cl/SO_4 (Molar ratio)	Cl thermal output (MW)	Heat flow (MW)
Hemo Gorge	18.3	16.8	2.95	10.6	103.6	14.7	12.1	3.30	8.5	95.2
Tatua Falls	18.9	17.8	2.88	11.0	107.0					
Geyser Flat	24.5	20.9	3.17	14.2	117.1	26.5	22.2	3.22	15.3	101.4
Whaka village	54.7	36.9	4.01	31.7	143.3	56.8	39.2	3.92	33.0	122.6
FRI (Scion)	79.0	48.5	4.41	45.8	140.7	78.0	51.4	4.11	45.2	125.2

4.3.2 Tawera Stream – Kuirau Park Outflow

Measurements made at deployment and collection of the logger recorded water temperatures of 43.5°C and 45.6°C respectively.

Figure 4.5 shows the recorded air and water temperatures, and stream flow (Perks 2018). In general, large drops in water temperature correlate to increases in stream flow. This is interpreted to be caused by rainfall events. Rainfall data would be required to confirm this.

Table 4.6 lists the flow, temperature and the calculated chloride, sulphate fluxes, heat flow and mass flow for the Tawera Kuirau Park outflow at the time the water sample was taken, 10:50 am, 27-4-2018.

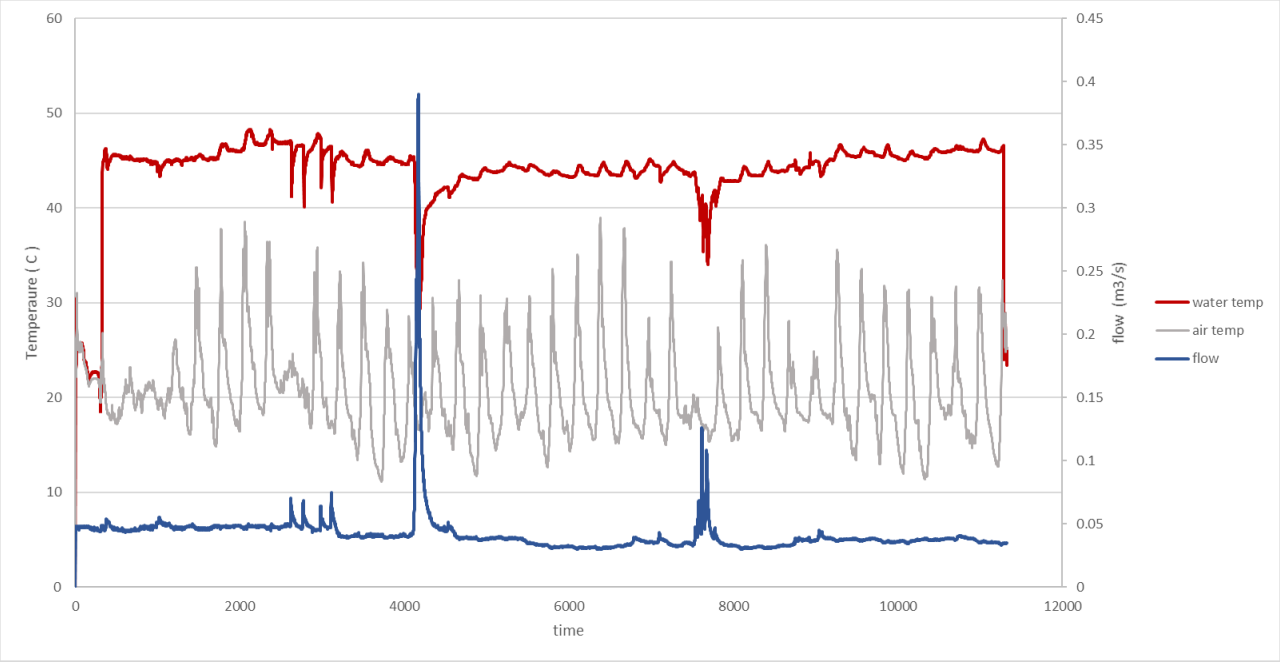

Figure 4.5 Water temperature, air temperature measured with the temperature logger compared with the flow data recorded by EK406461.

Table 4.6 Average measurements for the Tawera stream outflow of Kuirau Park.

Site	Flow (m^3/s)	Water temperature (°C)	Cl	SO_4	Cl flux (g/s)	SO_4 flux (g/s)	Cl/SO_4	Heat flow (KW)	Cl thermal output (KW)
Tawera	0.044	43.5	304	108	0.013	0.0045	2.81	8.2	24.2

4.4 Heat Flow from Heated Ground

Ground temperature and soil temperature profiles of measurements sites are shown in Appendix 5. Data and heat fluxes for each site are listed in Appendix A5.1. An ambient ground site located away from any geothermal influence was measured daily to ensure that the ground conditions remained consistent over the survey period (Appendix A5.2).

4.4.1 Calorimetry

Heat flux was measured at seven calorimeter sites around Rotorua (Appendix A5.3). Four of the sites were located in or around Whakarewarewa, while the other three sites were located in Kuirau Park and Sulphur Bay (Figure 4.6). Unfortunately, the data recorded at one site located at Whakarewarewa (W6) was corrupted and could not be recovered.

Table 4.7 summarises the calorimeter results.

The surface heat flux measured at the six calorimeter sites was used to determine a non-linear empirical relationship between total heat loss (Q_{tot}) and boiling point depth (Z_{BP}), but as there were only six data points to determine such a relationship, uncertainty is significant. The empirical relationship determined by Seward et al. (2018a), for 85 data points collected at the Wairakei and Tauhara Geothermal Fields was tested to see if the collected Rotorua data would fit the same equation. Figure 4.7 shows the measured Rotorua data points (red) compared to the Wairakei and Tauhara data points.

The relationship between Q_{tot} and Z_{BP} given below, was used to estimate a convective heat flux at other sites with calculated Z_{BP} values, where calorimetry was not measured.

$$Q_{ZB} = 147.87 \left[\frac{Z_{BP}}{Z_0}\right]^{-0.84}$$

Table 4.7 Measured heat fluxes (Wm^{-2}) and inferred boiling point depth (m).

Site	Q_{tot}	Q_{adv}	Z_{BP}	Q_{ZBconv}	Q_{Dawson}
R1	0	0	1.5	104.6	11.5
R2	410.5	114.3	0.5	260.7	60.1
R4	251.9	143.5	1.2	126.9	44.2
W1	739.5	241.5	0.51	260.3	196.5
W7	630.4	189.7	0.14	771.1	501.5
W8	55.5	15.7	0.72	194.9	29.3
99	751.8	331.3	0.16	689.3	479.6

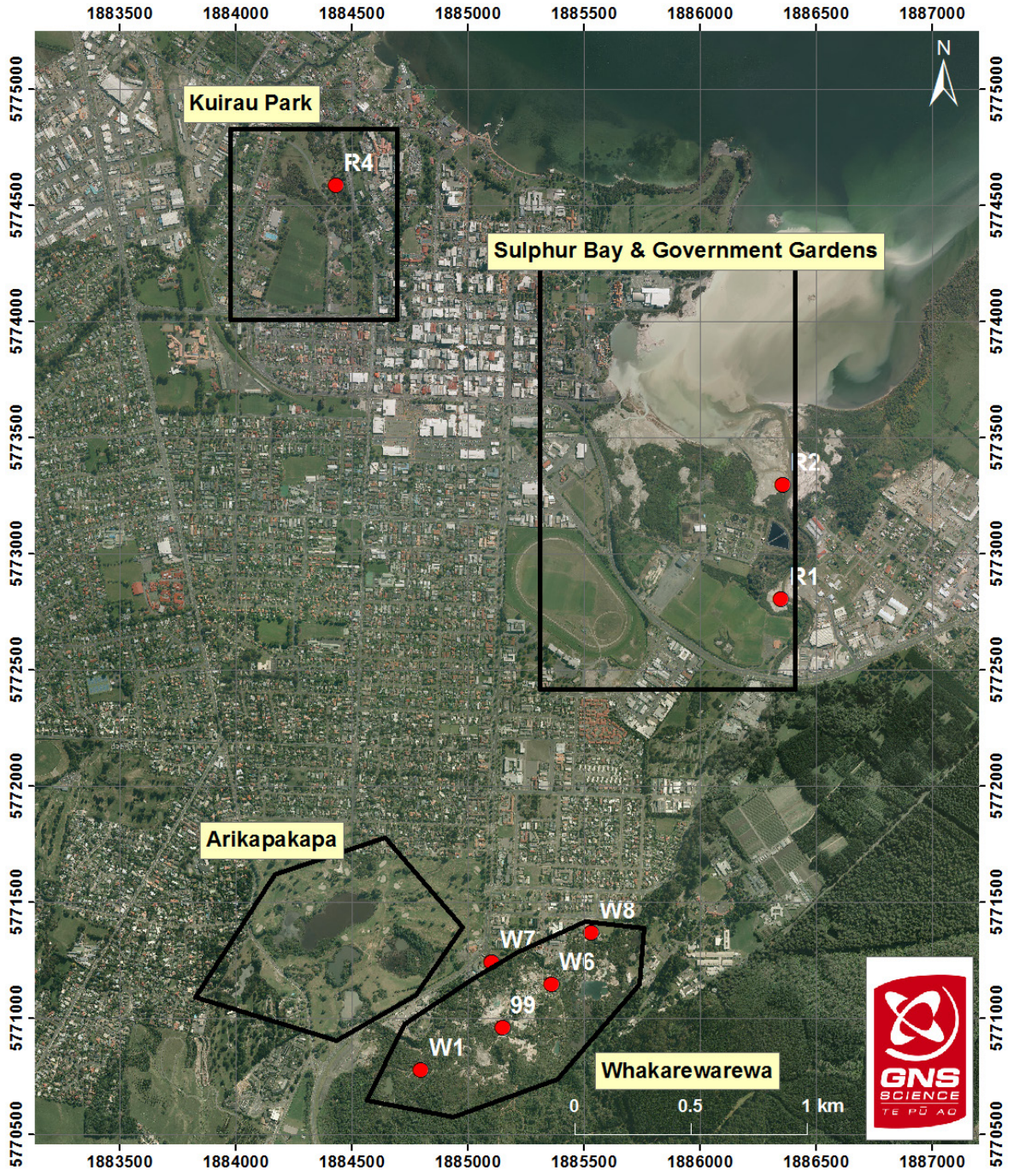

Figure 4.6 Locations of the Calorimeter sites of the 2018 heat flow survey. Aerial photography sourced from BOPLASS (2011)

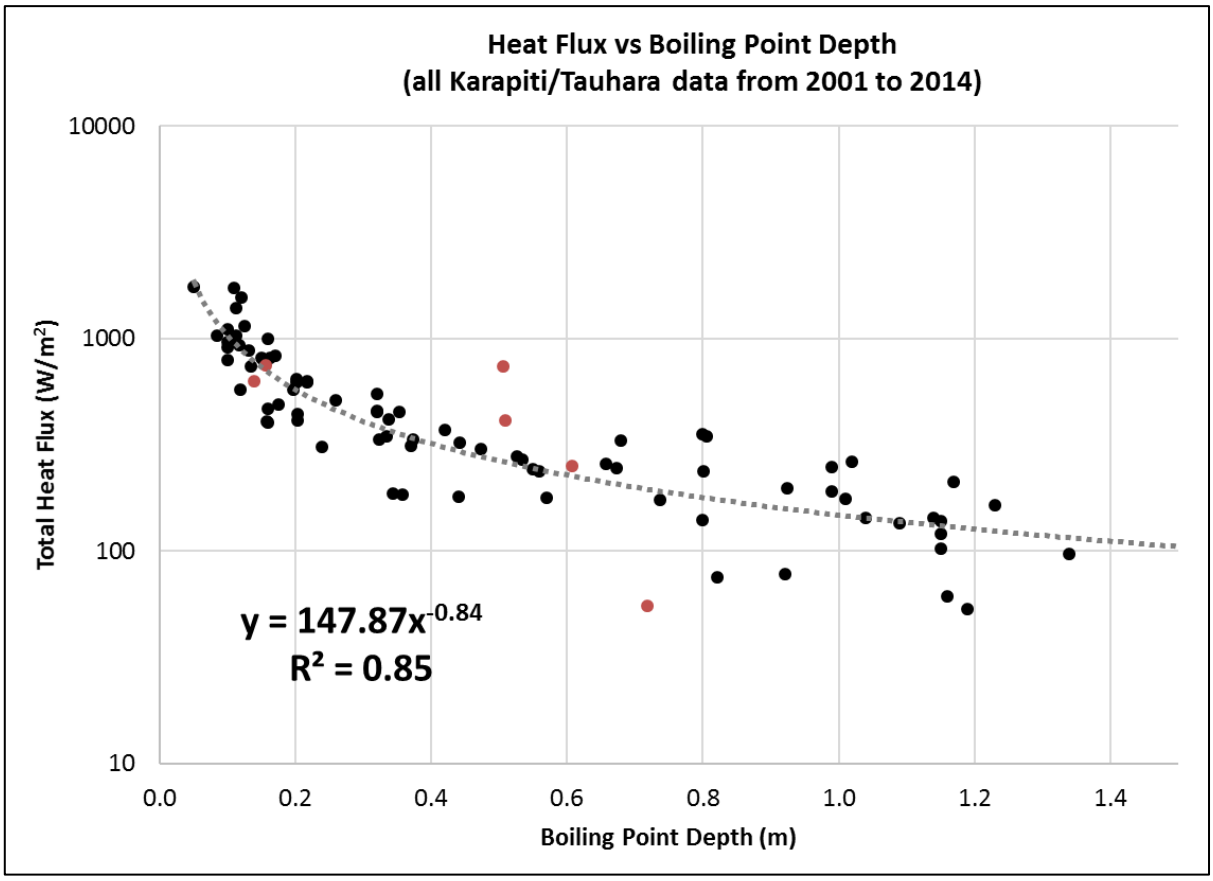

Figure 4.7 Total heat flux verses boiling point depth for the Wairakei – Tauhara sites (black circles) and from the six sites from this survey (red circles).

4.4.2 Soil Temperature Profiles

Ground temperatures were measured at 5, 10, 15, 20, 25, 50 and 100 cm depths at 138 sites across Whakarewarewa, Arikikapakapa, Kuirau Park and Sulphur Bay. Heat flux at the sites were calculated using both the relationship between the 15 cm ground temperature and heat flux determined by Dawson (1964), and the relationship between boiling point depth (Z_{BP}) total heat flux, as discussed in Section 3.4.4.

Historically, total heat loss from Whakarewarewa (e.g., Simpson 1985) has been estimated by contouring the measured heat fluxes, and summing the areas within each contour. The previous surveys contained over 1000 ground temperatures at 15 cm. However, that method was not appropriate for the recent dataset of 138 sites, as areas between measurement points had different ground cover and thermal properties. Instead, thermal areas detected by the 2014 TIR images (Reeves et al. 2014) were used to estimate the total area of ground with similar heat fluxes. Surface temperatures were banded into 2° intervals from 20 to 50°C. Apparent surface temperatures below 20°C are considered ambient conditions, with no geothermal signature. Inferred surface temperatures from the TIR were compared to measured ground temperatures at 5 cm, to determine a relationship that could be used to determine a heat flux for the measured data (Figure 4.8).

Appendix A5.4 lists the calculated heat loss for banded surface temperatures. Table 4.8 lists the total heat loss through the ground for the surveyed regions.

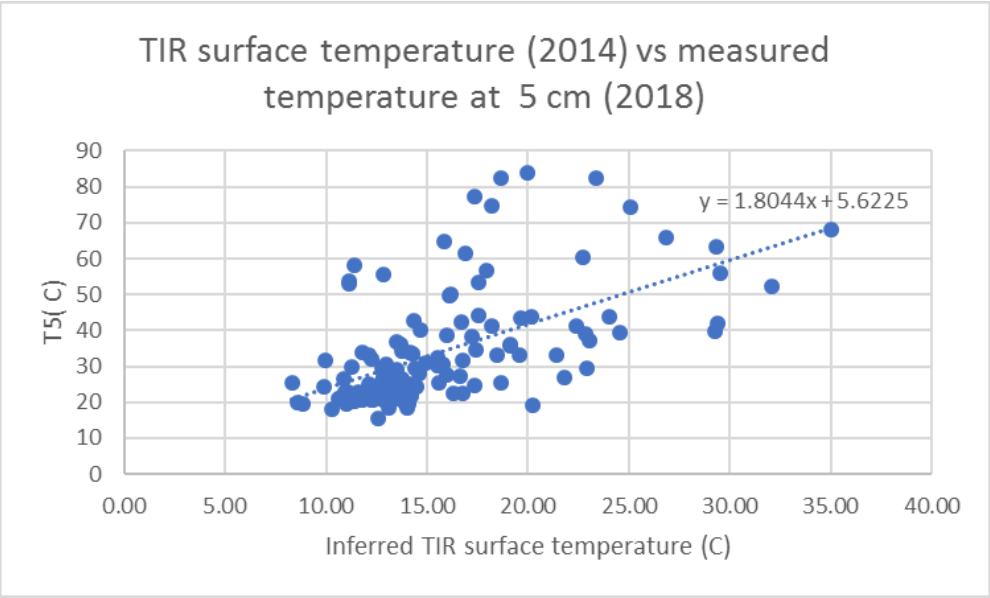

Figure 4.8 Comparisons between temperatures measured at 5 cm, and the inferred temperature of the related pixel on the 2014 TIR.

Table 4.8 Total heat loss through the ground.

Area	Total heat loss (MW)
Whakarewarewa	9.81
Arikikapakapa	0.48
Sulphur Bay and Government Gardens	6.62
Kuirau Park	0.77

4.4.3 Uncertainties

Processing of surface heat flux data from areas of steam-heated ground, using established methods, has approximately 15% uncertainty in heat flux values (Figure 4.7). The uncertainty associated with using 15 cm temperatures is unknown, but is considered to be greater than those associated with ground temperatures at greater depth. At 15 cm depth, solar heating still influences ground temperature, particularly in ground of lower temperatures (e.g., van Manen and Wallin 2012). Comparisons (Figure 4.9), however, show that the results are in relatively good agreement, although the method of Dawson over estimates heat flux in hotter areas and under-estimates them in cooler sites.

Further uncertainty is incurred using individual site-based heat flux measurements to calculate the surface heat loss for an area. The total number of pixels in the TIR for 2°C temperature bands between 20 and 50°C is calculated using GIS software. These areas are used to total the heat flux for each temperature band. An approximate linear relationship between the near-surface (5 cm depth) temperatures and the resulting Q_{tot} (Figure 4.10), is determined. This relationship is used to estimate the heat flux at non-measured points from the TIR imagery.

Combining the uncertainty related to each relationship used to determine the total surface heat flux through the soil the uncertainty in total heat loss is estimated to be ~35%.

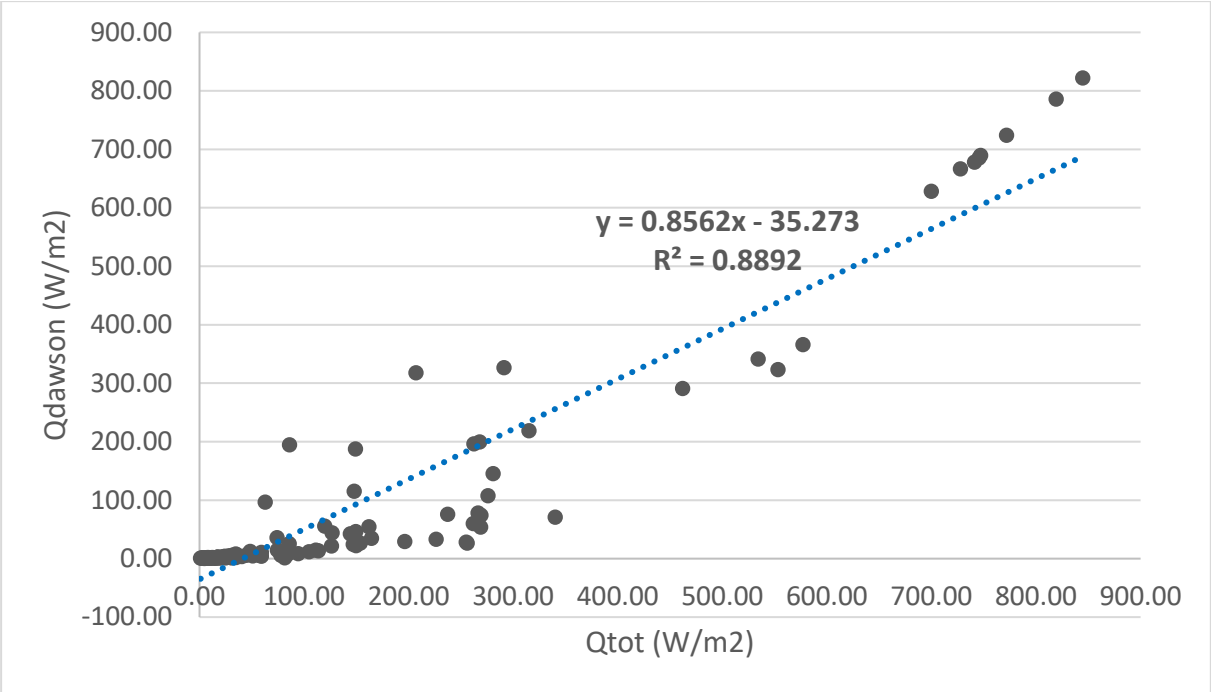

Figure 4.9 Comparison between ground heat flux calculated using the measured 15 cm ground temperature (Qdawson), and the heat flux determined using conductive and convective heat flux calculated by the methods of Seward et al. (2018a), showing a linear best fit correlation.

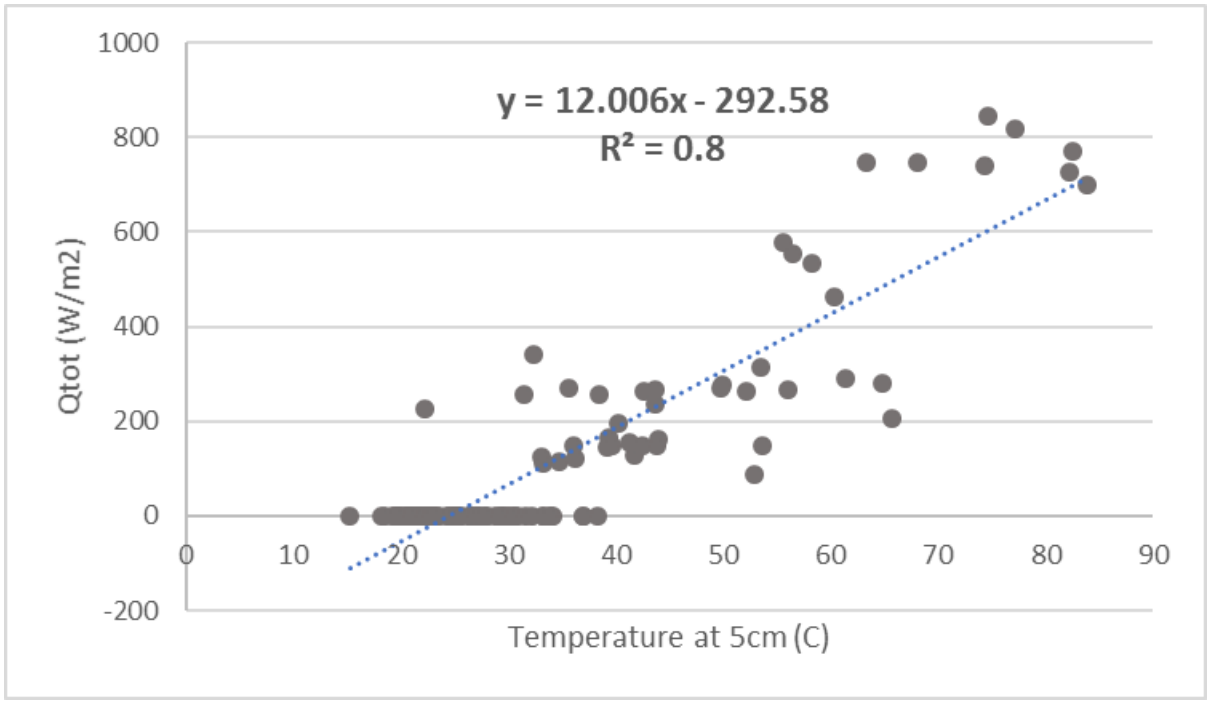

Figure 4.10 Inferred relationship between Q_{tot} and the 5 cm deep ground temperature for collected Rotorua soil data.

5.0 SUMMARY AND DISCUSSION

5.1 Results Summary

The total heat loss for each area in the RGF are summarised in Table 5.1. The heat loss from discharging spring and pool overflow was smaller than the heat loss from pool surfaces and from steam-heated ground. The heat loss through discharging springs at Sulphur bay is unaccounted for, as access to much of the area is unsafe with unstable ground.

Arikikapakapa has no measurable spring discharges, with most heat loss derived from geothermal activity associated with large pools and mud features. This is similar to observations at Kuirau Park, where approximately 99% of the measured heat loss results from evaporative and radiated heat loss from pool surfaces.

Whakarewarewa contains the largest number of surveyed features, and has significant geothermal water discharging into the Puarenga Stream. The Puarenga Stream has an average flow rate of water between 1860 and 1940 Ls^{-1} as it flows between Hemo Gorge and FRI (Scion) sites based on the two gaugings done as part of this survey. A water temperature increase of between 5.6°C and 3.7 is measured between gauging site Hemo Gorge and FRI (Scion) on 20 March 2018 and 19 April 2018, respectively. The flow rates and water temperature changes are consistent with previous surveys of the Puarenga Stream (Bradford and Glover (1984), Glover (1988, 1992)). Calculated heat loss from Whakarewarewa into the Puarenga Stream of between 30 and 37 MW is similar to the values determined by Glover (1988, 1992). The small discrepancy in heat loss between these surveys are within the error range of the measurements. The chloride and sulphate mass fluxes (Table 4.5) show that there is a significant increase in geothermal water downstream of the geothermal area confirming that a large proportion of the measured temperature increase in the Puarenga Stream is due to the input from heated geothermal water.

Table 5.1 Summary of results. Heat flows are given MW. An average Cl heat flow from the two Puarenga Stream gauging is given.

Area	Evaporation and radiation (pools)		Discharge (Spring Cl)	Ground heat flow	Total	
	Dawson	Adam			Dawson	Adam
Whakarewarewa	97.7	55.3	36.0	9.81	141	98.6
Sulphur Bay	6.2	4.0	Not accounted for	6.62	12.8	10.6
Arikikapakapa	71.5	32.3	-	0.48	72	32.8
Kuirau Park	72.6	41.6	0.024	0.77	73.4	42.4
Summed	**248**	**133.2**	**36.0**	**17.7**	**299.2**	**184.4**

5.2 Comparisons to Historical Heat Loss Surveys

Historic heat loss estimations have predominately been made in the Whakarewarewa area and are discussed in Section 2.1. This section will compare the heat loss estimates from this survey to those in 1969 and 1984 (Cody and Simpson 1985). The 2011 (Scott et al. 2016) survey has been excluded from the comparison because of the limited extent and lack of detail in reported measurement of this survey.

In order to compare this survey to the 2 previous surveys, several changes to how heat loss has been calculated must be noted:

1. The evaporative component of heat loss for the 2018 data has been **recalculated** using a wind speed of 1 ms^{-1} and an ambient air temperature of 12°C to be consistent with the 1969 and 1984 surveys. This limits the accuracy of the 2018 calculations, but ensures similar assumptions are made as site-specific wind speed and air temperature data are not available for the 1969 and 1984 surveys.
2. Different methods of determining the extent of steam-heated ground heat loss have been used. The historic datasets were estimated from 1000+ 15 cm temperature points and areas estimated by contouring the data, while the ground heat loss in 2018 was calculated using areas derived from the 2014 TIR thermal signatures.

Forty-five pools in Whakarewarewa were surveyed during this survey. It is estimated that the 45 features contribute to the majority of the heat output in the valley, due to their surface area, water temperature and / or flowrate and thermal anomaly on 2014 TIR images (Reeves et al. 2014). Of the 45 features surveyed in 2018, 38 were also surveyed in 1969, and 1984.

We have split the heat loss comparison into 2 parts:

a) heat loss of Whakarewarewa using features that are in common with each survey (Table 5.2), and

b) heat loss from Whakarewarewa calculated from all data available for each survey (Table 5.3).

When the results from the 1969, 1984 and 2018 surveys are compared for the 45 features common to all surveys (Table 5.2), a clear reduction in heat loss is evident between 1969 and 1984. This is likely a result of the increased uptake in use of geothermal heat from the shallow aquifer (Cody and Simpson 1985; Scott et al. 2016) during this period. The data collected in the 2018 survey indicate an increase in total heat loss from geothermal surface features since 1984, although not to the same levels of heat output recorded in 1969.

By excluding features not common between the surveys, there appears to be reduced recovery of heat output between 1984 and 2018. Part of the explanation is likely due to the exclusion of the heat output from RRF0952 (THC blow-out feature). This feature accounts for about 4 MW of surface heat output and was formed in 1987 as a result of a bore blowout. The high temperature and chloride concentration of this feature points to it being fed via deep fluids. Consequently, this discharge may be affecting the amount of deep geothermal fluid and heat that is reaching the surface and discharging from surrounding features. Table 5.3 compares the heat output in Whakarewarewa from evaporative and radiative components (pools), discharge to the Puarenga Stream and through ground surface heat flux.

An increase of approximately 22 MW is evident between 1984 and 2018. The heat loss measured in 2018 is equivalent to about 80% of the total heat loss measured in 1969. Faster recovery in mass discharge than pool temperatures is consistent with expectation from modelling studies (e.g., O'Sullivan and Mannington 2005). Following pressure recovery, recovery of surface mass discharge typically occurs long before full recovery of surface temperature.

Table 5.2 Comparison between heat loss calculated using Dawson (1964) for 38 features common between the surveys at Whakarewarewa. Constant wind and ambient air temperatures are assumed.

Survey	1969	1984	2018
Total reported Heat loss (MW)	108	76	97.7
Heat loss (MW) (Common features)	95.5	58.7	62.9

Table 5.3 Comparison of heat loss results from Whakarewarewa over time. Evaporation and radiation values correspond to historical results published by Cody and Simpson (1985) and totalled from the same water features surveyed in the 2018 survey. Discharged heat loss is calculated from water temperatures relative to 12°C.

Survey	1969	1984	2018
Evaporation and radiation	95.5	58.7	62.9
Discharge	27	17	33.5
Ground surface heat flux	10.3	7.9	9.8
Total	132.8	83.6	106.2

6.0 CONCLUSIONS

Surface heat losses are calculated for the Whakarewarewa, Arikikapakapa, Sulphur Bay, Government Gardens and Kuirau Park areas in the Rotorua Geothermal Field (Ngapuna and Ohinemutu were not included in this study). A total surface heat loss of 184 MW is calculated using the evaporative heat flux method of Adam et al. (1990) and 299 MW using the method of Dawson (1964). Note neither of these assessments account for heat loss through geysers, or mud pools and there are some features that could not be accessed due to safety concerns.

Comparing current results from historic assessments of heat loss in Whakarewarewa suggest an overall increase in heat output of ~22 MW since the 1985 survey. The 2018 data show that the current heat loss from Whakarewarewa is approximately 80% of the heat loss measured in 1969 (when compared using the same methods).

6.1 Recommendations

1. We recommend that future heat loss assessments of Rotorua include the heat loss from the Ohinemutu and Ngapuna areas.
2. We suggest that any future analysis of evaporative heat output from Rotorua be assessed using the methods of Adam et al. (1990).
3. A repeat heat loss survey should be conducted in 10 years' time (or earlier if large changes in geothermal use occur in Rotorua).

7.0 REFERENCES

Adam EE, Cosler DJ, Helfrich KR. 1990. Evaporation from heated water bodies: predicting combined forced plus free convection. *Water Resources Research.* 26(3):425-435.

Bradford E, Glover RB. 1984. Heat and chloride inflow into the Puarenga Stream for Whakarewarewa. In: *Proceedings of the 6th New Zealand Geothermal Workshop;* 1984 Nove 7-9; Auckland, New Zealand. Auckland (NZ): Geothermal Institute.

Bromley CJ, van Manen SM, Mannington W. 2011. Heat flux from steaming ground: reducing uncertainties. In: *Proceedings, 36th Workshop on Geothermal Reservoir Engineering;* 2011 Jan 31-Feb 2; Stanford, CA. Stanford (CA): Stanford University. p. 925-931.

BOPLASS. 2011. Tauranga (NZ): BOPLASS Ltd. http://www.boplass.govt.nz/

Cody AD, field team. 1984a. Rotorua: Whakarewarewa hydrothermal features survey 1983-1984, features S001-S299. 300 p. Located at GNS Science, Wairakei, NZ. Originator: New Zealand Geological Survey – Rotorua.

Cody AD, field team. 1984b. Rotorua: Whakarewarewa hydrothermal features survey 1983-1984, features S300-S599. 300 p. Located at GNS Science, Wairakei, NZ. Originator: New Zealand Geological Survey – Rotorua.

Cody A, Simpson B. 1985. Natural hydrothermal activity. In: New Zealand Department of Scientific and Industrial Research. *The Rotorua geothermal field: technical report of the Geothermal Monitoring Programme 1982-1985.* Wellington (NZ): Ministry of Energy, Oil and Gas Division. p. 227-273.

Dawson GB. 1964. The nature and assessment of heat flow from hydrothermal areas. *New Zealand Journal of Geology and Geophysics.* 7(1):155-71.

Ede D. 2018. Personal communication. Senior Regulatory Compliance Officer at Bay of Plenty Regional Council, Whakatane, New Zealand.

Fridriksson T, Kristjansson BR, Armannsson H, Margretardottir E, Olafsdottir S, Chiodini G. 2006. CO_2 emissions and heat flow through soils, fumaroles, and steam heated mud pools at the Reykjanes geothermal area, SW Iceland. *Applied Geochemistry*. 21(9):1551-1569. doi:10.1016/j.apgeochem.2006.04.006.

Glover RB. 1988. Chemical and physical changes in the outflow from Whakarewarewa to the Puarengua stream, Rotorua. In: *Proceedings of the 10th New Zealand Geothermal Workshop*; 1988; Auckland, New Zealand. Auckland (NZ): Geothermal Institute. p. 269-273.

Glover RB. 1992. Integrated heat and mass discharges from the Rotorua geothermal system. *Geothermics*. 21(1-2):89-96.

GNS Science. 2017a. Geothermal SOP: Mapping and monitoring natural geothermal surface features. Version 1.1. Wairakei (NZ): GNS Science.

GNS Science. 2017b. Geothermal SOP: Geothermal water sample collection for water chemistry. Version 1.1. Wairakei (NZ): GNS Science.

Gordon DA, O'Shaughnessy BW, Grant-Taylor DG, Cody AD. 2001. Rotorua geothermal field management monitoring. Whakatane (NZ): Environment Bay of Plenty. (Environmental report; 2001/22).

Hochstein MP, Bromley CJ. 2005. Measurement of heat flux from steaming ground. *Geothermics*. 34(2):131-158.

Lloyd EF. 1969a. Rotorua: Whakarewarewa hydrothermal features survey 1967-1969, features S001-S269. 269 p. Located at GNS Science, Wairakei, NZ. Originator: New Zealand Geological Survey – Rotorua.

Lloyd EF. 1969b. Rotorua: Whakarewarewa hydrothermal features survey 1967-1969, features S270-S538. 268 p. Located at GNS Science, Wairakei, NZ. Originator: New Zealand Geological Survey – Rotorua.

[LINZ] Land Information New Zealand. 2018. Bay of Plenty 0.125m Urban Aerial Photos (2015-16). Wellington (NZ): LINZ. https://data.linz.govt.nz/layer/88129-bay-of-plenty-0125m-urban-aerial-photos-2015-16/data/489/?mv=1

Macdonald N, Reeves R, Brakenrig T, Graham D. Forthcoming 2018. Water level mapping of Whakarewarewa geothermal valley using an unmanned aerial vehicle (UAV). Lower Hutt (NZ): GNS Science. (GNS Science report).

Miotti L, Mroczek E, Hurst T. 2010. Review of heat flow surveys at Whakarewarewa. Lower Hutt (NZ): GNS Science. 28 p. (GNS Science report; 2010/41).

Mroczek E, Scott B, Graham D. 2011. Chemistry of the Rotorua Geothermal Field – update of spring and well compositions 2008-2009. 91 p. Located at: GNS Science, Wairakei, NZ; GNS Science internal report 2011/02.

O'Sullivan MJ, Mannington W. 2005. Renewability of the Wairakei-Tauhara geothermal resource. In: *Proceedings of the World Geothermal Congress 2005*; 2005 Apr 24-29; Antalya, Turkey. Reykjavik (IS): International Geothermal Association.

Pearson-Grant SC, Scott BJ, Mroczek EK, Graham DJ. 2015. Rotorua surface feature monitoring data review: 2008-2014. Wairakei (NZ): GNS Science. 108 p. (GNS Science consultancy report; 2015/124).

Perks A. 2018. Personal communication. Environmental Data Analyst at Bay of Plenty Regional Council, Whakatane, New Zealand.

Ratouis TMP, O'Sullivan MJ, O'Sullivan JP. 2016. A numerical model of Rotorua geothermal field. *Geothermics*. 60:105-125.

Reeves RR, Rae L. 2016. Changes in aerial thermal infrared signature over the Rotorua Geothermal Field, New Zealand: 1990–2014. *Geothermics*. 64:262-270. doi:10.1016/j.geothermics.2016.06.007.

Reeves RR, Scott BJ, Hall J. 2014. 2014 Thermal infrared survey of the Rotorua and Lake Rotokawa-Mokoia Geothermal Fields. Lower Hutt (NZ): GNS Science. 28 p. (GNS Science report; 2014/57).

Ryan PJ, Harleman DRF, Stolzenbach KD. 1974. Surface heat loss from cooling ponds. *Water Resources Research.* 10(5):930-938.

Sartori E. 2000. A critical review on equations employed for the calculation of the evaporation rate from free water surfaces. *Solar Energy*. 68(1):77-89.

Scott BJ, Mroczek EK, Burnell JG, Zarrouk SJ, Seward A, Robson B, Graham DJ. 2016. The Rotorua Geothermal Field: an experiment in environmental management. *Geothermics*. 59(B):294-310. doi:10.1016/j.geothermics.2015.09.004.

Seward A, Ashraf S, Reeves R, Bromley C. 2018a. Improved environmental monitoring of surface geothermal features through comparisons of thermal infrared, satellite remote sensing and terrestrial calorimetry. *Geothermics.* 73:60-73. doi:10.1016/j.geothermics.2018.01.007.

Seward AM, Sanders F, Rodriguez C, Bromley C, Keen D. Forthcoming 2018b. Measuring surface heat flow: development of new equipment and field procedures. Lower Hutt (NZ): GNS Science. (GNS Science report).

Simpson B. 1985. An assessment of heat flow at Whakarewarewa. In: *Proceedings of the 7th New Zealand Geothermal Workshop;* 1985 Nov 6-8; Auckland, New Zealand. Auckland (NZ): Geothermal Institute. p.147-148.

Sorey ML, Colvard EM. 1994. Measurements of heat and mass flow from thermal areas in Lassen Volcanic National Park, California, 1984-93. Denver (CO): U.S. Geological Survey. 35 p. Water Resources Investigations Report No.: 94-4180-A.

Spang B. 2002. Water97_v13.xla – Excel Add-In for properties of water and steam in SI-units. [updated 2002 Feb 10; accessed 2018 Jun 15]. http://alexmichinel.com/web_documents/water97_v13.pdf

Sutton PM. 1953. Variation of the elastic constants of crystalline aluminum with temperature between 63K and 773K. *Physical Review.* 112:2139.

Van Manen SM, Wallin E. 2012. Ground temperature profiles and thermal rock properties at Wairakei, New Zealand. *Renewable Energy*. 43:313-321.

APPENDICES

APPENDIX 1: DATA COLLECTION AND FIELD NOTES

A1.1 Field Notes

Field observations and notes are provided on the enclosed USB drive.

A1.2 Weather Details for Survey Dates

Table A 1.1 Survey details. Dates of data collections, field personnel, area and sites surveyed, local average daily climate information. Sites in blue are soils temperature sites.

Date	Survey area	Field staff	Sites surveyed	Maximum air temperature (°C)	Daily rain (mm)	Average wind (m/s)
27-02-2018	Kuirau Park	FS, SL	Kuirau Stream, RRF3022, RRF3059, RRF3061, RRF3062	16.3	1.8	1.6
28-02-2018	Kuirau Park	FS, SL, NM, TB	K12, K14, RRF0601, RRF0605, RRF0613, RRF0614, RRF0621, RRF0622, RRF0623, RRF0624, RRF0633, RRF0644, RRF0646, RRF0647, RRF0648, RRF0649, RRF0650, RRF0651, RRF0653, RRF0657, RRF0662, RRF0713, RRF0714, RRF0715, RRF0721, RRF0722, RRF3014, RRF3041, RRF3042, RRF3051, RRF3058, RRF3059, RRF3062, RRF3065, RRF3069, RRF3079, RRF6031	17.8	0	3.0
01-03-2018	Arikikapakapa \ Kuirau Park \ Sulphur Bay	FS, SL, NM, TB	A2, A2-2, A5, K11, K14, K9, Main lake outflow, RRF1365, RRF2041, RRF2042, RRF2050, RRF2051, RRF2052, RRF2064, RRF2070, RRF2094, RRF2098, RRF2107, RRF2122, RRF2124, RRF2128, RRF2135, RRF3140, RRF3168, RRF3175, RRF3177, RRF3178, RRF4040, RRF4041	18.2	0.8	2.7
02-03-2018	Kuirau Park \ Sulphur Bay	FS, SL, NM, TB	K1, K10, K2, K3, K4, K5, K6, K8, R4, R7, RRF3127, RRF3182, RRF3196, RRF3197, S1, S10, S11, S2, S3, S4, S5, S6, S7, S8, S9	19.1	0	2.6
05-03-2018	Sulphur Bay	AS, TB	S16, S17, S24, S26, S27	21.4	0	2.5
13-03-2018	Whakarewarewa \ Te Puia	FS, TB, DG, SL	RRF0093, RRF0284, RRF0286, RRF0296, RRF0306, RRF0323, RRF0325, RRF0328, RRF0330, RRF0337, RRF0358, RRF0414, RRF0422, RRF0426, RRF0427, RRF0428, RRF0430, RRF0435, RRF0443, RRF0444, RRF0446, RRF0447, RRF0448, RRF0488, RRF0825	17.5	0.2	4.5
14-03-2018	Whakarewarewa \ Te Puia	FS, TB, DG, SL	RRF0096, RRF0097, RRF0333, RRF0450, RRF0453, RRF0952	16.8	0.4	3.2
15-03-2018	Whakarewarewa \ Te Puia	RR, TB, DG, SL	139, 140, 141, 142, 143, 144, 146, 147, 150, 155, 156, 162, 168, 169, 170, 171, 181, 188, 190, RRF0028, RRF0055, RRF0076, RRF0089, RRF0160, RRF0172, RRF0194, RRF0229, RRF0230, RRF0401, RRF0505, RRF0529, RRF0599	15.2	0	2.2

Date	Survey area	Field staff	Sites surveyed	Maximum air temperature (°C)	Daily rain (mm)	Average wind (m/s)
16-03-2018	Whakarewarewa	AS, TB, FS, SL	132, 172, 173, 174, 178, 129, 145, 148, 149, 152, 153, 163, 164, 165, 166, 167, 175, 176, 177, 179, RRF3105	17.6	0	1.0
20-03-2018	Puarenga Stream	AS and NIWA	Hemo Gorge, Tatua Falls, Geyser Flat, Whakarewarewa Village, FRI (Scion)	18.1	0	2.4
26-03-2018	Kuirau Park	FS, SL	K13, K16, K17, K19, RRF0622, RRF3042, RRF3167	17.5	0	2.1
27-03-2018	Whakarewarewa	FS, SL	2, 4, 31, 33, 34, 37, 38, 40, 42, 44, 61, 63, 69, W1	18.9	0	2.4
28-03-2018	Whakarewarewa \ Te Puia	FS, SL	1, 2, 38, 61, 63, 64, 69, 70, 73, 74, 75, 76, 97, 98, 99, 136, 137	18.1	1	1.5
29-03-2018	Te Puia	FS, SL	51, 54, 57, 58, 59, 60, 100, 101, 108, 110, 111, 116, 117	18.2	1.6	1.2
03-04-2018	Te Puia	AS, FL	10, 55, 56, 109, 118, 200	15.5	0	0.7
04-04-2018	Whakarewarewa village	AS, FL	W1-calorimeter, W6-calorimeter	18.2	1.6	0.8
05-04-2018	Whakarewarewa / Kuirau Park	AS, FL	99-calorimeter, R4-calorimeter, W7-calorimeter, W8-calorimeter	17.3	0	2.6
06-04-2018	Sulphur Bay / Arikikapakapa	AS, FL	A20, A8, R1-calorimeter, R2-calorimeter	16.3	0	1.8
19-04-2018	Puarenga Stream	RR and NIWA	Hemo Gorge, Geyser Flat, Whakarewarewa Village, FRI (Scion)	11.2	0	2.8

Field Personnel:

FS – Fiona Sanders

SL – Sabine Lor (Student)

TB – Thomas Brakenrig

NM – Nick Macdonald

DG – Duncan Graham

AS – Anya Seward

RR – Rob Reeves

NIWA – NIWA subcontractors (Graham Timpany and Ben Harding)

APPENDIX 2: SPRING DATA CHEMICAL ANALYSIS

The chemical analysis results from the water samples are provided on the enclosed USB drive. Field notes, recorded data and photos of the springs sites can be found in Appendix 1.

Table A 2.1 Heat flow and chloride concentrations of surveyed springs.

Site	Area	Water temperature (°C)	Flow rate (Ls^{-1})	Discharging heat flow (W)	Chloride content (mgl^{-1})	Sulphate content (mgl^{-1})	Cl/SO_4 mass ratio
RRF0622	Kuirau Park	45.8	3	0.25	281	111	2.53
Kuirau Stream at Tarewa Rd (1114682)	Kuirau Park	44.1	83	9.68	306	108	2.83
RRF0653	Kuirau Park	76.6			316	86	3.67
RRF0657	Kuirau Park	76.2			327	74	4.42
RRF0714	Kuirau Park	87.1			329	66	4.98
RRF3051	Kuirau Park	72.6	0		333	227	1.47
RRF3042	Kuirau Park	40.2	33	2.10	346	110	3.15
RRF0601	Kuirau Park	58.7	50	8.30	353	105	3.36
RRF0722	Kuirau Park	99.9	0		356	47	7.57
RRF0624	Kuirau Park	67	0		368	95	3.87
RRF3014	Kuirau Park	99.7	0		396	44	9.00
RRF3175	Sulphur Bay	67.5	0		542	38	14.26
RRF3178	Sulphur Bay	70.1			551	131	4.21
RRF3177	Sulphur Bay	89.9	0		658	61	10.79
RRF3168	Sulphur Bay	68.4	0.1	0.02	1242	486	2.56
RRF3167	Sulphur Bay	93.8	0.3	0.08	1851	157	11.79
RRF3105	Whakarewarewa	32.7	0.1	0.01	71	329	0.22
RRF0160	Whakarewarewa	97.3	1.5	0.46	467	449	1.04
RRF0028	Whakarewarewa	100	0.6	0.21	497	76	6.54
RRF0529	Whakarewarewa	97.2			541	74	7.31
RRF0505	Whakarewarewa	95.2	1	0.32	554	69	8.03
RRF0055	Whakarewarewa	94.7	0.2	0.06	577	68	8.49
RRF0076	Whakarewarewa	60.1	3	0.47	602	111	5.42
RRF0172	Whakarewarewa	26.7	1.5	0.03	619	113	5.48
RRF0447	Whakarewarewa	29.7			280	332	0.84
RRF0446	Whakarewarewa	45.6	3.7	0.37	454	268	1.69
RRF0337	Whakarewarewa	47.4	20	2.21	481	283	1.70
RRF0428	Whakarewarewa	50.7	35	4.96	492	285	1.73
RRF0296	Whakarewarewa	93	3	0.88	495	174	2.84
RRF0328	Whakarewarewa	42	10	0.96	556	190	2.93
RRF0284	Whakarewarewa	96.6	0.5	0.16	557	79	7.05
RRF0306	Whakarewarewa	94	3	0.85	557	92	6.05
RRF0426	Whakarewarewa	54.8	0.1	0.02	613	248	2.47
RRF0488	Whakarewarewa	91.9	0.1	0.03	627	129	4.86
RRF0952	Whakarewarewa	90	2.5	0.71	1036	62	16.71

APPENDIX 3: POOL DATA

Field notes, recorded data and photos of the pool sites can be found in Appendix 1.

Table A 3.1 Surface heat loss from pools.

Feature ID	Location			Weather		Pool temperature (°C)	Pool area (m^2)	Calculated heat flow (Dawson 1964)				Calculated evaporative heat flow (Adams et al. 1990)		
	Easting (NZTM)	Northing (NZTM)	Region	Air temperature (°C)	Wind (ms^{-1})			Q_E (KW)	Q_C (KW)	Q_R (KW)	Q_{tot} (KW)	Q_{Efree} (KW)	$Q_{Eforced}$ (KW)	Q_{Etot} (KW)
RRF4040	1886357	5773391	Sulphur Bay	19	5.4	70	50	967.0	34.6	17.8	**1019.4**	190.4	682.4	**708.4**
RRF4041	1886357	5773391	Sulphur Bay	19	5.4	80	8	238.7	9.7	3.6	**252.1**	50.4	186.7	**193.3**
Kuirau Stream at Tarewa Rd (1114682)	1884063	5774602	Kuirau Park	16.2	0	44.1		0.0	0.0	0.0	**0.0**			**0.0**
RRF2100	1884072	5771248	Arikikapakapa	20	0	29.5	3585	1306.7	27.4	195.1	**1529.2**	480.7	0.0	**480.7**
RRF0028	1884778	5770800	Whakarewarewa	16.8	0	100	3	56.4	3.0	2.0	**61.4**	46.3	0.0	**46.3**
RRF0055	1884928	5770988	Whakarewarewa	19.5	0	94.7	2	31.0	1.5	1.2	**33.8**	24.4	0.0	**24.4**
RRF0076	1885093	5771031	Whakarewarewa	23	2	60.1	38	244.0	7.3	9.6	**260.8**	77.3	115.6	**139.1**
RRF0089	1885206	5770905	Whakarewarewa	20.2	0	32.5	1535	786.2	16.9	109.9	**913.0**	317.2	0.0	**317.2**
RRF0093	1885275	5771044	Whakarewarewa	21	2.4	28.4	475	280.9	5.8	20.1	**306.9**	45.4	122.9	**131.0**
RRF0096	1885252	5770994	Whakarewarewa	20.2	3.6	33.7	182	276.3	6.0	14.4	**296.7**	44.0	153.6	**159.8**
RRF0097	1885239	5770973	Whakarewarewa	20	3.6	42.1	520	1613.5	38.9	70.2	**1722.7**	305.5	858.3	**911.0**
RRF0160	1885065	5771032	Whakarewarewa	24.5	2.1	97.3	3	98.0	4.7	1.8	**104.4**	39.5	56.3	**68.8**
RRF0172	1885134	5771080	Whakarewarewa	21.2	2	26.7	874	332.7	6.8	27.3	**366.8**	53.9	130.4	**141.1**
RRF0194	1885167	5771110	Whakarewarewa	22.5	1.7	59.7	152	892.3	26.8	38.2	**957.2**	304.3	360.8	**472.0**
RRF0229	1885036	5770765	Whakarewarewa	23.7	2	33	90	72.5	1.6	5.0	**79.1**	14.1	32.0	**35.0**
RRF0230	1885028	5770769	Whakarewarewa	24	2	42.4	27	55.3	1.3	3.1	**59.7**	13.6	26.2	**29.5**
RRF0284	1885276	5771168	Whakarewarewa	20	2.1	96.6	46	1498.1	73.7	28.2	**1600.0**	605.7	740.3	**956.5**
RRF0286	1885241	5771147	Whakarewarewa	25.2	1.4	100	17	520.2	25.3	10.6	**556.3**	249.7	215.6	**329.9**
RRF0296	1885234	5771215	Whakarewarewa	23	2.9	93	9	302.1	13.9	5.0	**321.0**	99.7	188.1	**212.8**
RRF0306	1885222	5771183	Whakarewarewa	26	5	94	9	438.6	19.8	5.0	**463.4**	101.9	334.7	**349.8**
RRF0323	1885258	5771059	Whakarewarewa	21	0.7	56.4	37	139.8	4.1	8.6	**152.5**	61.8	32.9	**70.0**
RRF0325	1885312	5771143	Whakarewarewa	20	2.2	71.6	34	413.4	15.0	12.4	**440.8**	139.3	206.6	**249.1**
RRF0328	1885401	5771175	Whakarewarewa	19	1.8	42	704	1553.0	37.7	98.4	**1689.1**	426.1	581.7	**721.1**
RRF0330	1885437	5771188	Whakarewarewa	21.3	2.6	46	195	645.8	16.2	30.2	**692.2**	152.1	312.3	**347.3**
RRF0333	1885405	5771197	Whakarewarewa	17.8	2	66	7	62.8	2.2	2.3	**67.3**	21.8	32.5	**39.1**
RRF0337	1885560	5771166	Whakarewarewa	21	4.8	47.4	10371	55095.9	1415.4	1725.4	**58236.8**	9133.6	27760.7	**29224.7**
RRF0358	1885492	5771185	Whakarewarewa	19	3.5	36.4	151	307.3	7.0	15.5	**329.8**	53.8	169.2	**177.6**
RRF0401	1885465	5771112	Whakarewarewa	19.1	0	80	7	61.1	2.5	3.1	**66.7**	44.1	0.0	**44.1**
RRF0414	1885617	5771212	Whakarewarewa	17.2	3.8	39	53	146.9	3.5	6.9	**157.2**	26.4	88.2	**92.0**
RRF0422	1885614	5771242	Whakarewarewa	16	0	67.3	261	1341.0	47.8	91.1	**1479.9**	889.5	0.0	**889.5**
RRF0426	1885575	5771217	Whakarewarewa	16	1	54.8	18	72.1	2.2	4.5	**78.7**	29.7	22.8	**37.5**
RRF0427	1885572	5771224	Whakarewarewa	16	1	63.8	95	598.9	20.4	30.4	**649.6**	267.3	175.6	**319.9**
RRF0428	1885600	5771221	Whakarewarewa	16.8	0	50.7	603	1322.5	37.0	128.4	**1487.9**	751.1	0.0	**751.1**
RRF0430	1885558	5771225	Whakarewarewa	17.7	3.6	75.7	309	5969.7	233.9	128.1	**6331.6**	1597.2	3338.5	**3700.9**
RRF0435	1885562	5771187	Whakarewarewa	17	5.6	46.5	15	89.5	2.4	2.7	**94.6**	13.8	65.5	**66.9**
RRF0443	1885511	5771030	Whakarewarewa	20	0	42.8	1369	1732.1	42.2	191.3	**1965.6**	855.1	0.0	**855.1**
RRF0444	1885469	5770991	Whakarewarewa	19	0	40	360	380.8	9.0	45.5	**435.3**	182.4	0.0	**182.4**
RRF0446	1885487	5771074	Whakarewarewa	22	2.3	45.6	1684	5015.5	124.9	249.4	**5389.7**	1239.6	2052.4	**2397.7**
RRF0447	1885508	5770992	Whakarewarewa	20	0.5	29.7	2963	1370.7	28.8	164.8	**1564.3**	410.8	193.3	**454.0**
RRF0448	1885398	5770842	Whakarewarewa	19.2	2.5	37.6	1419	2617.4	60.0	155.3	**2832.6**	565.8	1115.8	**1251.0**
RRF0450	1885708	5771350	Whakarewarewa	21	0	28	1285	339.9	7.0	51.4	**398.3**	112.7	0.0	**112.7**
RRF0453	1885637	5771318	Whakarewarewa	21	0	29.8	150	52.3	1.1	7.6	**61.0**	18.8	0.0	**18.8**
RRF0462	1884559	5774253	Kuirau Park	17.6	0.1	25.7	500	137.5	2.8	22.5	**163.7**	45.9	5.0	**46.2**
RRF0488	1885446	5771291	Whakarewarewa	19.6	0.9	91.9	0.5	9.9	0.5	0.3	**10.7**	5.4	3.6	**6.5**
RRF0505	1884892	5770935	Whakarewarewa	18.1	0	95.2	1	15.8	0.8	0.6	**17.2**	12.6	0.0	**12.6**
RRF0529	1884738	5770750	Whakarewarewa	13.2	1.1	97.2	3	76.5	4.0	2.0	**82.6**	42.0	29.9	**51.6**
RRF0599	1884889	5770924	Whakarewarewa	18.6	0	88.9	3.1	38.6	1.8	1.7	**42.1**	29.5	0.0	**29.5**
RRF0601	1884362	5774748	Kuirau Park	19	3.6	58.7	4450	37890.1	1160.8	1167.2	**40218.1**	8907.0	18488.2	**20521.9**
RRF0605	1884344	5774696	Kuirau Park	19	1	52.8	30	103.0	2.9	6.5	**112.4**	41.1	32.1	**52.2**
RRF0613	1884447	5774552	Kuirau Park	18	1	60	25	127.2	4.0	7.0	**138.2**	55.0	40.3	**68.2**
RRF0614	1884443	5774530	Kuirau Park	19	1	73.2	2	18.9	0.7	0.8	**20.3**	9.0	6.9	**11.3**
RRF0621	1884460	5774437	Kuirau Park	19.8	0.3	69.9	12.5	79.4	2.8	4.4	**86.6**	46.9	10.1	**48.0**
RRF0622	1884473	5774403	Kuirau Park	25.8	0.4	45.8	115	179.7	4.4	14.7	**198.8**	73.7	25.7	**78.1**
RRF0622	1884463	5774409	Kuirau Park	19	1.5	41.8	115	228.1	5.5	15.9	**249.8**	68.4	85.5	**109.5**
RRF0623	1884497	5774397	Kuirau Park	19.3	0.2	64	120	556.0	18.3	36.4	**610.9**	327.1	43.4	**330.0**
RRF0624	1884497	5774368	Kuirau Park	20	0.3	67	25	138.6	4.7	8.1	**151.5**	79.9	16.9	**81.7**
RRF0633	1884451	5774373	Kuirau Park	19	1	67.9	10	74.2	2.6	3.4	**80.1**	34.0	24.8	**42.1**

Feature ID	Location			Weather		Pool temperature (°C)	Pool area (m^2)	Calculated heat flow (Dawson 1964)				Calculated evaporative heat flow (Adams et al. 1990)		
	Easting (NZTM)	Northing (NZTM)	Region	Air temperature (°C)	Wind (ms^{-1})			Q_E (KW)	Q_C (KW)	Q_R (KW)	Q_{tot} (KW)	Q_{Efree} (KW)	$Q_{Eforced}$ (KW)	Q_{Etot} (KW)
RRF0644	1884385	5774498	Kuirau Park	19	1	40.5	580	907.2	21.6	75.2	**1004.0**	307.6	240.9	**390.7**
RRF0646	1884280	5774588	Kuirau Park	17	3	47.3	650	2682.9	71.3	121.7	**2875.9**	634.9	1323.1	**1467.5**
RRF0647	1884184	5774610	Kuirau Park	18	1	80.1	50	634.8	26.2	22.7	**683.8**	319.4	198.5	**376.1**
RRF0648	1884165	5774615	Kuirau Park	17	3	84	20	482.2	21.1	9.9	**513.3**	154.5	294.2	**332.3**
RRF0649	1884157	5774643	Kuirau Park	17	1	53.1	9	32.1	0.9	2.1	**35.1**	13.1	10.6	**16.9**
RRF0650	1884153	5774648	Kuirau Park	17	1	73.7	15	145.7	5.6	6.0	**157.3**	70.6	48.0	**85.4**
RRF0651	1884147	5774653	Kuirau Park	17	0.5	76.4	10	92.2	3.7	4.2	**100.2**	53.8	18.4	**56.9**
RRF0653	1884122	5774660	Kuirau Park	17	1.1	76.6	30	340.2	13.6	12.8	**366.6**	163.1	116.0	**200.2**
RRF0657	1884134	5774705	Kuirau Park	17	5.2	76.2	25	620.7	24.7	10.6	**655.9**	133.3	453.3	**472.5**
RRF0662	1884432	5774738	Kuirau Park	18	1.1	37.5	200	263.7	6.1	23.0	**292.9**	83.7	78.6	**114.8**
RRF0713	1884179	5774617	Kuirau Park	18	3.1	69	25	323.1	11.5	8.8	**343.4**	91.3	194.4	**214.8**
RRF0714	1884160	5774592	Kuirau Park	17	0.5	87.1	35	498.7	22.7	18.5	**539.9**	311.3	94.6	**325.3**
RRF0715	1884158	5774587	Kuirau Park	17	0.5	34.5	10	8.7	0.2	1.0	**10.0**	3.3	1.7	**3.7**
RRF0721	1884378	5774573	Kuirau Park	19	1.4	48.8	50	152.6	4.1	9.4	**166.1**	51.8	57.6	**77.4**
RRF0722	1884452	5774573	Kuirau Park	20	1	99.9	1	27.0	1.4	0.6	**29.0**	15.1	10.5	**18.4**
RRF0825	1885441	5771115	Whakarewarewa	20	2.1	83.6	18	356.4	15.1	8.6	**380.1**	133.4	181.9	**225.6**
RRF0952	1885489	5771367	Whakarewarewa	22	2	90	152	3723.1	166.5	80.7	**3970.4**	1485.4	1694.9	**2253.7**
RRF1365	1885603	5772481	Sulphur Bay	19	2.8	28	1510	1099.4	22.8	76.9	**1199.1**	176.3	492.8	**523.4**
RRF2041	1884327	5771229	Arikikapakapa	19	1.8	73.7	195	2353.0	88.6	75.9	**2517.4**	900.1	981.6	**1331.8**
RRF2042	1884431	5771159	Arikikapakapa	19	2.4	28.9	9930	7502.1	156.6	558.7	**8217.4**	1350.3	2851.9	**3155.4**
RRF2050	1884635	5771305	Arikikapakapa	19	0.8	26.5	1220	428.9	8.8	51.4	**489.0**	107.1	91.9	**141.1**
RRF2051	1884717	5771330	Arikikapakapa	19	0	27.7	3190	990.2	20.4	156.8	**1167.4**	353.1	0.0	**353.1**
RRF2052	1884772	5771298	Arikikapakapa	19	1.5	27.2	655	315.6	6.5	30.3	**352.3**	66.1	106.4	**125.2**
RRF2070	1884837	5771177	Arikikapakapa	19	0	33	4845	2793.5	60.8	393.6	**3247.9**	1173.4	0.0	**1173.4**
RRF2094	1883975	5771118	Arikikapakapa	20	0.8	25	405	93.5	1.9	11.3	**106.7**	20.4	21.1	**29.4**
RRF2098	1883991	5771153	Arikikapakapa	20	1.5	33.2	75	70.0	1.5	5.8	**77.3**	17.3	26.5	**31.6**
RRF2107	1884179	5771283	Arikikapakapa	18	1	29.2	15	8.8	0.2	1.0	**9.9**	2.4	2.8	**3.6**
RRF2122	1884398	5771327	Arikikapakapa	19	0.7	25.5	265	76.0	1.5	9.6	**87.2**	18.7	15.9	**24.5**
RRF2124	1884266	5771458	Arikikapakapa	19	0.8	22.2	9285	1241.3	24.6	163.2	**1429.0**	232.5	239.3	**333.6**
RRF2128	1884561	5771515	Arikikapakapa	20	1	36.4	40515	44381.1	998.8	3942.4	**49322.3**	13634.6	9452.0	**16590.4**
RRF2135	1884462	5771020	Arikikapakapa	19	3.2	23.6	7690	2744.5	54.9	195.7	**2995.1**	324.7	1195.7	**1239.0**
RRF3014	1884431	5774580	Kuirau Park	20	1.8	99.7	1	33.4	1.7	0.6	**35.7**	15.0	18.7	**24.0**
RRF3022	1884476	5774118	Kuirau Park	17.3	0.1	32.4	50	30.6	0.7	4.3	**35.6**	12.7	1.3	**12.7**
RRF3041	1884336	5774560	Kuirau Park	18	1.3	36	250	309.5	7.0	26.4	**342.9**	90.1	101.5	**135.7**
RRF3042	1884295	5774563	Kuirau Park	17	3	47.3	655	2703.5	71.8	122.7	**2898.0**	639.8	1332.7	**1478.4**
RRF3042	1884279	5774552	Kuirau Park	25	0.6	40.2	655	712.7	16.4	61.7	**790.8**	246.7	129.3	**278.5**
RRF3051	1884385	5774385	Kuirau Park	20	0.8	72.6	9	77.2	2.8	3.4	**83.5**	38.8	22.2	**44.8**
RRF3058	1884471	5774329	Kuirau Park	17.4	2.2	29.4	1405	1196.0	25.2	95.3	**1321.3**	241.0	482.5	**539.3**
RRF3059	1884488	5774253	Kuirau Park	17.4	2	26.4	2600	1459.9	29.9	130.2	**1620.0**	279.0	542.1	**609.7**
RRF3061	1884476	5774177	Kuirau Park	18.4	0	26.6	75	20.9	0.4	3.4	**24.9**	7.3	0.0	**7.3**
RRF3062	1884559	5774253	Kuirau Park	18.6	0	32.8	60	34.5	0.7	4.9	**40.1**	14.6	0.0	**14.6**
RRF3065	1884524	5774106	Kuirau Park	20	1.5	40.1	120	204.6	4.8	14.6	**224.0**	58.7	76.4	**96.3**
RRF3069	1884438	5774517	Kuirau Park	19	0.8	55.3	35	129.5	3.8	8.3	**141.6**	56.6	34.3	**66.1**
RRF3079	1884396	5774811	Kuirau Park	18	3	71.5	960	13629.3	503.6	360.0	**14493.0**	3997.4	6758.8	**7852.4**
RRF3105	1884811	5770847	Whakarewarewa	18.8	1.7	32.7	420	418.1	9.1	33.8	**461.0**	99.4	155.6	**184.7**
RRF3127	1885753	5773892	Sulphur Bay	23.3	6	47.8	145	876.4	22.2	22.7	**921.5**	122.3	589.6	**602.1**
RRF3140	1886307	5773420	Sulphur Bay	19	4	38.2	330	837.1	19.4	37.8	**894.2**	141.0	471.9	**492.5**
RRF3167	1886355	5772773	Sulphur Bay	26.8	1.5	93.8	2.5	61.1	2.7	1.4	**65.3**	27.9	29.4	**40.5**
RRF3168	1886304	5772816	Sulphur Bay	19	1.5	68.4	30	264.0	9.3	10.3	**283.7**	104.8	108.2	**150.7**
RRF3175	1885740	5773122	Sulphur Bay	19	0	67.5	5	25.3	0.9	1.7	**27.8**	16.6	0.0	**16.6**
RRF3177	1885376	5774066	Sulphur Bay	19	0.5	89.9	15	238.1	11.0	8.2	**257.3**	149.0	47.1	**156.3**
RRF3178	1885477	5774041	Sulphur Bay	20	1.2	70.1	45	391.8	13.9	15.8	**421.6**	170.3	137.2	**218.7**
RRF3182	1885943	5774132	Sulphur Bay	25	4.4	36	150	250.5	5.5	10.0	**266.2**	32.8	151.3	**154.8**
RRF3196	1885946	5774042	Sulphur Bay	21.8	7.1	53.3	15	148.4	4.1	3.1	**155.6**	20.0	117.4	**119.0**
RRF3197	1885939	5774047	Sulphur Bay	21.5	8.5	87.3	5	280.0	12.2	2.5	**294.8**	43.4	252.6	**256.3**
RRF6031	1884562	5774225	Kuirau Park	19.2	0.2	37.8	40	38.0	0.9	4.4	**43.4**	16.3	3.1	**16.6**

APPENDIX 4: CHEMICAL ANALYSIS OF PUARENGA STREAM

A4.1 Puarenga Stream Gauging Reports

The Puarenga stream gauging reports provided by NIWA are provided on the enclosed USB drive.

A4.2 Puarenga Stream Chemistry

Chemistry reports of water sample analysed by NZGAL are provided on the enclosed USB drive.

APPENDIX 5: GROUND TEMPERATURE DATA

A5.1 Soil Temperature Data

Field notes, recorded data and photos of the Ground temperature sites can be found in Appendix 1.

Table A 5.1 Temperatures and heat flux determined at ground temperature sites.

Site details						Conductivity	Ground temperatures (°C)							Heat flux using Fridriksson et al. (2006) (Wm^{-2})		Heat flux from Calorimeter measurements (Wm^{-2})		Conductive heat flux (Wm^{-2})		Convective heat flux (Wm^{-2})	
Area	Site	Date	Time	Northing	Easting		T5	T10	T15	T20	T25	T50	T100	q15	q15[BP<15]	qtot	qadv	ΔT/z	qc (W/m^2)	ZBP	qzb
Arikikapakapa	A2	2018-03-01	11:10	1884463	5771641	0.683	58.2	75.1												0.2	531.7
Arikikapakapa	A20	2018-04-06	13:19	1884035	5771237	0.7	19.8	19.5	19.4	19.2	19.5	20.8	22.1	0.7				2.3	1.6	92.0	3.3
Arikikapakapa	A2-2	2018-03-01	11:40	1884461	5771646	0.768	22.8	26.3	30.2	33.8	39.4	55.6	65.3	4.3						3.6	50.9
Arikikapakapa	A5	2018-03-01	09:27	1884670	5771113	0.597	55.6	76	91.6	99.1				366.1						0.2	575.0
Arikikapakapa	A8	2018-04-06	13:39	1884211	5771143	0.7	26.2	26.1	25.1	25.2	26.2	33.5		2.1						6.7	30.0
Kuirau Park	K1	2018-03-02	10:59	1884429	5774797	0.676	27.2	27.7	29.1	30.1	32.1	37.8	49.3	3.7				22.1	14.9	5.9	33.2
Kuirau Park	K10	2018-03-02	09:47	1884431	5774619	0.7	49.8	54	61.4	69.6	75.5	99.4		73.9						0.5	267.8
Kuirau Park	K11	2018-03-01	16:57	1884437	5774580	0.585	43.7	53.7	62.2	77.4	88.9	99		77.8						0.5	265.9
Kuirau Park	K12	2018-02-28	16:52	1884368	5774577	0.775	25.1	24	24.1	24.9	25.3	30.9	39.8	1.8				14.7	11.4	9.5	22.4
Kuirau Park	K13	2018-03-26	16:01	1884483	5774484	0.499	31.6	33.8	35.9	38.6	43			8.6				57.0	28.4	1.7	94.1
Kuirau Park	K14	2018-02-28	15:31	1884353	5774387	0.644	52.9	67.6	78.2	92.6	92.8			194.5						1.9	86.2
Kuirau Park	K14	2018-03-01	15:25	1884353	5774387	0.683	53.6	63.6	77.5	94.4	94.7			187.6						1.0	149.0
Kuirau Park	K16	2018-03-26	15:34	1884512	5774279	0.707	24.3	23.2	22.1	21.9	22	23	24.9	1.2				0.6	0.4	58.8	4.8
Kuirau Park	K17	2018-03-26	15:14	1884484	5774154	0.701	26.5	26.1	25.2	24.8	25.2	28.2	33.1	2.1				6.6	4.6	19.1	12.4
Kuirau Park	K19	2018-03-26	14:56	1884359	5774218	0.787	25.3	23.5	22.8	22.8	23.2	25.9	30.5	1.4				5.2	4.1	21.8	11.1
Kuirau Park	K2	2018-03-02	10:43	1884314	5774764	0.98	21.8	22	22.3	22.6	23.47	26.5	32.6	1.3				10.8	10.6	16.0	14.4
Kuirau Park	K3	2018-03-02	11:17	1884147	5774696	0.694	21.2	22.2	23.9	26.3	28	36.6	49.2	1.7				28.0	19.4	5.6	35.0
Kuirau Park	K4	2018-03-02	11:46	1884121	5774678	0.807	50	59.6	67.4	79.3	85.3	100		107.3						0.5	274.9
Kuirau Park	K5	2018-03-02	11:31	1884203	5774671	0.713	20.8	21.2	22.4	23.2	24.6	30	37	1.3				16.2	11.6	12.5	17.7
Kuirau Park	K6	2018-03-02	10:44	1884379	5774703	0.992	35.6	44.2	56.7	63.4	73.1	99.3		53.7						0.5	267.0
Kuirau Park	K8	2018-03-02	09:59	1884351	5774648	0.78	31.5	38.8	48.2	53.7	59.6	96.4		28.1						0.5	253.3
Kuirau Park	K9	2018-03-01	16:02	1884371	5774628	0.31	30.4	37.7	44.3	51.2	56.2	87.2		20.0						0.7	210.3
Kuirau Park	R4	2018-03-02	10:14	1884445	5774595	0.943	41.8	46.9	54	63.5	71.6	86.1	95.6	44.2		251.9	143.5			1.2	126.6
Sulphur Bay	R1	2018-04-06	09:34	1886357	5773300	0.7	30.6	32.5	38.6	43.6	49.1	70.7	87.1	11.5		0.0	0.0			1.5	104.6
Sulphur Bay	R2	2018-04-06	10:54	1886352	5772805	0.7	42.7	45.9	58.3	66.1	76.8	98.3		60.1		410.5	114.3			0.5	260.7
Sulphur Bay	S1	2018-03-02	12:34	1886156	5774298	1.238	77.2	97.1	100					520.0	1079.8					0.1	817.5
Sulphur Bay	S10	2018-03-02	15:11	1885620	5773727	0.658	43.6	54.5	61.8	71.6	77.3	95		75.9						0.6	236.5
Sulphur Bay	S16	2018-03-05	13:49	1886344	5773402	0.503	34	32.2	32.3	34.4	36.9	47.1	70.7	5.7				36.7	18.5	2.1	77.8
Sulphur Bay	S17	2018-03-05	13:25	1886356	5773304	0.825	41.3	45.2	47.5	54.6	61.3	84.5	100	26.5						1.0	153.3

Site details						Conductivity	Ground temperatures (°C)							Heat flux using Fridriksson et al. (2006) (Wm^{-2})		Heat flux from Calorimeter measurements (Wm^{-2})		Conductive heat flux (Wm^{-2})		Convective heat flux (Wm^{-2})	
Area	Site	Date	Time	Northing	Easting		T5	T10	T15	T20	T25	T50	T100	q15	q15[BP<15]	qtot	qadv	ΔT/z	qc (W/m^2)	ZBP	qzb
Sulphur Bay	S2	2018-03-02	12:44	1886129	5774270	0.997	61.4	78.7	89	92.6	94.5	100		326.3						0.4	290.7
Sulphur Bay	S24	2018-03-05	12:59	1886354	5772800	0.398	44	50.1	56.8	65.8	70.3	86.7	101.5	54.1						0.9	161.8
Sulphur Bay	S26	2018-03-05	11:58	1886143	5772545	0.844	30.9	28.9	29.5	32.6	35.2	44.6	62.9	3.9				32.0	27.0	3.0	59.0
Sulphur Bay	S3	2018-03-02	12:57	1886037	5774153	0.653	23.3	22.7	23	23.5	23.6	27.4		1.5				9.1	5.9	14.2	15.9
Sulphur Bay	S5	2018-03-02	13:13	1885926	5774114	0.729	25.5	27.5	30.3	33.6	36.5	46.3	71.7	4.4				46.2	33.7	2.0	81.4
Sulphur Bay	S6	2018-03-02	14:19	1885826	5774034	0.33	82.3	95.5	96	96				441.7						0.2	636.5
Sulphur Bay	S7	2018-03-02	16:52	1885685	5774026	0.529	29.6	31.5	34.9	38.2	41.8	47.8	56.8	7.7				27.2	14.4	5.6	34.6
Sulphur Bay	S8	2018-03-02	14:29	1885760	5773922	0.792	24.9	23.2	23.9	26	28.2	33	39	1.7				14.1	11.2	13.5	16.7
Whakarewarewa	1	2018-03-28	16:53	1884712	5770928	*0.7*	21.4	21	20	19.9	20	20.6	22.2	0.8				0.8	0.6	75.0	3.9
Whakarewarewa	2	2018-03-27	14:05	1884865	5771006	0.184	20.9	20.5	20.3	20.3	20.3	20.3	20.6	0.9				-0.3	-0.1	408.0	0.9
Whakarewarewa	2	2018-03-28	09:17	1884865	5771006	0.163	18.6	18.3	18.6	19.2	19.4	19.4	20.5	0.6				1.9	0.3	113.4	2.8
Whakarewarewa	4	2018-03-27	09:36	1884823	5770913	0.467	20.7	20.4	21.5	22.5	23.5	27.2	35.2	1.1				14.5	6.8	11.8	18.6
Whakarewarewa	10	2018-04-03	14:13	1884624	5770983	*0.65*	19.6	19.5	19.8	20.2	20.8	22.7	24.5	0.8				4.9	3.2	62.6	4.6
Whakarewarewa	31	2018-03-27	10:52	1884734	5770657	0.768	20.2	20	20.2	21.4	21.1	30.1	28.4	0.9				8.2	6.3	6.2	32.0
Whakarewarewa	33	2018-03-27	11:20	1884855	5770772	0.341	22.7	23.5	25.3	24.6	27.4	34.4	46.4	2.1				23.7	8.1	6.2	31.8
Whakarewarewa	34	2018-03-27	11:41	1884818	5770768	0.697	74.7	97.7	100					520.0	1079.8					0.1	844.0
Whakarewarewa	37	2018-03-27	12:17	1884785	5770795	1.416	42.5	49.1	54.6	63.6	70.5	92.8	99	46.2						1.0	149.0
Whakarewarewa	38	2018-03-27	12:36	1884743	5770795	0.372	33.3	34.2	34.1	33.7	35.4	49	62.4	7.0				29.1	10.8	3.6	50.2
Whakarewarewa	38	2018-03-28	16:18	1884743	5770751	*0.7*	33.8	38	39.2	41.4	43.1	49.1	61.9	12.3				28.1	19.7	3.8	48.4
Whakarewarewa	40	2018-03-27	09:48	1884817	5770856	0.569	30.1	35.8	37.6	39.8	42.8	49.1	65.3	10.4				35.2	20.0	3.0	59.2
Whakarewarewa	42	2018-03-27	10:13	1884694	5770819	0.711	20.8	21.7	22.4	22.9	23.5	25.6	29.5	1.3				8.7	6.2	26.1	9.5
Whakarewarewa	44	2018-03-27	10:29	1884624	5770789	0.366	28	31.9	34.8	38	43.8	50.2	65.6	7.6				37.6	13.8	3.0	58.2
Whakarewarewa	51	2018-03-29	11:57	1884892	5770918	*0.7*	39.2	48.1	53.5	65.2	71.9	89.4	98.4	42.6						1.0	144.1
Whakarewarewa	54	2018-03-29	12:28	1884939	5770930	*0.7*	24.5	25.4	27.2	28.9	30.1	35.1	34.6	2.8				10.1	7.1	8.9	23.7
Whakarewarewa	55	2018-04-03	12:20	1884967	5770952	*0.7*	37	38.7	41	50.2	55.2	69.7	80.3	14.7						2.3	74.2
Whakarewarewa	56	2018-04-03	12:41	1884943	5770985	*0.7*	33.3	35.9	41	52.9	51.9	71.1	88.7	14.7						1.4	110.9
Whakarewarewa	57	2018-03-29	16:08	1884985	5770994	*0.7*	25.5	25	25.4	25.7	27.6	33.4	42.2	2.2				16.7	11.7	8.9	23.5
Whakarewarewa	58	2018-03-29	11:28	1884982	5770910	*0.7*	36.2	49.2	57.2	66.5	73.4	85.3		55.7						1.3	119.6
Whakarewarewa	59	2018-03-29	16:35	1884979	5770874	*0.7*	27.7	28.6	29.5	30.6	33.7	44.9	51.4	3.9				23.7	16.6	8.6	24.3
Whakarewarewa	60	2018-03-29	09:50	1884938	5770878	*0.7*	20.8	21.9	26.3	26.8	28.4	34.5	40.3	2.5				19.5	13.7	13.3	16.8
Whakarewarewa	61	2018-03-27	14:54	1884886	5771057	0.183	25.6	24.8	24	24.6	25.1	26.5	29.6	1.7				4.0	0.7	32.2	8.0
Whakarewarewa	61	2018-03-28	12:27	1884888	5771053	0.7	22.1	22.5	23.3	23.9	24.2	26.2	29.6	1.5				7.5	5.3	29.6	8.6
Whakarewarewa	63	2018-03-27	15:17	1884978	5771057	0.24	34.1	30.9	29.9	30.3	30.6	34.6	45.3	4.2				11.2	2.7	7.0	28.8
Whakarewarewa	63	2018-03-28	12:10	1884978	5771057	0.7	26.5	27.1	28.4	29.3	30.6	34.9	45.3	3.4				18.8	13.2	7.2	28.3

Site details						Conductivity	Ground temperatures (°C)							Heat flux using Fridriksson et al. (2006) (Wm^{-2})		Heat flux from Calorimeter measurements (Wm^{-2})		Conductive heat flux (Wm^{-2})		Convective heat flux (Wm^{-2})	
Area	Site	Date	Time	Northing	Easting		T5	T10	T15	T20	T25	T50	T100	q15	q15[BP<15]	qtot	qadv	ΔT/z	qc (W/m^2)	ZBP	qzb
Whakarewarewa	64	2018-03-28	11:52	1885033	5771056	0.451	22.4	22.8	23.4	24.1	25.1	27.4	34.3	1.6				11.9	5.4	13.7	16.4
Whakarewarewa	69	2018-03-27	15:44	1885036	5771136	1.12	23.5	23.4	22.8	28.4				1.4				32.6	36.5	2.0	81.0
Whakarewarewa	69	2018-03-28	11:31	1885035	5771132	1.194	22.3	22.2	22.8	22.9	23.6	26	32.1	1.4				9.8	11.7	16.2	14.2
Whakarewarewa	70	2018-03-28	15:15	1885065	5770989	0.65	23	22.9	22.9	23.1	23.5	25.2	27.4	1.4				4.4	2.9	47.5	5.8
Whakarewarewa	73	2018-03-28	11:06	1885137	5771019	0.578	33.1	39.3	45.1	51.4	55.7	76.6	93.5	21.5						1.2	126.0
Whakarewarewa	74	2018-03-28	09:52	1885144	5771062	0.417	22.1	24.5	27.4	28.9	30.2	34.4	42.3	2.9				20.2	8.4	9.7	21.9
Whakarewarewa	75	2018-03-28	10:15	1885140	5771102	0.157	22.3	23.1	25.6	25.1	27.3	30.6	37.5	2.2				15.2	2.4	12.5	17.7
Whakarewarewa	76	2018-03-28	10:44	1885189	5771045	0.469	60.4	75.5	86.5	92.7				291.1						0.3	460.9
Whakarewarewa	97	2018-03-28	15:37	1885068	5771017	*0.7*	33.3	40.3	47.1	52.2	59.2	80.7	88.1	25.6						1.9	85.6
Whakarewarewa	98	2018-03-28	14:57	1885116	5770991	0.7	68.1	87.9	99.6					511.7	790.1					0.1	742.0
Whakarewarewa	99	2018-03-28	14:31	1885141	5770972	0.356	63.4	90.5	99.6					511.7	790.1					0.1	745.6
Whakarewarewa	100	2018-03-29	10:17	1885129	5770875	*0.7*	27.9	32.4	36.2	39.1	42.4	54.6	74.4	8.9				46.5	32.6	2.1	79.9
Whakarewarewa	101	2018-03-29	10:35	1885107	5770875	*0.7*	24.4	25.3	26.6	27.6	28.8	34.4	44.2	2.6				19.8	13.9	7.7	26.5
Whakarewarewa	108	2018-03-29	14:53	1885079	5770783	*0.7*	25.1	24.3	25.1	25.5	25.2	30.4		2.1				11.8	8.2	9.8	21.7
Whakarewarewa	109	2018-04-03	11:50	1885077	5770847	*0.7*	65.7		88.4		94.7	95.8		317.6						0.7	207.8
Whakarewarewa	110	2018-03-29	14:33	1885037	5770807	*0.7*	38.3	45.1	51.3	58.5	65.4	85.1	89.5	36.0						2.3	74.2
Whakarewarewa	111	2018-03-29	15:26	1885033	5770814	*0.7*	41.3	51	61.2	61.8	69.4	68.7	63	72.9				21.7	15.2	0.6	238.9
Whakarewarewa	116	2018-03-29	11:11	1885032	5770909	*0.7*	29.1	32.4	34.6	38	41.1	50.9	74.3	7.5				45.2	31.6	2.0	84.0
Whakarewarewa	117	2018-03-29	10:52	1885056	5770906	*0.7*	36.9	55.7	65.6	72.5	76.3	90.5	92.5	96.3						2.8	62.7
Whakarewarewa	129	2018-03-16	14:27	1885257	5771063	0.536	34.7	37.2	40.2	41.8	47.9	63	87.2	13.6				52.5	28.1	1.4	113.2
Whakarewarewa	132	2018-03-16	14:50	1885253	5771041	0.526	43.8	56.7	68.6	74.8	78.5	98.3	98.9	115.2						1.0	147.9
Whakarewarewa	136	2018-03-28	13:51	1885219	5770926	1.147	21.7	21.5	21.1	21.2	21.4	22.3	24.4	1.0				2.7	3.1	54.2	5.2
Whakarewarewa	137	2018-03-28	14:12	1885219	5770926	1.538	27.3	29.8	32.6	35.4	36.7	44.1	57.6	5.9				30.3	46.6	4.2	44.7
Whakarewarewa	139	2018-03-15	15:06	1885275	5770824	0.266	39.4	45.2	50.8	55.3	66.3	87.3	101.7	34.6					0.0	0.9	163.4
Whakarewarewa	140	2018-03-15	14:29	1885291	5770813	1.132	25	25.4	26.3	27.3	28.7	33.2	39.6	2.5				14.6	16.5	12.5	17.7
Whakarewarewa	141	2018-03-15	14:16	1885310	5770859	0.639	22.8	21	20.6	21.3	21.2	24.5	28.1	0.9				5.3	3.4	29.3	8.7
Whakarewarewa	142	2018-03-15	15:22	1885315	5770905	1.016	30.6	32.1	32.6	34.2	35.4	44.1	61.9	5.9				31.3	31.8	3.1	56.9
Whakarewarewa	143	2018-03-15	14:06	1885342	5770887	1.337	29.4	32.1	34.5	37.9	41.3	53.6	65.1	7.4				35.7	47.7	3.7	49.8
Whakarewarewa	144	2018-03-15	13:53	1885371	5770826	0.242	22.9	22.5	22.3	22.7	22.8	29.3	36.9	1.3				14.0	3.4	11.7	18.7
Whakarewarewa	145	2018-03-16	10:58	1885397	5770875	0.515	21.3	20.8	21.6	22.8	24.1	29.4	42.6	1.1				21.3	11.0	6.5	30.7
Whakarewarewa	146	2018-03-15	13:41	1885413	5770930	0.198	23.3	23.5	23.6	24	24.1	29.4	39.8	1.6				16.5	3.3	8.4	24.8
Whakarewarewa	147	2018-03-15	13:27	1885428	5770986	0.166	32.2	31.6	32.3	34.3	35.2	39.5	49.8	5.7				17.6	2.9	6.3	31.5
Whakarewarewa	148	2018-03-16	10:42	1885413	5771053	0.7	30	31.8	33	34.6	36.8	43.8	54.4	6.2				24.4	17.1	5.4	35.9
Whakarewarewa	149	2018-03-16	12:05	1885312	5771014	0.354	27						27.6					0.6	0.2	316.5	1.2

Site details						Conductivity	Ground temperatures (°C)							Heat flux using Fridriksson et al. (2006) (Wm^{-2})		Heat flux from Calorimeter measurements (Wm^{-2})		Conductive heat flux (Wm^{-2})		Convective heat flux (Wm^{-2})	
Area	Site	Date	Time	Northing	Easting		T5	T10	T15	T20	T25	T50	T100	q15	q15[BP<15]	qtot	qadv	ΔT/z	qc (W/m^2)	ZBP	qzb
Whakarewarewa	150	2018-03-15	15:32	1885311	5770940	0.457	21.6	21.6	21.3	22.3	23.1	26.5	33.1	1.1				11.5	5.3	14.7	15.4
Whakarewarewa	152	2018-03-16	11:51	1885366	5771002	0.272	20.6	20.2	20.9	22.8	22.7	25.8	31.9	1.0				11.3	3.1	16.3	14.2
Whakarewarewa	153	2018-03-16	11:32	1885275	5770934	0.7	20.1	19.7	20.2	20.8	21.3	21.8	24.8	0.9				4.7	3.3	38.2	6.9
Whakarewarewa	155	2018-03-15	12:16	1885496	5770987	0.439	20.8	21.2	21.3	21.5	22	24.3	25	1.1				4.2	1.8	155.0	2.1
Whakarewarewa	156	2018-03-15	11:49	1885553	5770944	0.611	18.2	18.1	18.5	19.2	19.7	21.5	24.5	0.6				6.3	3.8	38.5	6.9
Whakarewarewa	162	2018-03-15	12:01	1885526	5770876	0.673	19.7	20.2	19.9	21.2	21.9	24.4	26.6	0.8				6.9	4.6	48.6	5.7
Whakarewarewa	163	2018-03-16	14:01	1885254	5771194	0.225	27.2	30.5	33.2	35.4	44.2	53.9	67.4	6.3				40.2	9.0	3.1	57.3
Whakarewarewa	164	2018-03-16	13:44	1885227	5771163	0.629	28.8	28.9	30.4	31	31.8	37.8	47.2	4.4				18.4	11.6	7.3	27.8
Whakarewarewa	165	2018-03-16	10:06	1885432	5771188	0.68	19.4	20.1	22.3	23.1	24.2	31.7	35.4	1.3				16.0	10.9	23.0	10.6
Whakarewarewa	166	2018-03-16	09:56	1885464	5771243	0.973	20.5	20.5	20.7	21.5	22.4	26.5	30.5	1.0				10.0	9.7	24.8	10.0
Whakarewarewa	167	2018-03-16	09:44	1885447	5771277	0.481	74.4		99.3					505.6	723.4					0.1	736.6
Whakarewarewa	168	2018-03-15	10:36	1885479	5771166	0.556	21.8	22.3	24.3	27.8	29.3	35.7	42.8	1.8				21.0	11.7	10.4	20.6
Whakarewarewa	169	2018-03-15	11:00	1885462	5771110	1.319	64.8		72.7	86.3	94	99.6		145.3						0.5	280.4
Whakarewarewa	170	2018-03-15	11:15	1885491	5771069	0.443	29.5	31.1	34.6	39	43.8	54.8	66.1	7.5				36.6	16.2	3.6	50.6
Whakarewarewa	171	2018-03-15	11:31	1885521	5771016	0.282	19.8	22.1	23.1	24	24.9	28.8	31.3	1.5				11.5	3.2	37.5	7.0
Whakarewarewa	172	2018-03-16	15:01	1885380	5771239	0.687	38.5	40.1	47.5	50.5	58.7	96.8		26.5						0.5	255.3
Whakarewarewa	173	2018-03-16	14:04	1885255	5771230	0.521	32.4	51.1	60.8	71.7	81.6	72		71.1						0.4	338.3
Whakarewarewa	174	2018-03-16	13:20	1885322	5771164	0.79	26.7	27	28.2	30	32	48.3	58.9	3.3				32.2	25.4	4.7	40.4
Whakarewarewa	175	2018-03-16	12:12	1885304	5771080	0.507	21	20.6	20.9	21.3	21.7	24.4		1.0				7.6	3.8	21.3	11.3
Whakarewarewa	176	2018-03-16	15:06	1885228	5771124	0.776	24.6	23.8	23.8	24.6	26.4	31.3		1.7				14.9	11.6	10.1	21.2
Whakarewarewa	177	2018-03-16	13:18	1885321	5771126	0.7	53.5	65.2	80.5		97.7	99.6		218.4						0.4	315.0
Whakarewarewa	178	2018-03-16	13:37	1885291	5771169	0.637	56.5	72.4	88.8	97.5				323.3						0.2	550.5
Whakarewarewa	179	2018-03-16	10:23	1885357	5771143	0.7	36.1	40.4	45.3	51.8	56.3	91.2	99.1	21.9						1.0	149.6
Whakarewarewa	181	2018-03-15	10:22	1885532	5771184	0.794	18.5	19.3	20.2	21.1	22.6	24.2	25.3	0.9				6.8	5.4	98.6	3.1
Whakarewarewa	188	2018-03-15	09:39	1885635	5771228	0.905	15.3	15.5	16.8	17.9	18.8	20.7	22.6	0.4				7.3	6.6	62.8	4.6
Whakarewarewa	190	2018-03-15	10:01	1885582	5771218	*0.7*	19.3	20.9	22.8	24.7	27.8	32.2	42	1.4				22.7	15.9	8.2	25.1
Whakarewarewa	118	2018-04-03	12:57	1884987	5770974	0.7	33.5	39.7	45.6	50.7	57.1	75.4		22.5						1.0	143.1
Whakarewarewa	99-calorimter	2018-04-05	10:23	1885152	5770961	*0.7*	83.9		98					479.6	723.4	751.8	331.3			0.2	689.3
Whakarewarewa	New1	2018-04-03	14:41	1885510	5771384	*0.7*	22.3	45.6	50.3	57.3	63.9	91.4		33.3						0.6	227.1
Whakarewarewa	W1	2018-03-27	11:59	1884798	5770782	1.729	56.1	70.5	78.7	92.8	94.6	99		199.5						0.5	264.7
Whakarewarewa	W1-calorimter	2018-04-04	11:50	1884800	5770778	1.729	52.2	67.9	78.4	87.6		98.7		196.5		739.5	241.5			0.5	260.3
Whakarewarewa	W6-calorimeter	2018-04-04	09:31	1885361	5771147	*0.7*	39.6	45.7	46.4	48.3	50.3	53.5	98.1	24.1						1.0	146.6
Whakarewarewa	W7-calorimeter	2018-04-05	15:36	1885105	5771242	*0.7*	82.6	98.1	99.1					501.5		630.4	189.7			0.1	771.1
Whakarewarewa	W8- calorimeter	2018-04-05	14:08	1885533	5771371	*0.7*	40.3	44.1	48.7	54.2	60.3	85.3		29.2		55.5	15.7			0.7	194.9

A5.2 Soil Temperature Profiles

Figures A 5.1 to A 5.5 show the soil temperature profiles measured at each area.

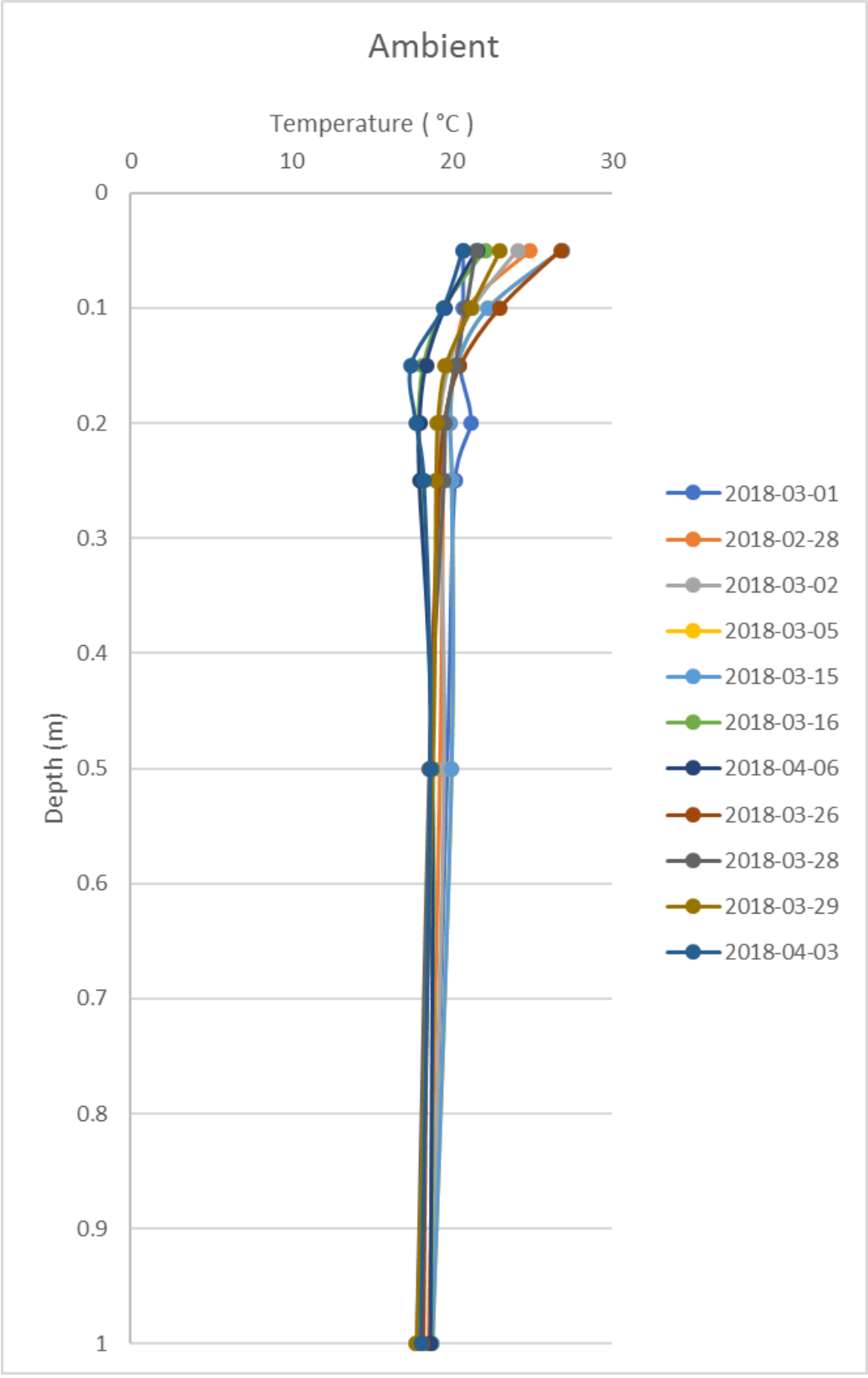

Figure A 5.1 Soil temperature profiles recorded at the ambient reference site.

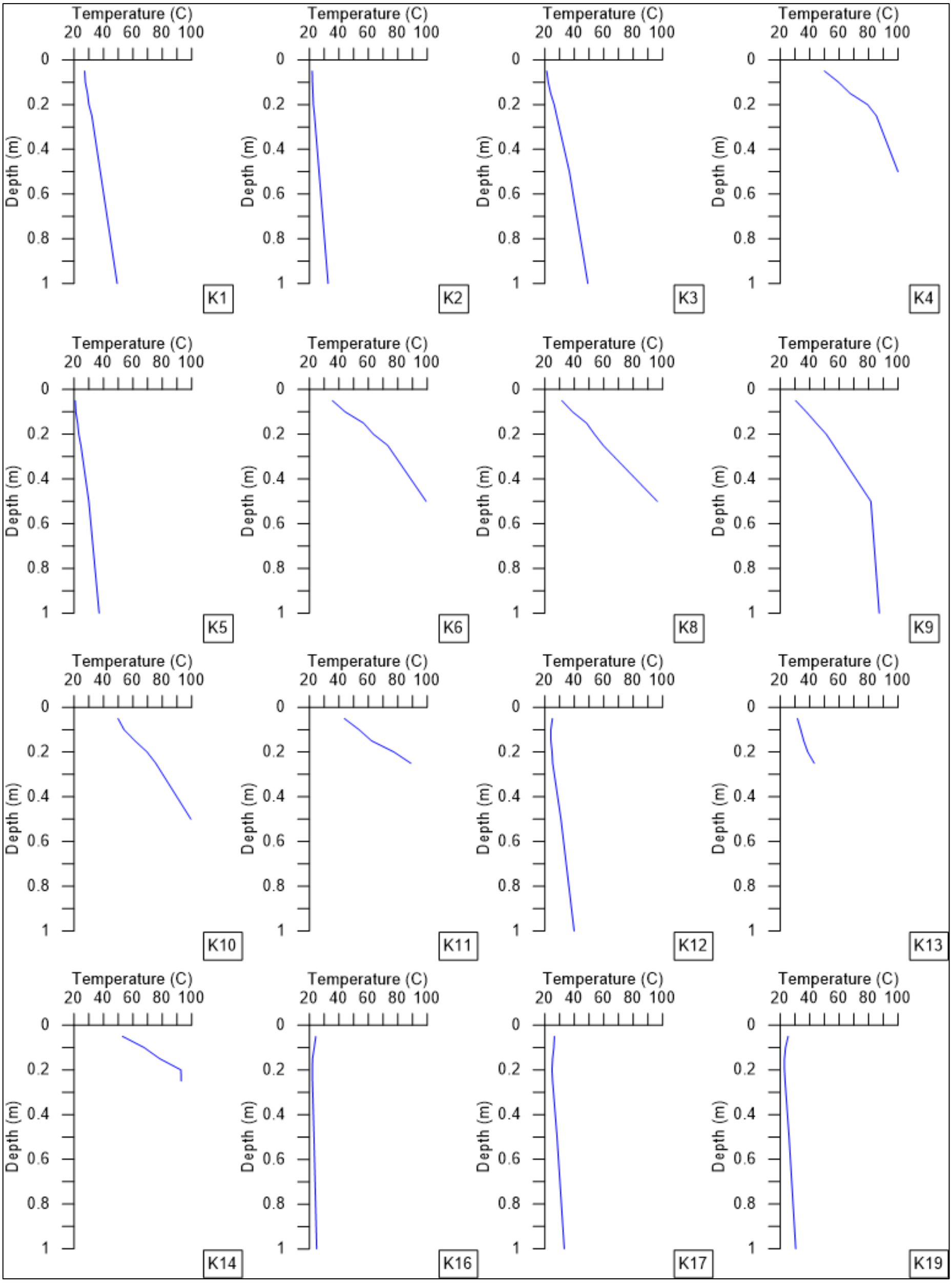

Figure A 5.2 Soil temperature profiles measured at Kuirau Park.

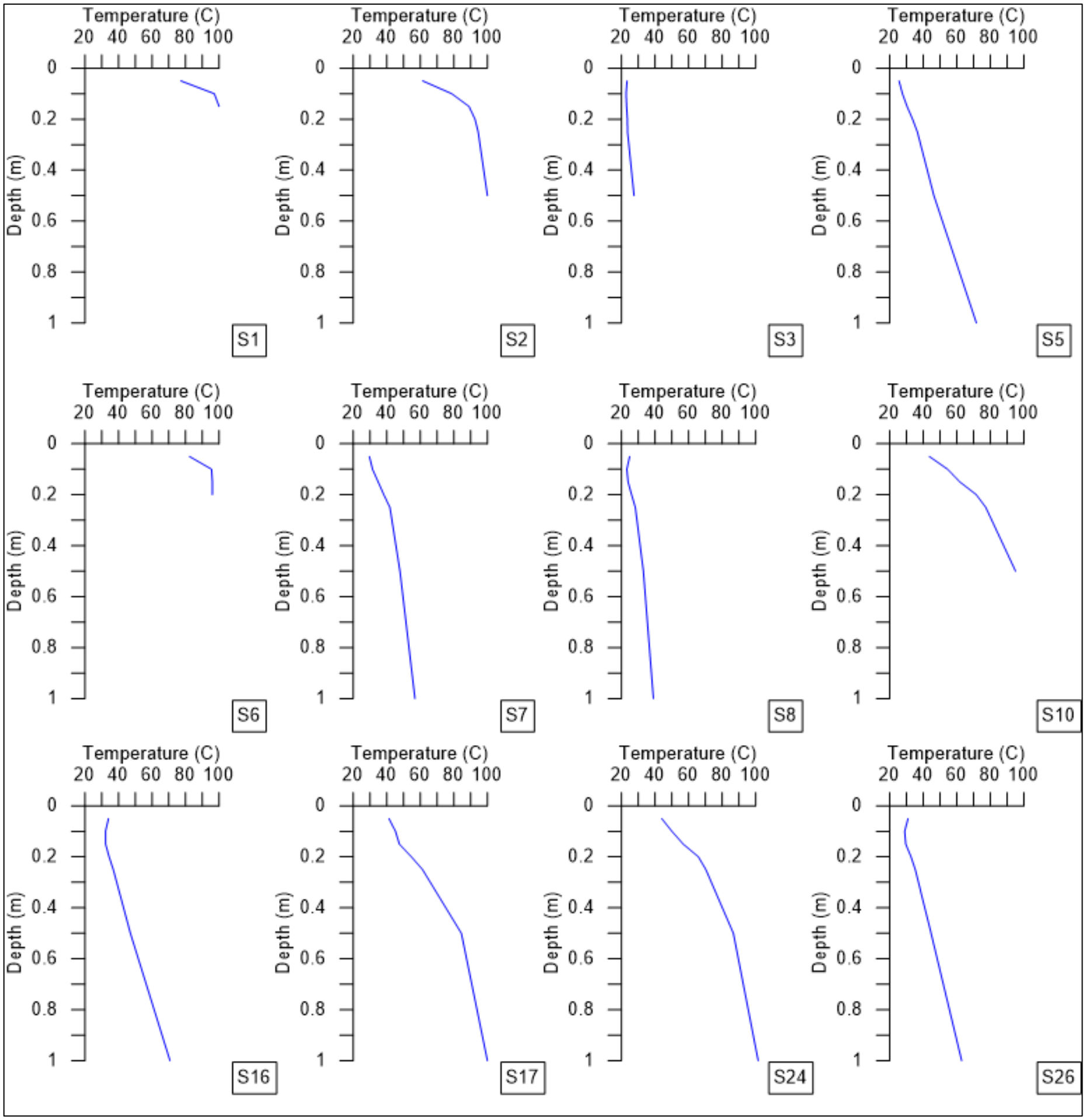

Figure A 5.3 Soil temperature profiles collected at Sulphur Bay / Government gardens.

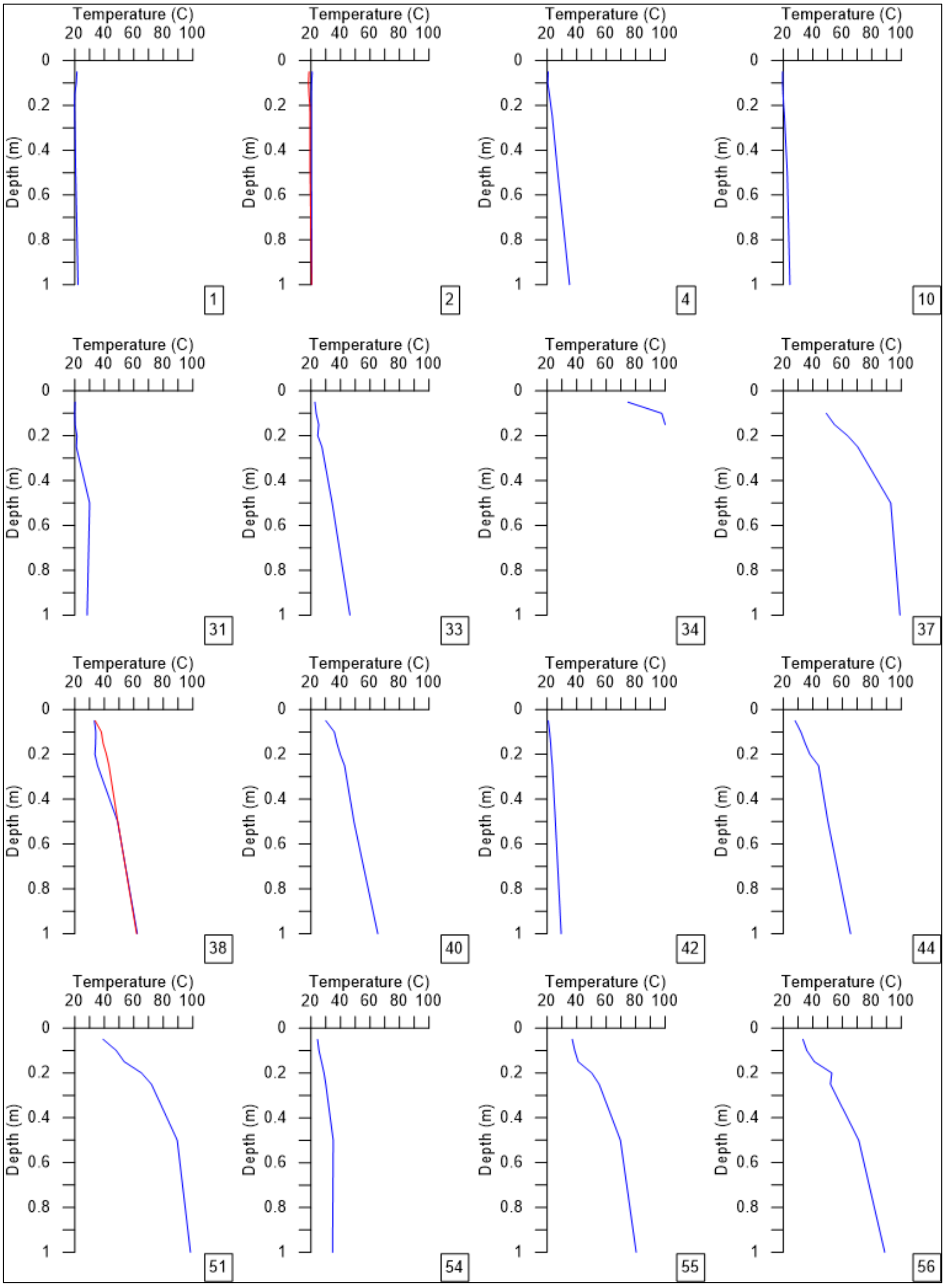

Figure A 5.4 Soil temperature profiles collected at Whakarewarewa / Te Puia.

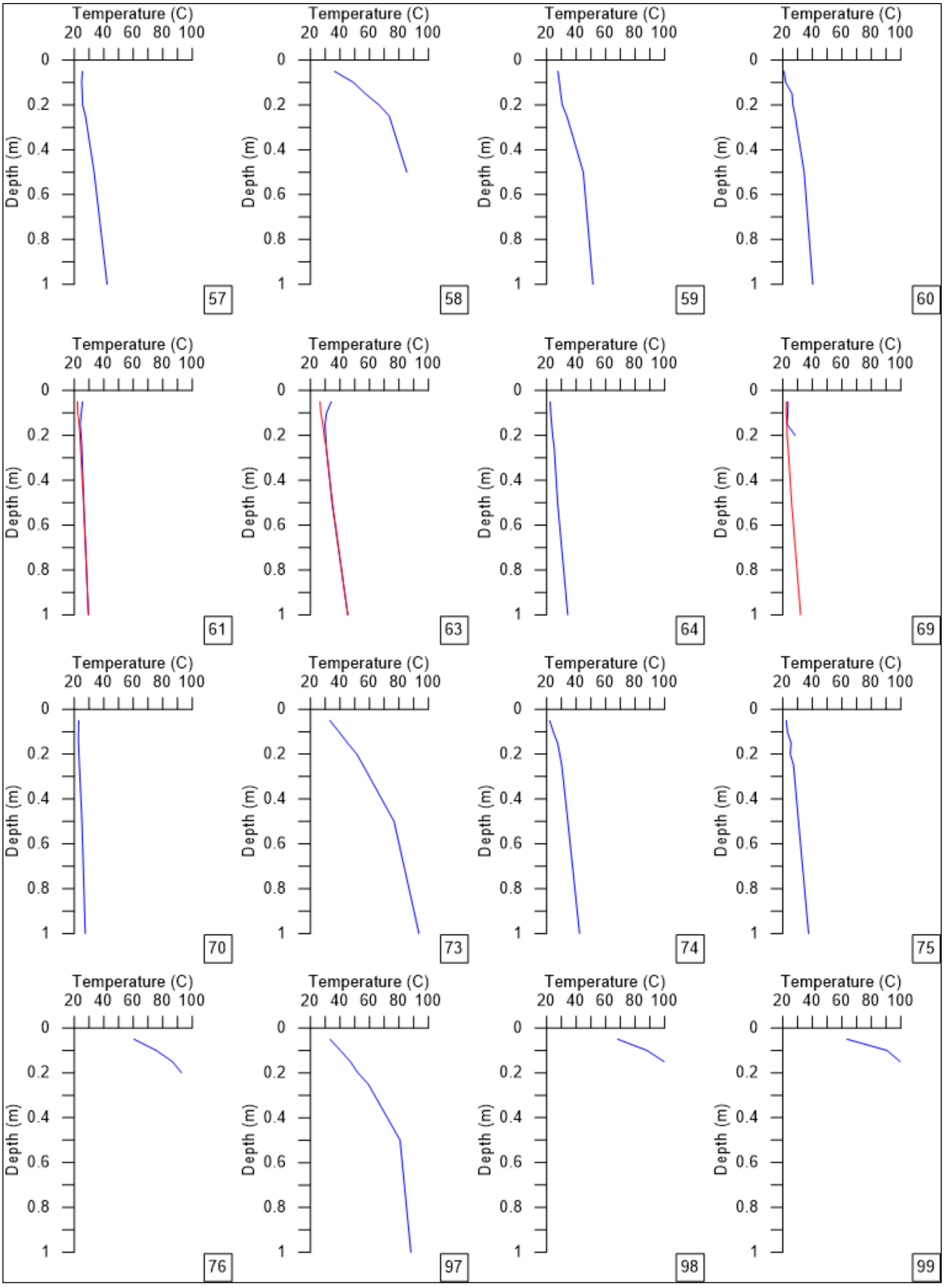

Figure A 5.4 continued. Soil temperature profiles collected at Whakarewarewa / Te Puia.

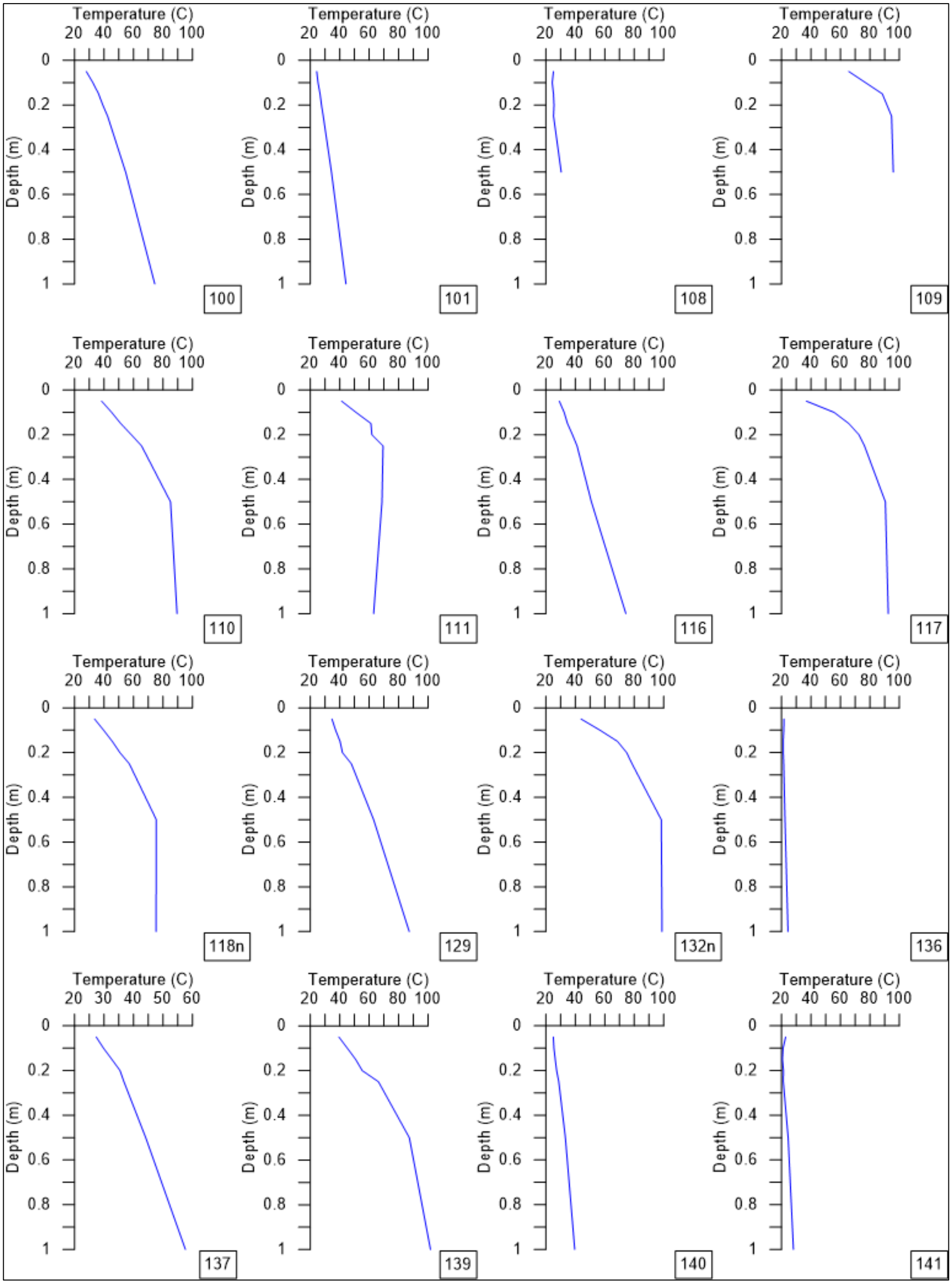

Figure A 5.4 continued. Soil temperature profiles collected at Whakarewarewa / Te Puia.

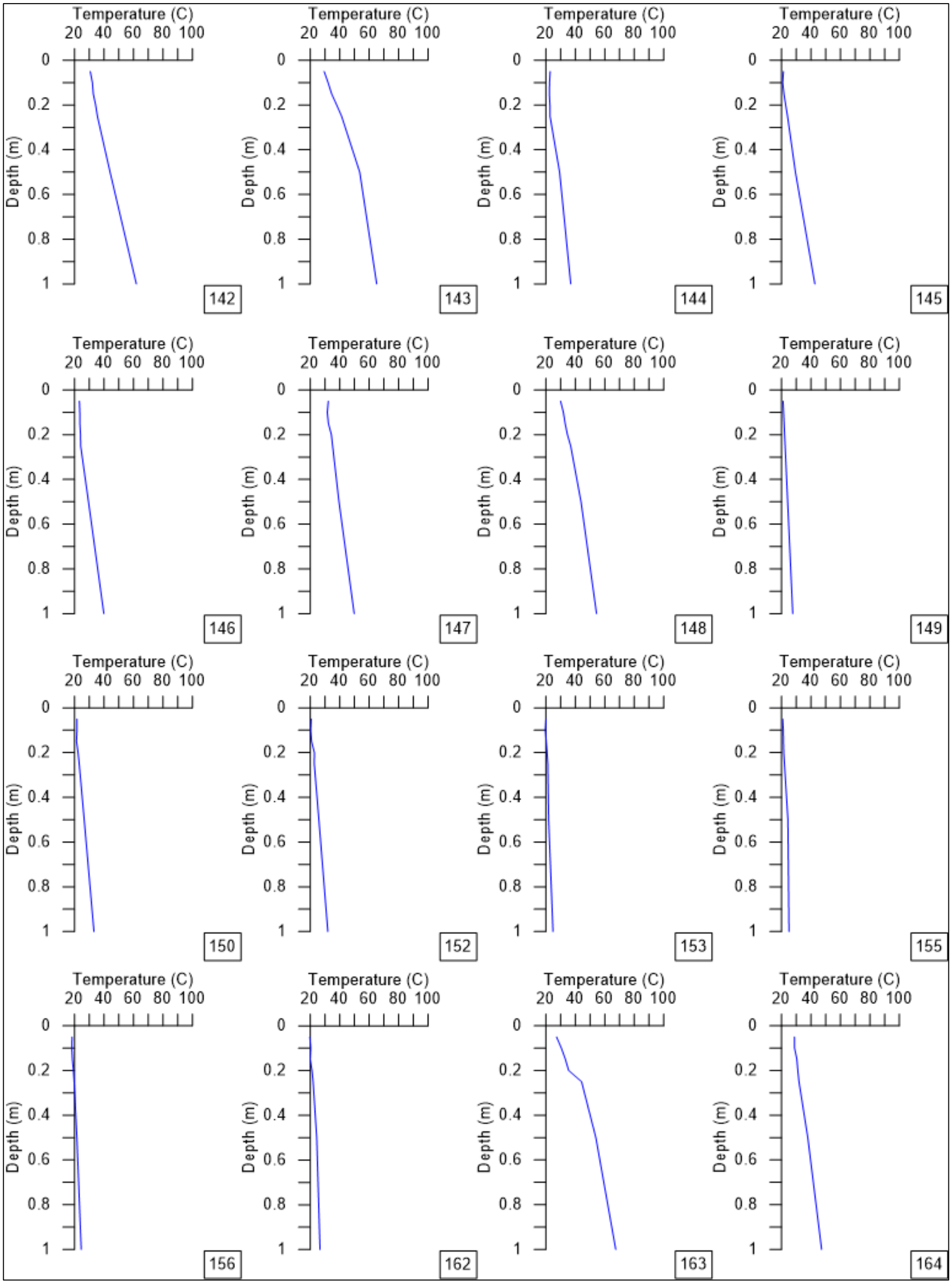

Figure A 5.4 continued. Soil temperature profiles collected at Whakarewarewa / Te Puia.

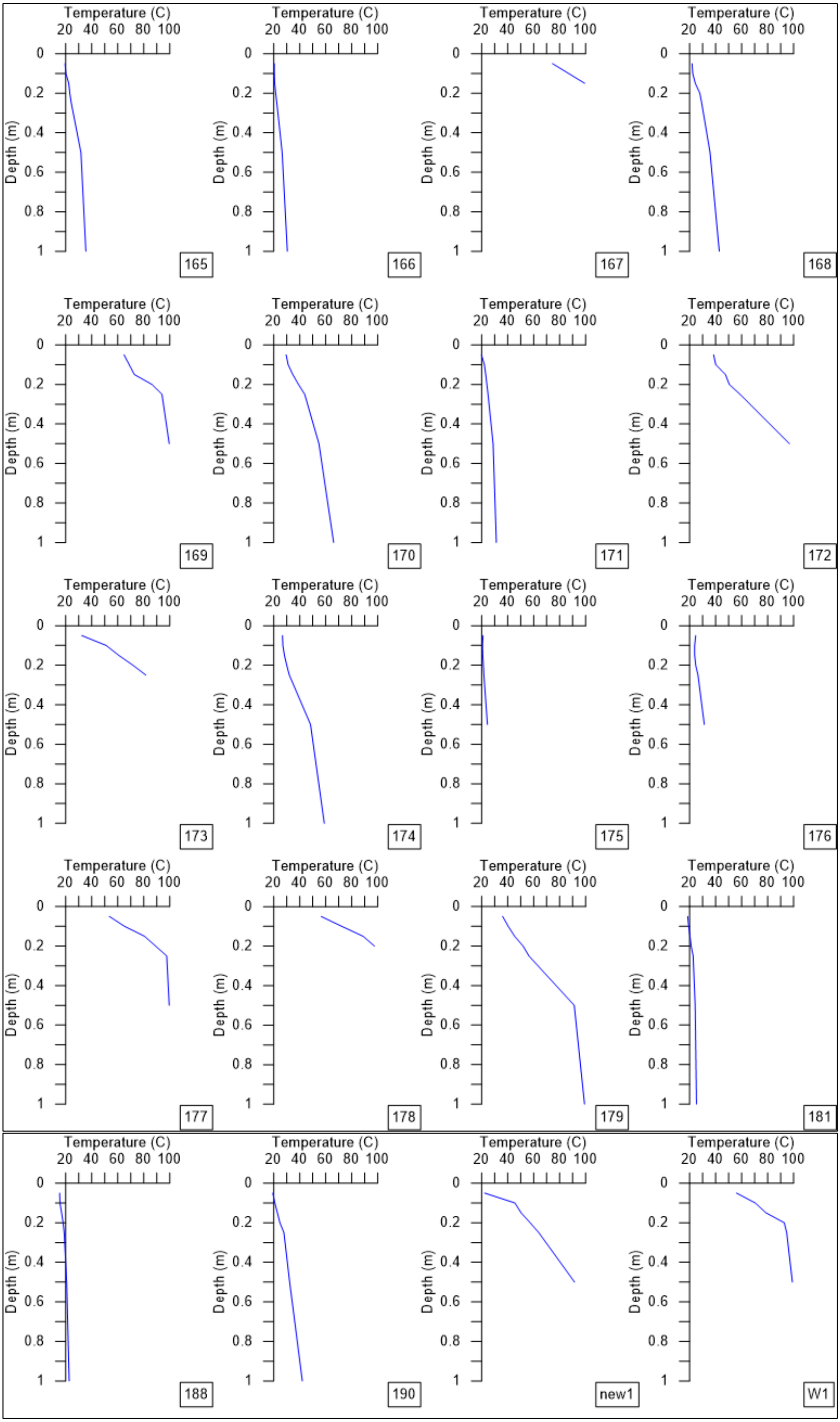

Figure A 5.4 continued. Soil temperature profiles collected at Whakarewarewa / Te Puia.

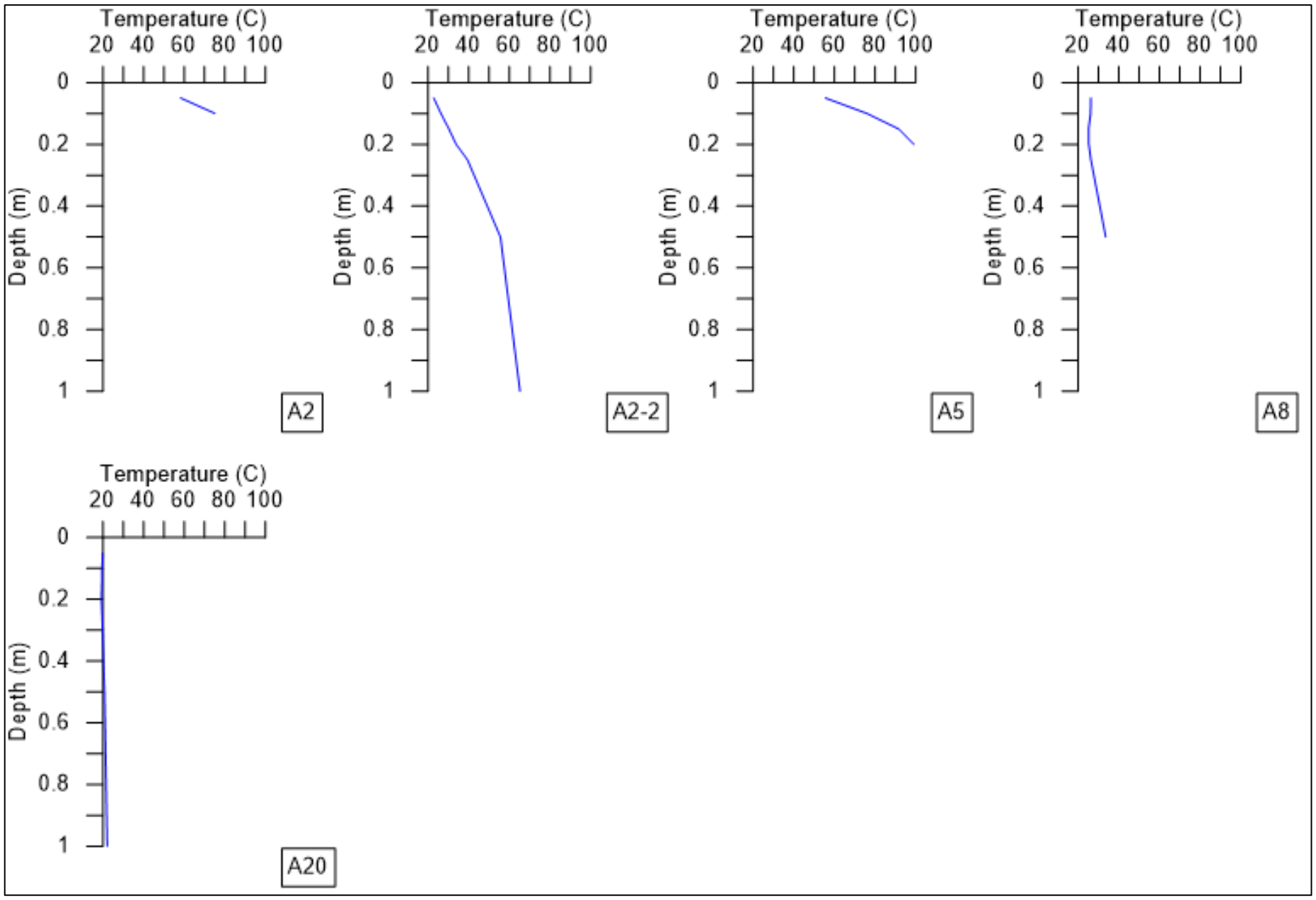

Figure A 5.5 Soil temperature profiles collected at Arikikapakapa.

A5.3 Calorimeter Data Plots

Field notes, recorded data and photos of the calorimeter sites can be found in Appendix 1. The raw data recorded at the calorimeter sites are plotted in Figures A 5.6 to A 5.12.

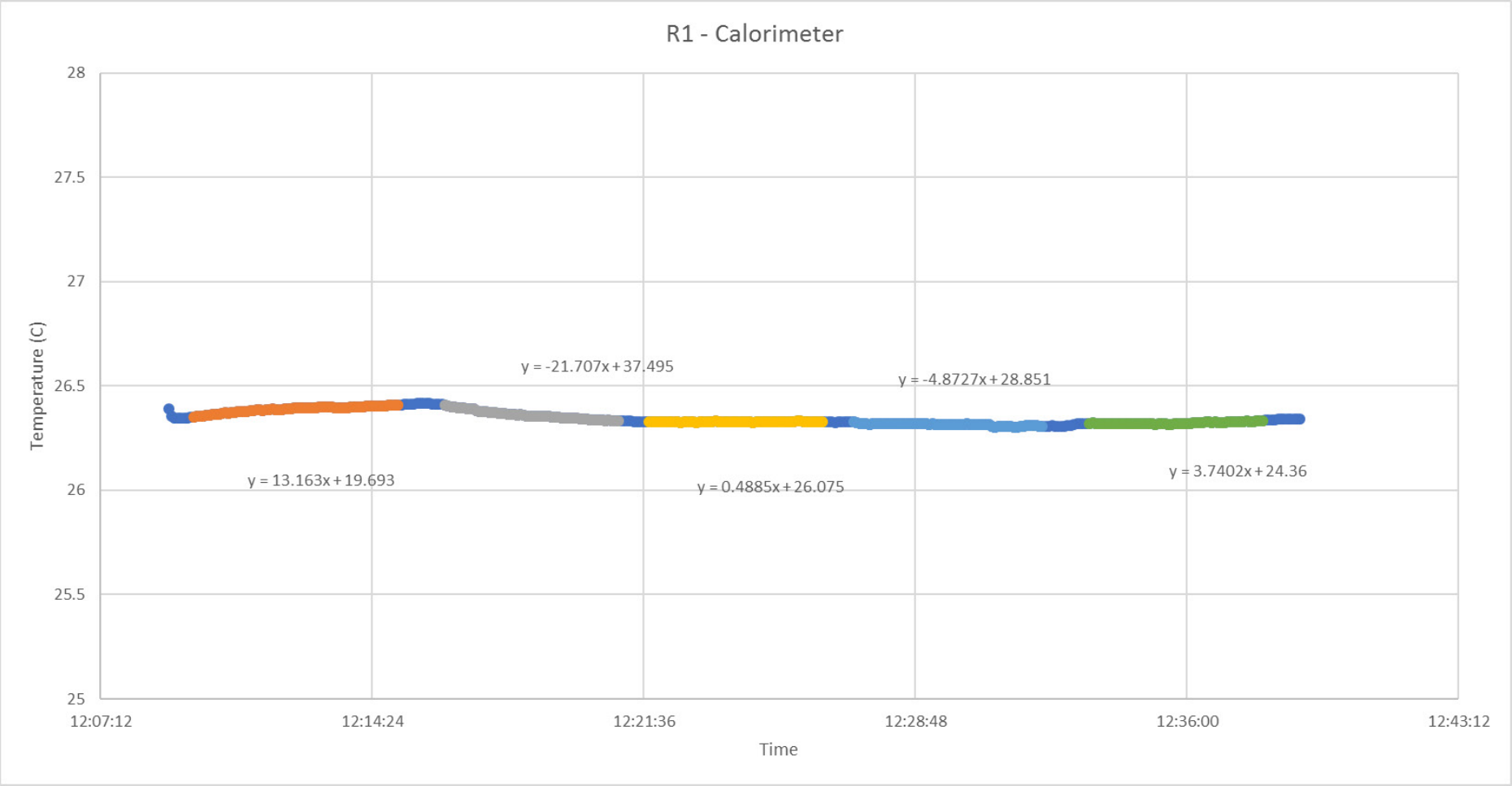

Figure A 5.6 Plot of raw data collected at Calorimeter site R1. Orange colour represents the time the calorimeter was first place on the insulated block; Grey represent when the Calorimeter was placed on the ground surface; yellow represented the 2nd time on the insulated block; light blue represents when the calorimeter is placed on the elevated ring; and green represented the 3rd time on the insulated block.

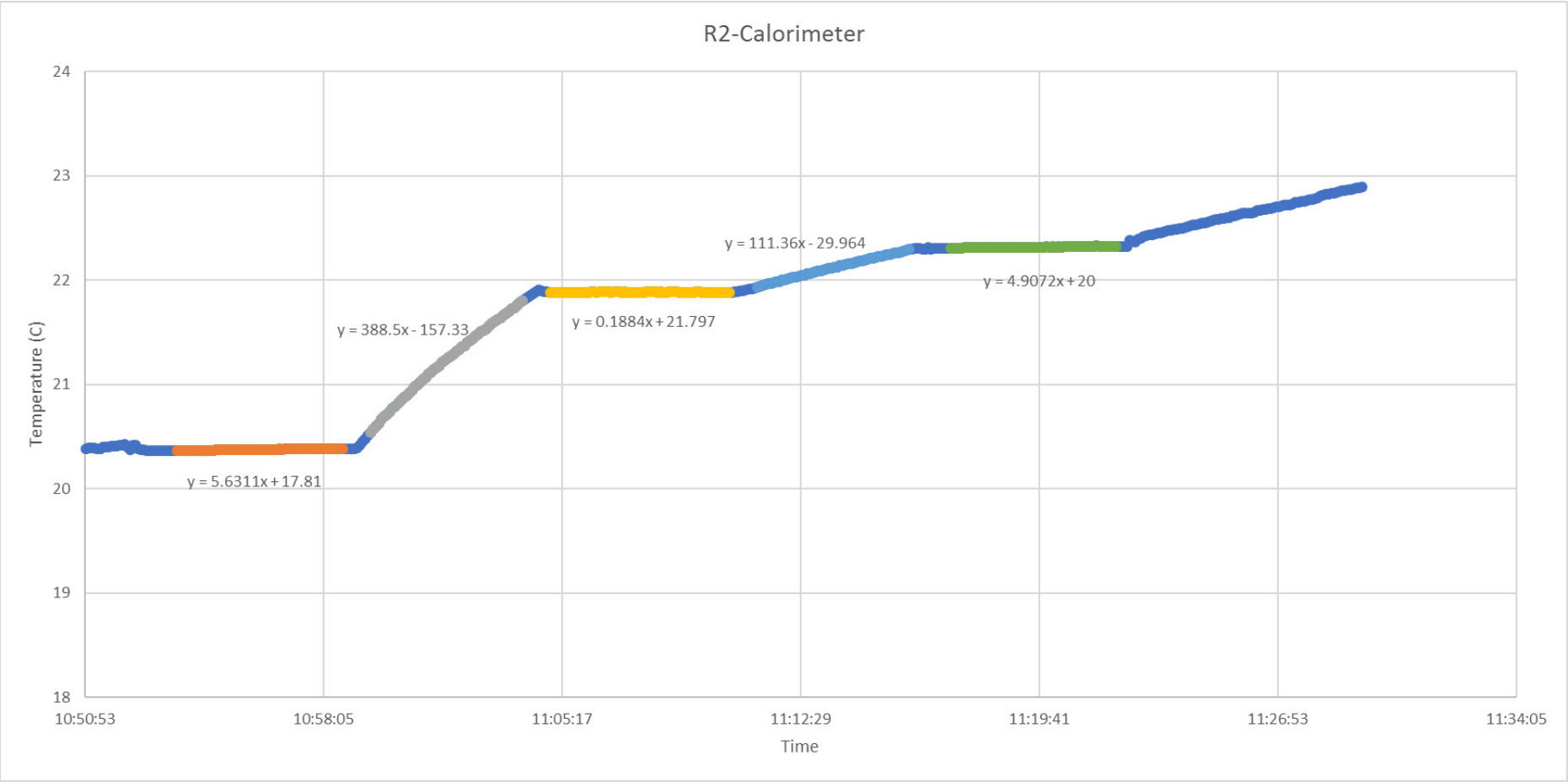

Figure A 5.7 Plot of raw data collected at Calorimeter site R2. Orange colour represents the time the calorimeter was first place on the insulated block; Grey represent when the Calorimeter was placed on the ground surface; yellow represented the 2nd time on the insulated block; light blue represents when the calorimeter is placed on the elevated ring; and green represented the 3rd time on the insulated block.

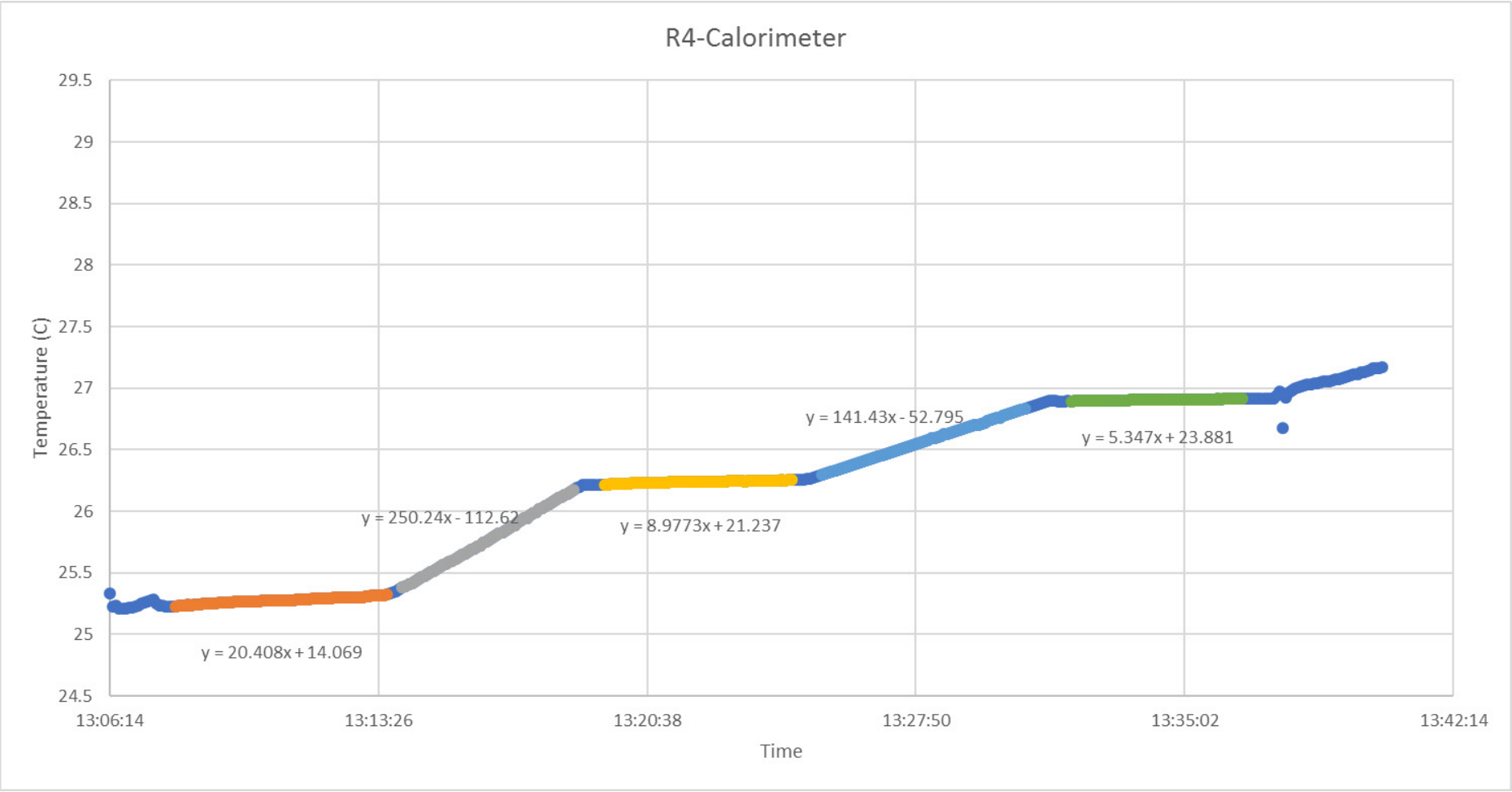

Figure A 5.8 Plot of raw data collected at Calorimeter site R4. Orange colour represents the time the calorimeter was first place on the insulated block; Grey represent when the Calorimeter was placed on the ground surface; yellow represented the 2nd time on the insulated block; light blue represents when the calorimeter is placed on the elevated ring; and green represented the 3rd time on the insulated block.

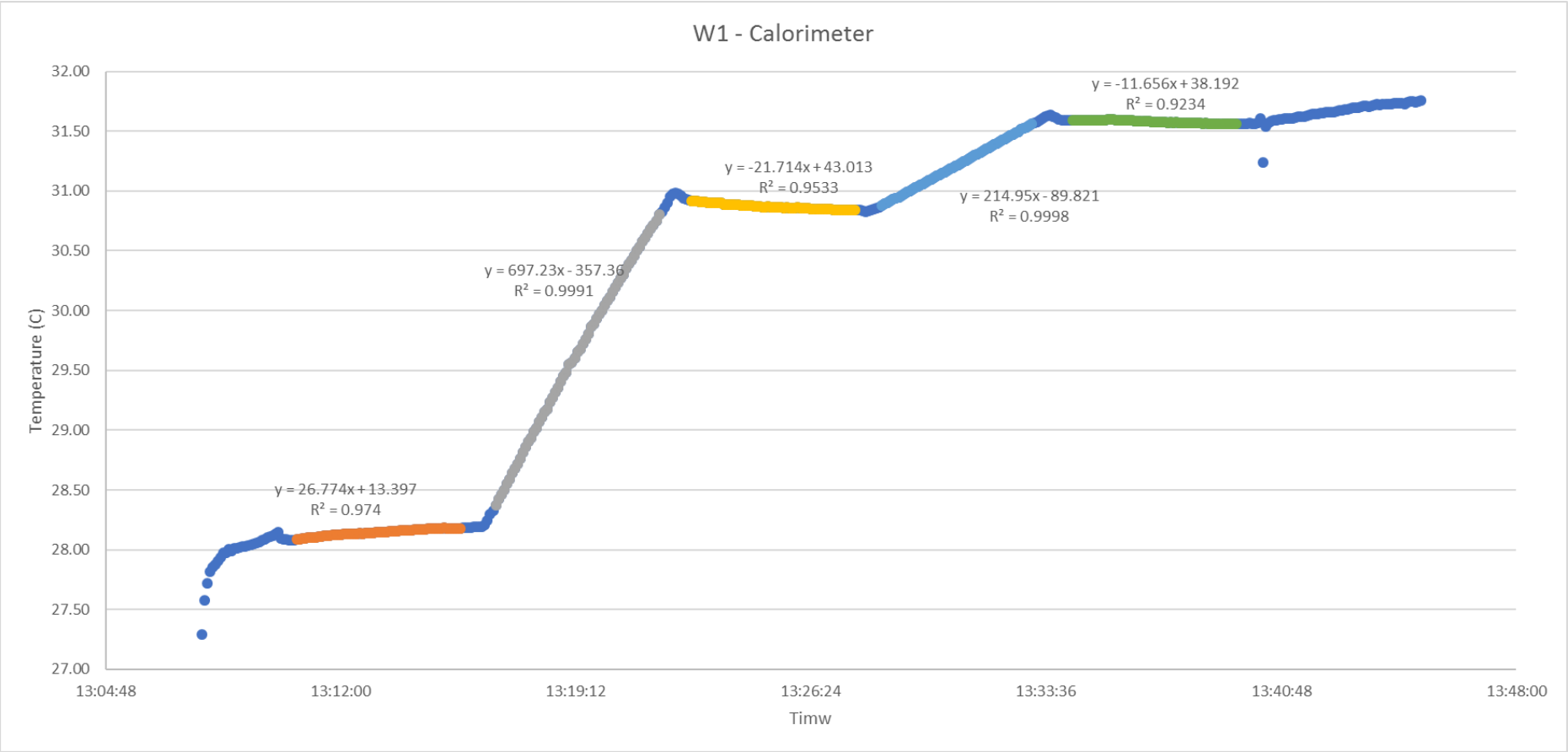

Figure A 5.9 Plot of raw data collected at Calorimeter site W1. Orange colour represents the time the calorimeter was first place on the insulated block; Grey represent when the Calorimeter was placed on the ground surface; yellow represented the 2nd time on the insulated block; light blue represents when the calorimeter is placed on the elevated ring; and green represented the 3rd time on the insulated block.

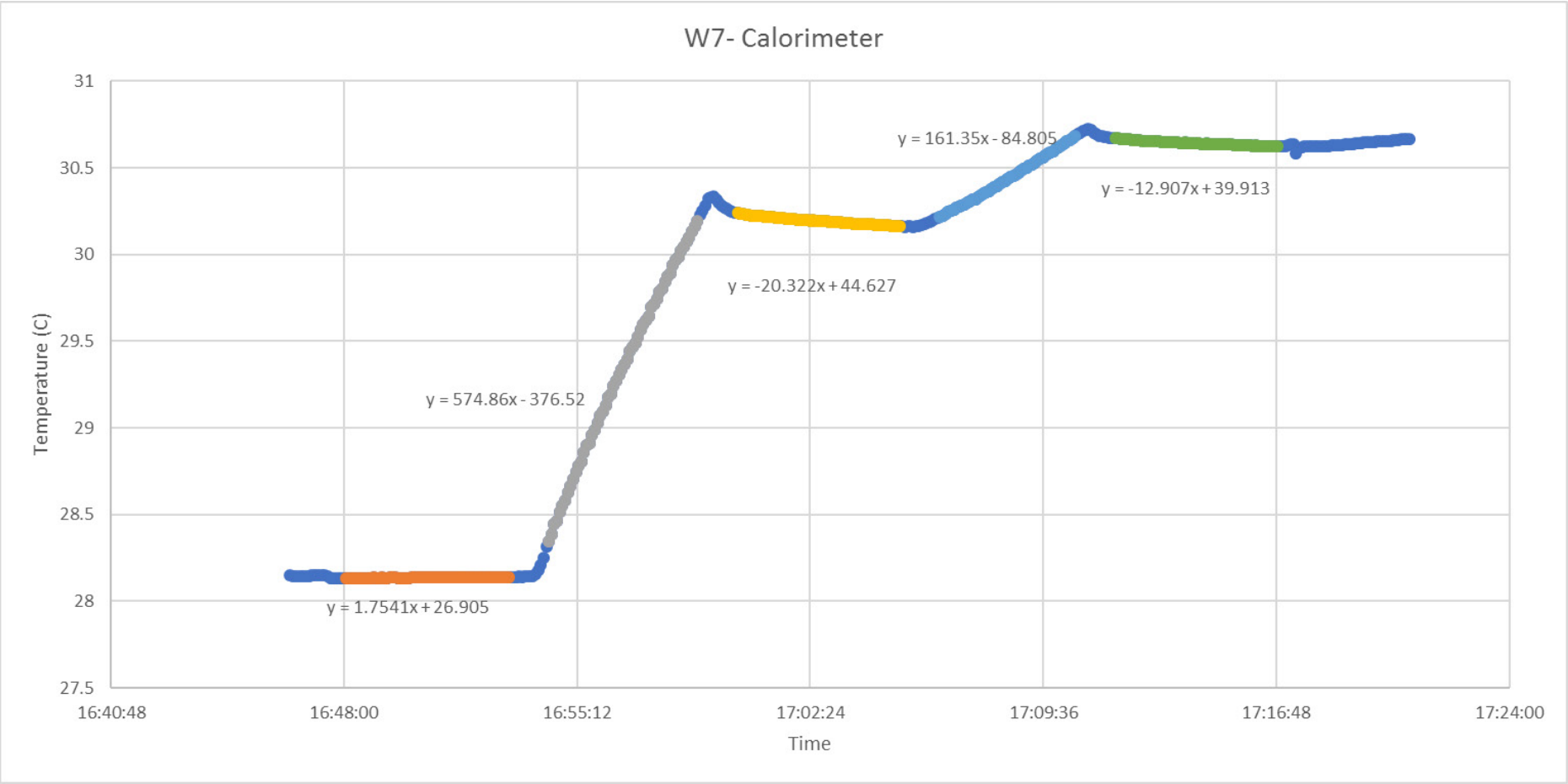

Figure A 5.10 Plot of raw data collected at Calorimeter site W7. Orange colour represents the time the calorimeter was first place on the insulated block; Grey represent when the Calorimeter was placed on the ground surface; yellow represented the 2nd time on the insulated block; light blue represents when the calorimeter is placed on the elevated ring; and green represented the 3rd time on the insulated block.

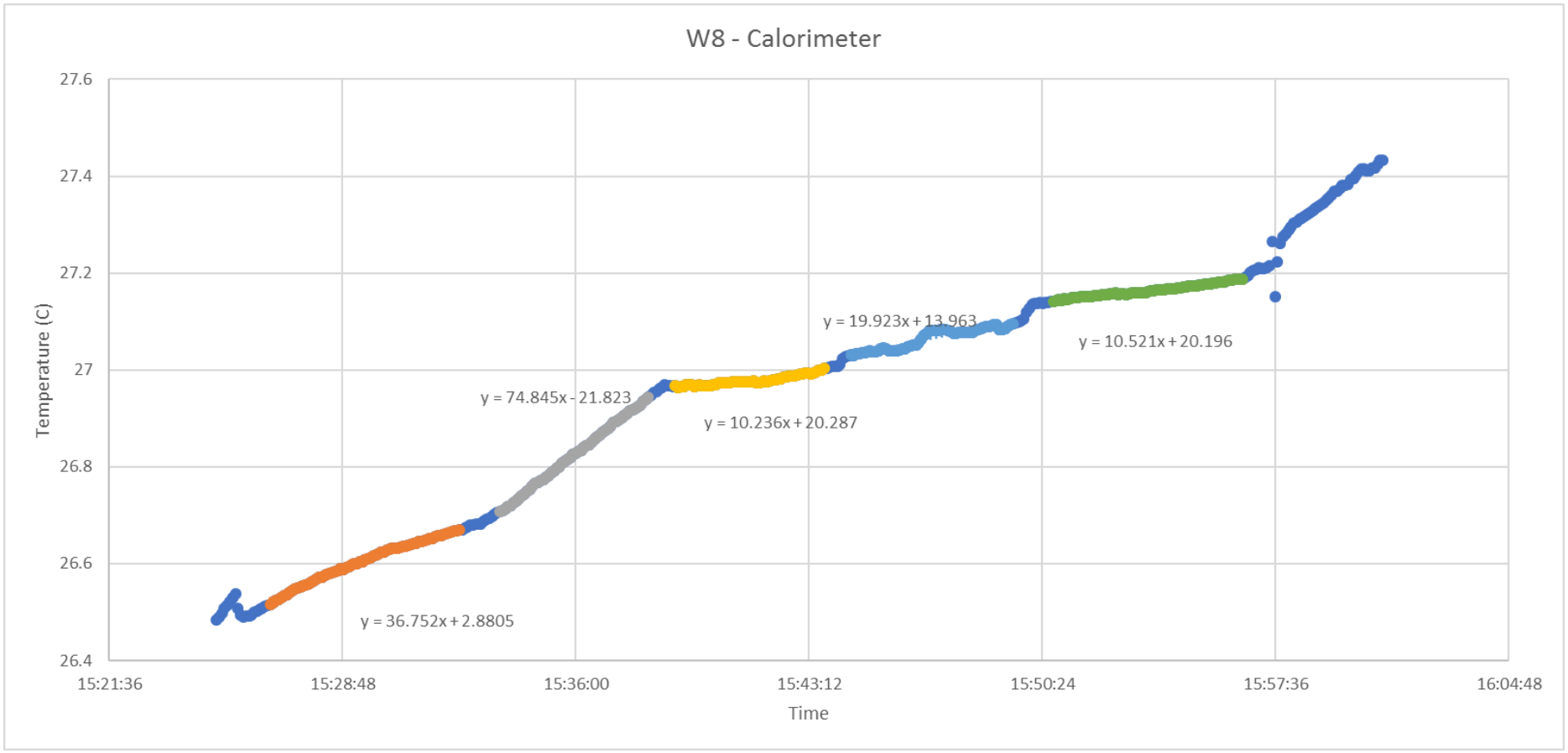

Figure A 5.11 Plot of raw data collected at Calorimeter site W8. Orange colour represents the time the calorimeter was first place on the insulated block; Grey represent when the Calorimeter was placed on the ground surface; yellow represented the 2nd time on the insulated block; light blue represents when the calorimeter is placed on the elevated ring; and green represented the 3rd time on the insulated block.

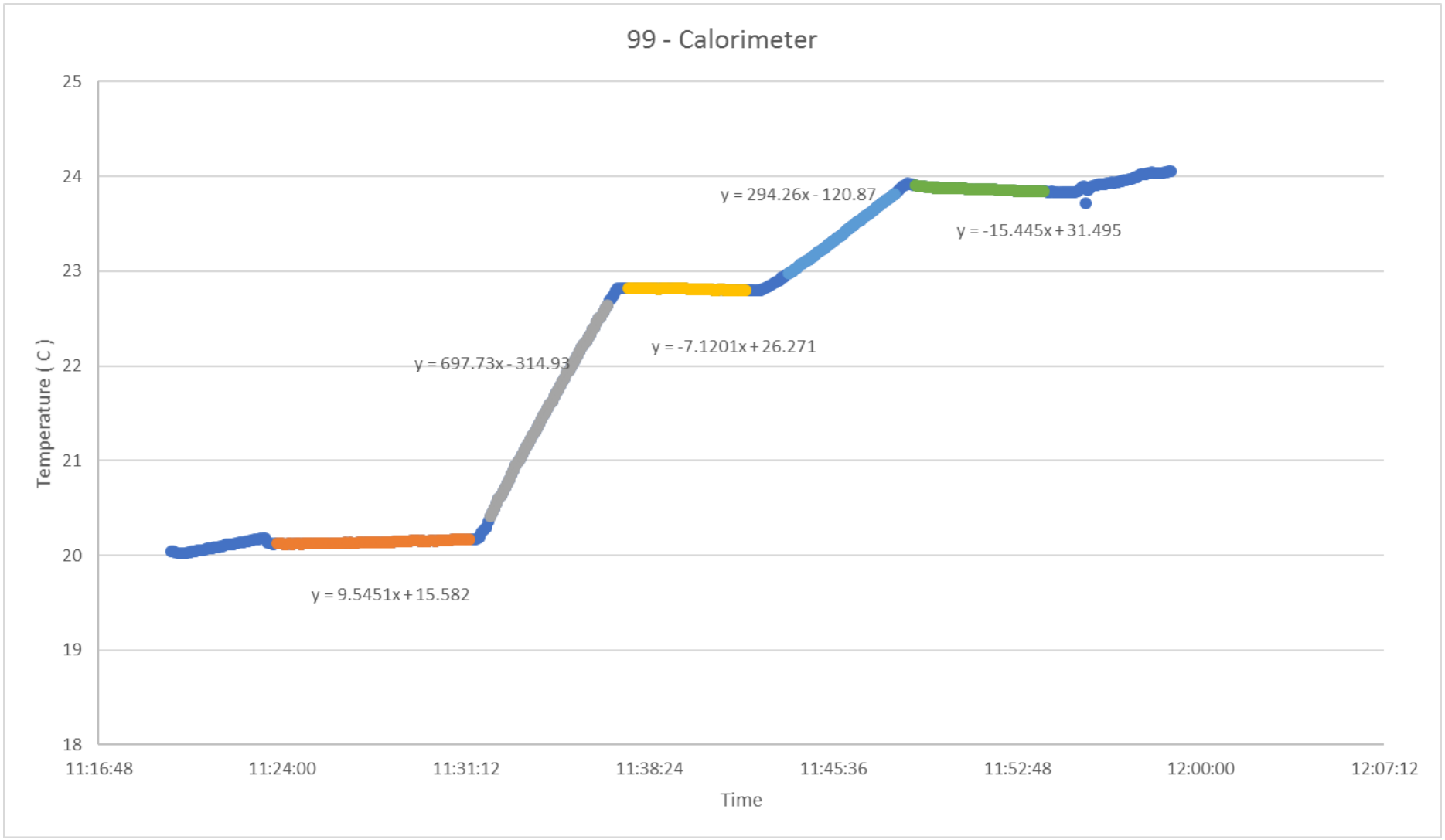

Figure A 5.12 Plot of raw data collected at Calorimeter site 99-calorimeter. Orange colour represents the time the calorimeter was first place on the insulated block; Grey represent when the Calorimeter was placed on the ground surface; yellow represented the 2nd time on the insulated block; light blue represents when the calorimeter is placed on the elevated ring; and green represented the 3rd time on the insulated block.

A5.4 Determining Heat Loss from TIR Heat Signature for Area Estimation

Table A 5.2 Summary of heat loss determined in each area using the TIR image.

Temperature (°C)		Whakarewarewa			Kuirau Park			Sulphur Bay			Arikikapakapa		
Inferred TIR	T5	# pixel	Area (m^2)	Qtot (W)	# pixel	Area (m^2)	Qtot (W)	# pixel	Area (m^2)	Qtot (W)	# pixel	Area (m^2)	Qtot (W)
<20	36	1139523	558366.3		1139523	558366.3		1139523	558366.3		1139523	558366.3	
20–22	37.8	18805	9214.45	1485828	18805	9214.45	1485828	18805	9214.45	1485828	18805	9214.45	1485828
22–24	41.4	13931	6826.19	1395761	13931	6826.19	1395761	13931	6826.19	1395761	13931	6826.19	1395761
24–26	45	9877	4839.73	1198767	9877	4839.73	1198767	9877	4839.73	1198767	9877	4839.73	1198767
26–28	48.6	7488	3669.12	1067401	7488	3669.12	1067401	7488	3669.12	1067401	7488	3669.12	1067401
28–30	52.2	5746	2815.54	940773.8	5746	2815.54	940773.8	5746	2815.54	940773.8	5746	2815.54	940773.8
30–32	55.8	4546	2227.54	840579.6	4546	2227.54	840579.6	4546	2227.54	840579.6	4546	2227.54	840579.6
32–34	59.4	3450	1690.5	710989.5	3450	1690.5	710989.5	3450	1690.5	710989.5	3450	1690.5	710989.5
34–36	63	2383	1167.67	541566.5	2383	1167.67	541566.5	2383	1167.67	541566.5	2383	1167.67	541566.5
36–38	66.6	1742	853.58	432784.4	1742	853.58	432784.4	1742	853.58	432784.4	1742	853.58	432784.4
38–40	70.2	1174	575.26	316533.5	1174	575.26	316533.5	1174	575.26	316533.5	1174	575.26	316533.5
40–42	73.8	827	405.23	240490.1	827	405.23	240490.1	827	405.23	240490.1	827	405.23	240490.1
42–44	77.4	597	292.53	186250.2	597	292.53	186250.2	597	292.53	186250.2	597	292.53	186250.2
44–46	81	432	211.68	143923.1	432	211.68	143923.1	432	211.68	143923.1	432	211.68	143923.1
46–48	84.6	287	140.63	101693.9	287	140.63	101693.9	287	140.63	101693.9	287	140.63	101693.9
48–50	88.2	220	107.8	82612.77	220	107.8	82612.77	220	107.8	82612.77	220	107.8	82612.77
50 +	90	334	163.66	128958	334	163.66	128958	334	163.66	128958	334	163.66	128958

www.gns.cri.nz

Principal Location

1 Fairway Drive
Avalon
PO Box 30368
Lower Hutt
New Zealand
T +64-4-570 1444
F +64-4-570 4600

Other Locations

Dunedin Research Centre
764 Cumberland Street
Private Bag 1930
Dunedin
New Zealand
T +64-3-477 4050
F +64-3-477 5232

Wairakei Research Centre
114 Karetoto Road
Wairakei
Private Bag 2000, Taupo
New Zealand
T +64-7-374 8211
F +64-7-374 8199

National Isotope Centre
30 Gracefield Road
PO Box 31312
Lower Hutt
New Zealand
T +64-4-570 1444
F +64-4-570 4657